THESIS FOR THE DEGREE OF DOCTOR OF PHILOSOPHY (PHD)

Szilvia Irina Ecsedi

GENETIC AND EPIGENETIC BACKGROUND OF MELANOMA PROGRESSION

UNIVERSITY OF DEBRECEN
DOCTORAL SCHOOL OF HEALTH SCIENCES
Debrecen, 2014

Table of contents

Abbreviations

AJCC: American Joint Committee on Cancer

AVG-Beta: average beta intensity values specific for each CpG in methylation bead assay

BRAF: v-raf murine sarcoma viral oncogene homolog B1

CCND1: cyclin D1 gene

aCGH: array comparative genome hybridization

CI: confidence interval

CIMP: CpG island methylator phenotype (in colon cancer)

CN: copy number

CpG island: genomic region rich in CpG dinucleotids ("p" refers to phospho-group)

DNMT1: DNA methyltrasferase type1

DNMT3a: de novo methyltransferase type 3a

DNMT3b: de novo methyltransferase type 3b

FISH: fluorescence *in situ* hybridization

GAPDH: glyceraldehyde 3-phosphate dehydrogenase

HR: hazard ratio (used in Cox regression analysis)

5mC: 5-methylcytosine

5-hmC: 5-hydroxymethylcytosine

KIT: v-kit Hardy-Zuckerman 4 feline sarcoma viral oncogene homolog

M-value: logit transfromation of averagre bete value

MYB: V-Myb Avian Myeloblastosis Viral Oncogene Homolog

NM: nodular melanoma

NRAS: neuroblastoma RAS viral (v-ras) oncogene homolog

PCA: Principal Components Analysis

OR: odds ratio (in logostic regression analysis)

OS: overall survival

QRT-PCR: quantitative reverse-transcription polymerase chain reaction

RGP: radial growth phase

ROC: receiver operating characteristic

RREB1: ras responsive element binding protein 1

SNP: single nucleotide polymorphism

SSM: superficial spreading melanoma

TNM: tumour – lymph node – metastasis

VGP: vertical growth phase

WT: wild type

WHO: World Health Organization

Introduction

Malignant melanoma is one of the most aggressive skin cancers with a constantly increasing incidence. As estimated by the World Health Organization worldwide number of newly diagnosed skin cancer cases is between 2 and 3 million each year, of which 132,000 are melanoma[1]. Additionally, in most western countries, the incidence of this malignancy doubles roughly every decade. Melanoma is a highly metastatic disease and as soon as the first distant metastasis appears, the disease becomes one of the most aggressive types of metastatic, chemoresistant lesions with poor survival rate as Figure 1 demonstrates[2].

Cutaneous melanoma originates from melanocytes, the pigment-producing skin cells that reside between keratinocytes in the basal layer of the epidermis, producing melanin in response to a variety of external stimuli, such as ultraviolet (UV) radiation which is the leading exogenous etiological risk factor for the development of the disease[3].

Melanoma often begins as a benign nevus (mole) consisting of a hyperplastic subpopulation locked in a state of cellular senescence. Once the senescence is overcome, the nevus will exhibit dysplastic features and readily progress to melanoma which progresses through a series of well-defined clinical and histopathological stages, advancing in a stepwise manner from either a common acquired or a dysplastic nevus through the primary radial growth phase (RGP) and the vertical growth phase (VGP) to distant metastasis[4]. The vertical progression of lesions is representative of the degree of tumour progression and is measured by the Breslow thickness, which was first used in the early 1970s and measures the thickness of the tumour from the top of the epidermal granular layer (or from the ulcer base if the tumour is ulcerated) to the innermost depth of invasion[5,6]. Ulceration of the tumour surface of melanoma covering the epidermis is one of the most sensitive parameters of metastatic potential[7,8]. Clark's level refers to how deep the tumour has penetrated into the layers of the skin[9]. Although the Clark's level has been demonstrated to be less predictive of outcome and less reproducible, it is still applied in the practice for some instances (e.g. to predict prognosis for level IV-V melanomas)[10].

According to the recent exome capture sequencing data, the median sample mutation rate of primary melanomas is 14.4 coding mutations per megabase, much higher than that reported for any other tumour type and a signature of UV mutagenesis (C > T transitions) is predominated[11,12].

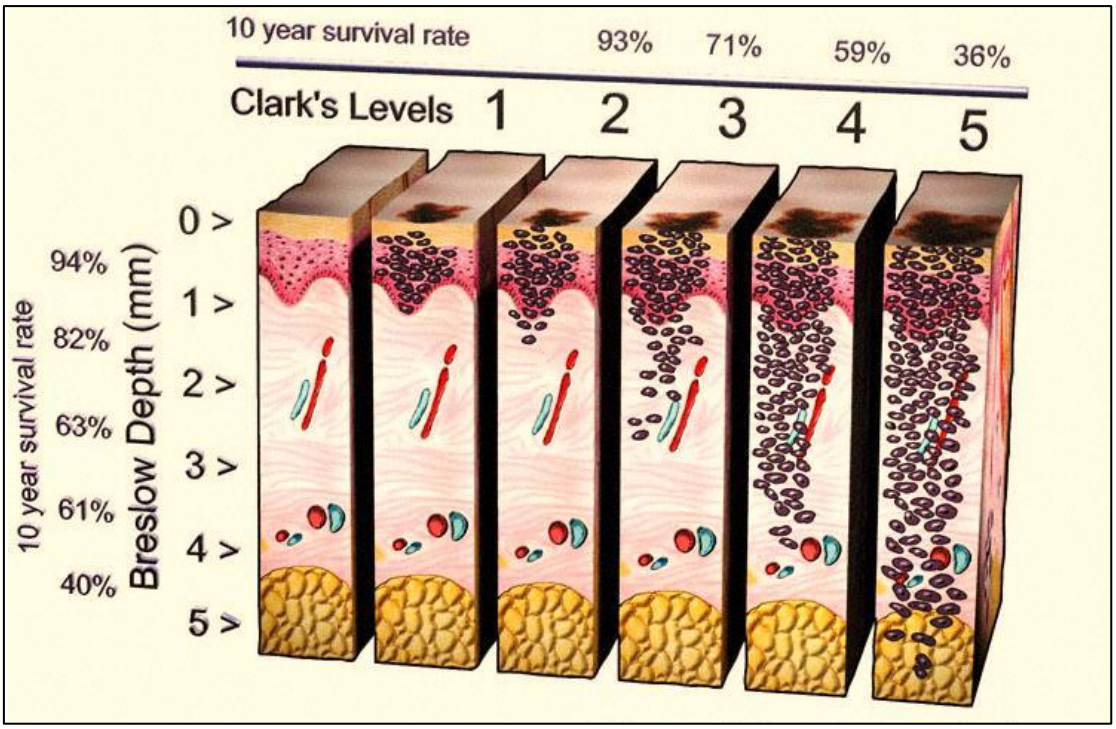

Figure 1 Clark's levels and Breslow depth with 10 years survival rate of melanoma patients.
Source: http://med-ars.it

The spectrum of somatic alterations in melanoma includes both genetic and epigenetic events that act in concert to promote tumour progression[13,14]. To date only a few experiments have focused mainly on elucidating the epigenetic differences in the DNA methylation patterns between melanomas and benign skin lesions. Notably, these studies have had a great impact regarding our understanding what drives melanocytic lesions to develop into malignant melanomas. However, the DNA methylation pattern associated with the progression of the disease is still under the question. In spite of having tremendous potential in improving our understanding in tumour progression, integrative genome approaches are still in their infancy. Considering the fact that melanomas are cured mainly surgically, providing new therapeutic targets with broader impact are especially urgent. As integrative genomics could provide deeper insights into the more generalized mechanisms driven by multiple types of alterations, it can play a major role in discovering an effective therapeutic intervention for melanoma patients.

Background

Epigenetic events in cancer

The commonly used term "epigenetics" has been rapidly spreading over the last decade. It emerged to define heritable changes in genome function that cannot be explained by direct influence over DNA sequences. As epigenetic mechanisms affect gene expression, resulting in different phenotypes without directly altering the underlying DNA sequence, it is reasonable that these factors should have an impact on cancer development[15,16]. Because the importance of epigenetic processes in gene regulation is currently a topic of doubt and discussion, standard nomenclature for different types of epigenetic modifications is not available in the literature, although it is reasonable to distinguish between them based on the phase during which a specific event influences gene expression[17]. There are classical two types of such alterations that are known to occur at the transcriptional level: DNA methylation and chromatin modification (post-transcriptional covalent change and chromatin rearrangement without chemical alteration). The third type of epigenetic alteration that has been discovered to date is RNA interference, which only affects a phenotype later, at the post-transcriptional level, as it directly cleaves mRNA, resulting in disrupted or no translation[18].

The best described factor involved in epigenetic inheritance is DNA methylation, a covalent modification of cytosines (mainly at position 5, but also at position 4 or 6) that results in 5-methyl-cytosine occurs in CpG dinucleotides that are part of CpG islands that can most commonly be found at or near promoter regions in mammals[19]. This process is accomplished through specific molecules: DNA methyltransferases (DNMTs), which are responsible for establishing and maintaining the unique methylation pattern on DNA[20]. Three different types of DNMT have been reported to date. DNMT2 has rather low activity and functions only in tRNA methylation. DNMT1 and DNMT3 play essential roles in both mammalian development and in cancer biology, as they catalyse the addition of a methyl group to cytosines from the donor S-adenosyl-methionine[14]. However, they require different substrates. Because DNMT1 is methylation dependent, it predominantly methylates hemimethylated CpGs[21]. Therefore, DNMT1 is responsible for maintaining the methylation pattern, which is extremely important in cell division. DNMT3a and DNMT3b are referred to as *de novo* methylases because they act independently of previous methylation of the complementary strand[22]. Both DNMT3a and DNMT3b could be important factors in establishing a new CpG methylation pattern, though DNMT3 exhibits a preference for centromeric regions[23].

Additionally, if a methyl group has already been added to a cytosine residue, methyl-CpG-binding proteins can attach to methylated regions. Therefore, a specific signature is constructed in assembling transcriptionally silent heterochromatin. It is widely accepted that DNA methylation of promoter regions, which are the main site of CpGs, can cause direct inactivation of specific genes[24].

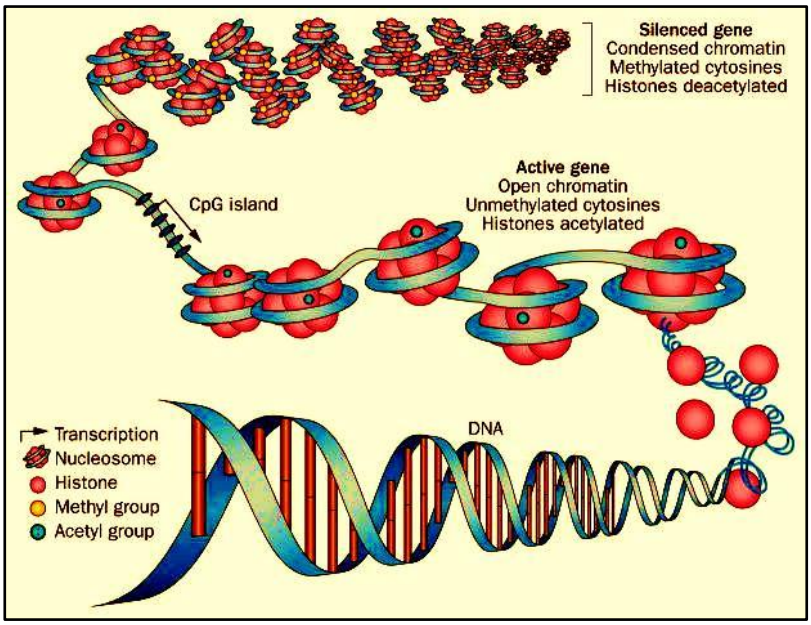

Figure 2 Epigenetic regulation of gene expression.
Gene expression is controlled in the promoter regions by a combination of DNA methylation and chromatin configuration. CpG islands that are rich in cytosine and guanine — and are typically unmethylated to promote gene expression — can be epigenetically silenced by hypermethylation in cancer. Adapted from Figueiredo et al.[25]

DNA methylation patterns in melanomas

Promoter hypermethylation

Given the existence of relatively easy approaches that require even minute amounts of tumour DNA, there are currently substantial amounts of data available that refer to gene silencing associated with the localised CpG hypermethylation of a specific gene promoter[19]. There are two options for investigating this epigenetic phenomenon: it can be estimated indirectly or measured directly. Indirect assessment consists of three steps: first, measuring mRNA or protein expression; next, treating samples with a specific drug that acts against the process of methylation, mainly by inactivating DNMT3a and finally, measuring gene expression again. Powerful arguments have been presented in the literature that supports direct experiments as being less ambiguous; additionally, because treatment is only possible in cell lines,

tissues are not appropriate for this purpose[26]. In spite of the existence of a large dataset that has revealed more than 80 genes downregulated by promoter methylation, to allow their clinical utilisation, the detected elements must be distinguished based on the number of primary tumour samples involved in the study and the frequency of positive results as eligibility criteria for diagnosis or to determine whether they are a candidate therapeutic target. Promoter hypermethylation of two molecules involved in the cell cycle, Ras association domain-containing protein 1 (*RASSF1A*) and the cyclin-dependent kinase inhibitor 2A-coding gene (*CDKN2A*), has been confirmed by multiple, substantive experiments; these findings have also been confirmed in melanoma cell lines[27-29]. A higher level of methylation of oestrogen receptor alpha (*ERα*) compared to normal tissues has also been revealed in both tumour specimens and cell lines[27,28]. Gaining 5-methyl-cytosines in the promoter regions of suppressor of cytokine signalling molecules (*SOCS1 and SOCS2*) has been demonstrated simultaneously with *MGMT*, which plays an essential role in DNA repair, and with *TIMP3*, which encodes a protein that protects the extracellular matrix from enzymatic degradation[30,31]. Downregulation of *RARB2* (retinoic acid receptor B2) has been validated in repeated studies: 6 groups have investigated the methylation level of the *RARB2* promoter, but their results are still inconsistent: some of these investigators have recorded high levels methylation in most of the examined specimens, while others have reported promoter methylation in only a few melanomas[27,31]. One of the most remarkable study concluded that *PTEN* methylation was a predictor for patient survival, even though it had not been associated with other clinical records[32].

In addition to the rapid progress that has been made in studying promoter hypermethylation at the single-gene level, only one group has attempted to conduct an array-based experiment, having chosen the most powerful and high-throughput bead array technology, to provide valuable information on the methylation pattern of the 1,505 gene promoter[26,33]. It is important to note that previous studies have given irrefutable proof of the reproducibility of this approach[34,35]. It is regrettable that researchers have focused on only comparing the methylation level of primary invasive melanomas with benign melanocytes; therefore, no data are available on the methylation markers of diverse melanomas with different clinical behaviours. However, the findings of these investigators support the claim that a covalent change from cytosine to 5-methyl-cytosine in the promoter region occurs as an early aberration event in melanomas. The group's results have clearly identified a group of genes in a statistically powerful interpretation that can be used to discriminate nevi from melanomas considering their methylation signature[26]. Furthermore, they adapted this high-throughput

methylation profiling to FFPE samples, which are generally prepared by pathologists, abundantly available and appropriate for further routine screening.

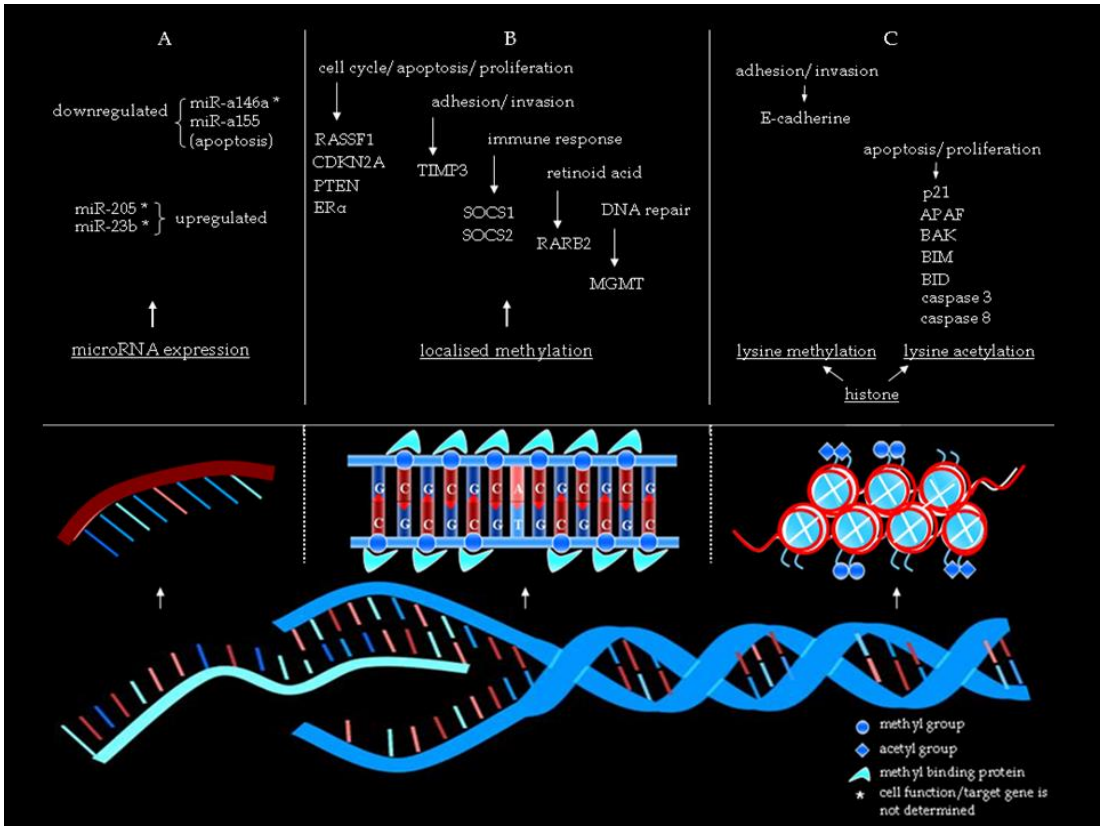

Figure 3 Main regulatory elements and pathways involved in epigenetic mechanisms in melanoma. ***(A)*** *MicroRNA regulation at post-transcriptional level results in decreasing in gene expression.* ***(B)*** *Localised methylation occurring at the promoter regions attracts methyl-CpG-binding proteins to construct transcriptionally silent heterochromatin and cause direct downregulation of genes involved in various pathways. C: histone post-transcriptional modifications alter gene expression of invasion and proliferation related molecules. (Balazs et al. 2011)*

Genome-wide hypomethylation

While most groups are studying extensively promoter-related hypermethylation, the importance of genome-wide demethylation or hypomethylation remains underestimated. However, these phenomena might also reflect important epigenetic alterations due to their ability to cause genetic instability[36]. Genome-wide hypomethylation is characterised by the overall loss of 5-methyl-cytosines, which is believed to correspond to the loss of methylcytosines of repetitive transposable elements. During evolution, these elements integrated into the human genome and became protected from transcription due to their higher levels of methylcytosines. Considering the abundance of repetitive elements, it is clear why scientists generalise the loss of their 5-methyl-cytosine content to the 'whole genome'. Repetitive elements constitute 40% of the human genome and mainly consist of two different

types: among *SINE* (short interspersed nucleotide element) sequences, only the Alu family is known, ranging from 400 to 500 bp, and it can be found in 10^5 copies across the human genome; *LINE* (long interspersed nucleotide element) sequences are longer than 5000 to 6000 bp, and 10^4 copies of these elements are spread throughout the genome[36-38].

Investigations of demethylation in carcinogenesis have raised a crucial question: how can genome-wide hypomethylation contribute to genetic instability? As described above, the overall loss of 5-methyl-cytosines can be explained by the modification of repetitive elements exhibiting strong homology. As these elements are reactivated by hypomethylation, they can recombine with each other, causing karyotypic instability[37,38].

The cause of their demethylation remains in question, as current evidence is divided between two hypotheses: hypomethylation could be an important early cancer-causing aberration, or it might occur as a passive inconsequential side effect of carcinogenesis. Both theories have gathered supporting data. Based on animal experiments, DNMTs have a higher affinity for recognising and affecting damaged DNA; therefore, their normal function of maintaining methylation patterns during replication might fail, suggesting passive demethylation as a subsequent genetic alteration. For many years, it has been hypothesised that indirect proof of active demethylation is provided by the imprinting of gametes and early embryos, which undergo massive epigenetic reprogramming involving demethylation followed by remethylation[39]. Regrettably, studies on melanomas have been unable to give evidence of active demethylation. However, results from breast cancer studies are promising: oestrogen receptor-alpha-responsive genes show remarkable demethylation followed by remethylation under the influence of oestrogen treatment[39]. These encouraging results might prompt scientists to extend their experiments to investigate the active demethylation of *ERα*-responsive elements in melanoma cell lines. As previous studies in melanoma have detected promoter hypermethylation of *ERα,* suggesting an important role of *ERα* epigenetics, in addition to hypermethylation, *ERα* might provide a significant contribution to the field of active demethylation[39].

To date the existence of genome-wide hypermethylation has been demonstrated in 16 melanoma cell lines compared to melanocytes via repetitive elements[40]. We are unable to conclude what the actual clinical effects of genome-wide methylation as the above-mentioned study focused only on comparing cell lines to controls, instead of drawing a demethylation-based distinction between cell lines with different characteristics. However, aberrant hypomethylation may be the best marker for early diagnosis, as the results of a number of studies agree on the relevance of *LINE* hypomethylation in both cell lines and tissues[29,41,42].

It is important to note that single-copy DNA regions can also feature hypomethylation, accompanied by mRNA and protein upregulation, as has been shown in colorectal, hepatocellular and breast cancers, although there is currently limited evidence to suggest the same characteristics for melanomas[43-47].

Notably, microRNA gene regulation and a limited number of histone modifications were also described in melanomas. Figure 2 summarizes the most important DNA methylation changes along with the other common epigenetic alterations published in melanomas[48-51].

A novel form of DNA methylation

In the early 1970s Penn et al. described 5-hydroxy-methylcytosine (5-hm-C),a novel form of DNA methylation[52], however, scientists were unable to reproduce their experiments and the 5hmC received scant attention over three decades. In 2009, Kriaucionis and Tahiliani rediscovered the 5-hm-C as novel epigenetic mechanism known as the sixth base of the DNA [53,54]. It was reported that Ten-eleven translocation (Tet) family proteins are responsible for the conversion of 5-m-C into 5-hm-C by oxidation in mammalian cells[55]. The new phenomenon has since been described at substantial amount in other mammalian tissues and studies are now under way to give functional relevance for 5-hm-C[56,57]. Regarding carcinogenesis and tumour progression, interesting clues to the role of 5-hydroxymethylcytosine are still emerging in most types of malignant diseases. Although a single remarkable study by Lian et al examined extensively this new epigenetic mark and gained strong evidence of 5hmC loss in melanoma tissues[14].

Further studies are warranted to investigate the distribution of 5-hm-C along with the timing and dynamics of the conversion of 5-m-C into 5-hm-C. More detailed descriptions of the sixth base can indicate new strategies for epigenetic therapy.

The role of DNA methylation in tumour diagnosis and therapy

Because DNA methylation is described as a reversible mechanism, inhibition of promoter hypermethylation might represent the most promising therapeutic target for the treatment of malignant diseases such as melanoma. DNMT inhibitors are compounds that are able to demethylate 5-methyl-cytosines by the direct obstruction of DNMT enzymes. To date, 3 types of DNMT inhibitors have been characterised:

1. Nucleoside analogues were the first of these inhibitors to be developed and include 5-azacitidine (Vidaza)[58] and 5-aza-2'-deoxycytidine (Decitabin)[59]. The common feature of these two drugs is their incorporation into DNA strands; because they contain an amino group instead of carbon at the 5 position of cytosine, they cannot be methylated[58]. Currently, both molecules are undergoing phase I or phase II clinical trials in several types of solid tumours[60]. In patients with advanced or metastatic cutaneous melanoma, these drugs are administered in combination with either interferon α-2b or temozolomide[61]. Zebularine, a new type of DNMT inhibitor introduced in 2003, is a less toxic agent compared to others because it does not contain an amino group[62-64]. It was demonstrated that Zebularine can inhibit colon cancer tumourigenesis[65].
2. Non-nucleoside analogue DNMT inhibitors currently include procainamide and procaine[66]. However, there are no data available related to their effect on melanoma.
3. Antisense oligonucleotides that target the DNMT1 enzyme (DNMT1 ASO) are currently undergoing clinical drug testing[66-68].

There is ample evidence for the direct influence of polyphenols on gene expression through several epigenetic pathways such as DNA methylation, chromatin remodelling or microRNA gene silencing[69,70]. Over the past few years, the term nutriepigenetics – the influence of bioactive food components on the epigenetic machinery – has emerged as an exciting new field in current epigenetic research[71]. Several dietary polyphenols was demonstrated to be able to inhibit DNMTs (mainly DNMT1) in cell cultures and animal models[72], hence, these active components offer a novel possibility for chemoprevention or even therapeutic interventions[73].
It is notable that efforts are now under way to develop methods to measure the methylation of genes in body fluids that are easy to obtain[74]. Additionally, it is firmly believed that the methylation pattern of a specific gene in cell-free DNA (serum or urine) should resemble the markings of that gene in tumour tissue. Regarding early diagnosis, this represents a rapidly growing field, and a blood test aimed at quantifying
suppressor genes has already been made commercially available for colon cancer samples. Similar attempts have also been made in melanomas: hypermethylation of *RASSF1A* in serum has been demonstrated, although 3 conflicting publications have reported that it occurs to a lesser (19%) or a greater (63%) extent in melanomas[27,31]. In serum, *CDKN2A* has also exhibited hypermethylation to a considerably higher level than in tumour tissues[28].
Because one of the most notable previous investigations demonstrated the prognostic relevance of *PTEN* methylation (as described above), studies were extended to quantify its

methylation pattern in serum. A significant correlation was found between the methylation level of tumour tissue specimens and blood serum. Moreover, *PTEN* methylation might function as an early event in carcinogenesis, rather than a progression-related mechanism, based on experiments that compared the methylation levels of tumours and melanocytes[75]. As it has been demonstrated that *PTEN* silencing is due to an epigenetic event[27], although it may have little impact on tumour progression, *PTEN* appears to be the most relevant candidate for the early diagnosis of melanoma by non-invasive tools.

Molecular classification of melanomas

During the last decade, microarrays have become the technology of choice for the selection of the genes responsible for the behaviour of malignant lesions. The technology has been extensively used in cancer research to identify tumour subclasses, predict disease outcomes and identify genes associated with drug resistance. The first molecular classification of malignant melanoma based on gene expression profiling was first described in 2000[76].

Many research groups have used different gene expression platforms to obtain a better understanding of the stepwise tumourigenesis involved in melanoma development. These studies have identified cohorts of genes that facilitate the distinction of benign nevi from malignant melanomas, sub-classification of metastatic melanomas into distinct subgroups and the prediction of distant metastasis-free survival.

One of the most remarkable study investigating 58 primary melanomas, described the relationship between the gene expression profiles and clinical outcomes and found 254 genes whose expression might have a role in predicting the clinical outcome of melanoma patients[77]. Global transcript profiling identified a signature characterised by decreased expression of lineage specification genes, including *MITF*, *EDNRB*, *DCT*, and *TYR*, and increased expression of genes involved in interactions with the extracellular environment, such as *PLAUR*, *VCAN*, and *HIF1a*.[78]

Migration assays showed that the gene expression signature was correlated with the invasive potential of the cell lines, and external validation using publicly available data indicated that tumours with the invasive gene signature were less melanocytic and might be more aggressive. It is significant that the invasion signature could be detected in both primary and metastatic tumours, suggesting that gene expression conferring increased invasive potential in melanoma may occur independently of tumour stage[78].

Several research groups have attempted to develop large gene classifier sets composed of several hundred or often thousands of genes. A critical analysis of gene expression studies relating to malignant melanoma progression was performed by Timár et al. in metastatic melanomas[79]. Despite the stunning success of genomics in defining genomic markers or gene signatures for breast cancer prognosis and for predicting therapies, there has been virtually no similar progress related to malignant melanoma. Microarray studies have been limited in utility because of the lack of concordance from one study to the next. Additionally, the investigated tumours may be heterogeneous even within a single study, containing limited numbers of primary melanomas or cutaneous, lymphatic or visceral metastases[80,81]. Furthermore, the biological behaviour and histological appearance of the tumours were not taken into account in some studies. Underlying the discrepancies in these data is the problem that the defined prognostic gene sets have not been validated in independent cohorts or datasets, with the exception of a few studies performed in primary tumours[77,82].

Studies applied integrative genomic approaches to describe altered genes with functional relevance are still limited[83,84]. Berger et al. applied a systematic genomic approach to characterise the spectrum of cancer-associated mRNA alterations through the integration of transcriptomic and structural genomic data has revealed new insights into melanoma biology and will likely lead to a new era of discovery in melanoma genomics that promises to reveal molecular mechanisms associated with the disease[83]. More than 700 non-synonymous coding variants have been identified. However, only a subset of these was validated to clarify whether they were bona fide somatic mutations. Based on the results described above, it is expected that most of these variants are inherited SNPs and that approximately 30% are somatic mutations[83]. The most interesting variants include a mutation observed in the melanoma cell line 501 Mel (*CTNNB1, chr3:41241117, C/T*), which was noted 135 times in the COSMIC database of somatic mutations in cancer. A new approach, paired-end massively parallel sequencing of cDNA, together with analyses of high-resolution chromosomal copy number data was used, as a result 11 novel melanoma gene fusions was identified, that produced by underlying genomic rearrangements and 12 novel read-through transcripts. These chimeric transcripts were mapped at base-pair resolution and traced to their genomic origins using matched chromosomal copy number information[83]. Furthermore, these data were used to discover and validate base-pair mutations that accumulated in these melanomas, revealing a surprisingly high rate of somatic mutations and lending support to the notion that point mutations constitute the major driver of melanoma progression.

Driver mutations and DNA copy number alterations in melanomas

Comparative genomic hybridisation represents the best approach for searching for DNA sequence copy number alterations in cancer genomes. Improvement of the resolution and sensitivity of CGH during the last decade has allowed the discovery of recurrent copy number alterations and new genetic targets in different cancer types, including malignant melanoma[85]. Although chromosomal and array CGH have revealed a large number of common non-random alterations, no obvious or validated melanoma-relevant molecular targets have yet been identified[85]. The non-random nature of melanoma-specific copy number alterations may allow the segregation of melanomas into subtypes based on distinct clinical and biological behaviours.

Chromosome copy number alterations and the mutational status of the *BRAF* and *NRAS* genes were compared in 126 primary melanomas by Curtin et al., and melanoma tissue samples were grouped based on their degree of exposure to ultraviolet light[86]. The four types of melanoma included in these groupings were as follows: acral melanoma (melanoma occurring on the non-hair-bearing skin of the palms or soles), mucosal melanoma (tumours arising on mucosal membranes), tumours arisen from skin with chronic sun-induced damage and lesions arisen from skin without chronic sun-induced damage[86]. Melanomas without chronic sun-induced damage frequently showed mutations in the *BRAF* oncogene, together with losses of chromosome 10q (site of *PTEN*), or mutations in the *NRAS* gene alone. In contrast, melanomas arising from skin with chronic sun-induced damage (mucosal and acral melanomas) did not exhibit *BRAF* or *NRAS* mutations but instead displayed an increased number of copies of the *CCND1* or *CDK4* genes[86]. The different genetic alterations identified in different anatomical sites of the skin and with varying levels of ultraviolet exposure indicate that several molecular pathways are involved in the development and progression of the disease[86]. Our group published the frequent amplification of the 11q13 region harbouring the *CCND1* gene along with other candidate genes that reside in the 11q13 amplicon core. Amplification of 11q13 region was associated with unfavourable outcomes of melanomas[87,88].

A systematic analysis of the melanoma genome led to the discovery of a new lineage survival oncogene, *MITF* (3p14), which is amplified or shows copy number gains in 10% of primary and 15% to 20% of metastatic melanomas[89]. Based on FISH analysis, the *MITF* copy number fluctuates between 4 and 13 copies per cell. However, no amplification can be detected in nevi samples. Comparing *MITF* copy number alterations and clinical parameters, it was found that patients presenting tissue carrying the amplified gene exhibited survival of less than five

years. A similar correlation was seen for MITF protein expression, which implicates *MITF* gene amplification in the progression and lethality of a subset of melanomas[90]. It was clearly demonstrated that *MITF* plays a crucial role in melanocyte biology and melanoma progression and potentially acts as a dominant oncogene[90]. *MITF* regulates the expression of a large variety of genes, including genes involved in pigmentation, cell cycle regulation, differentiation, survival and migration. Targeting MITF in combination with *BRAF* or cyclin-dependent kinase inhibitors may offer a rational therapeutic opportunity to successfully treat this aggressive, chemoresistant disease[91].

The discovery of new targets by array CGH was also reported by Gast et al.[92]. In this study, SNP arrays with 250,000 targets were applied to 60 cell lines derived from metastasised melanomas. Amplifications were found to be more common than deletions in these cell lines. Similar to the findings of other studies, homozygous and heterozygous deletions of the *CDKN2A* gene were the most frequent type of deletion found at the 9p21 locus, and these alterations were associated with a lack of gene expression[92]. In addition to the common alterations described above, it was observed that melanoma cell lines without *BRAF* and *NRAS* oncogenic mutations exhibited losses of the entire 13q and 16q chromosome regions[92]. These data further confirm that distinct molecular pathways are involved in malignant melanomas, driving melanoma initiation and progression in association with either oncogenic *BRAF* or *NRAS* mutations complemented mainly by the loss of tumour suppressor genes, including *CDKN2A* and *PTEN*[92].

Our group has already performed several experiments aiming at determining the copy number alterations of melanomas by candidate gene approaches as well as high-throughput microarray platforms. In line with the published data we demonstrated that primary melanomas with $BRAF^{V600E}$ mutations exhibit more frequent losses on 10q23-q26 and gains on chromosome 7 as well as 1q23-q25 genomic regions. Generally, we described marked differences in the genetic pattern of the *BRAF* and *NRAS* mutated subgroups[87,93].

A chromosome 6p gain is one of the most frequent alterations found in melanomas, as determined by CGH and classical cytogenetic studies. A novel melanoma metastasis gene on 6p25-p24 (*NEDD9*: neural precursor cell expressed, developmentally downregulated-9) showing recurrent focal amplification in 35% of human melanomas and melanoma cell lines was discovered by a cross-species comparison[94]. The expression of *NEDD9* is significantly upregulated relative to nontransformed melanocytes and benign melanocytic neoplasia, and this gene is overexpressed in 52% of melanomas, but only 14% of nevi. It was found that *NEDD9* amplification and overexpression were strongly associated with enhanced invasion

and metastasis formation related to malignant melanomas. The large regional gain on chromosome 6p and the high recurrence of the alteration likely indicate the presence and synergistic activities of multiple oncogenes on 6p, in addition to *NEDD9*[94]. The observation that more than 50% of human primary melanomas exhibit higher NEDD9 expression relative to benign nevi suggests the possibility that the amplification or overexpression of NEDD9 in a regional/focal manner may identify a subset of primary melanoma tumours with increased risk of metastasis[94].

Although epidemiological data have already established the role of intense UV exposure during melanoma development and several model systems have also linked UV-dependent tumourigenic effects to modulation of signalling pathways, the direct mutagenic role of UV exposure has remained controversial as the most recurrent base mutations (*BRAF* and *NRAS*) are not C>T (by UVB) and G>T (by UVA) transitions indicative of UV mutagenesis.

Using the same approach, known as exome capture new generation sequencing, on more than 100 melanoma samples, two independent research groups addressed the direct effect of UV-induced DNA damage as a cause of melanoma driver mutations[11,12]. The groups found more than 100,000 specific mutations in the sequenced specimens which are not present in the corresponding healthy tissue[11]. More than 80 per cent of described mutations were the result of pyrimidine dimers associated with UV exposure. Using permutations, the researchers successfully sorted driver mutations from passenger alterations and identified 262 driver mutations in 21 genes of which 46% were caused by C>T or G>T mutations[11,12].

Interestingly, *TP53* possessed the highest number of total putative UV-induced mutations among mutated melanoma genes identified by the study of Hodis et al.[11], which stands in contrast to the published data which often cites the wild-type status of TP53 as a characteristic melanomas. Besides the well-known melanoma tumour suppressors such as *PTEN*, *p14ARF and p16INK4a*), newly discovered genes (PPP6C, RAC1, SNX31, TACC1, STK19 and ARID2) were also found to be mutated and exhibited the C>T transitions[11,12].

Nearly one in ten sun-exposed tumours had the same specific UV-induced mutation patterns in the *RAC1* gene, indicating that the *RAC1* is the third most commonly mutated gene besides the *BRAF* and *NRAS*[11].

Hodis et al. also revealed that *BRAF* and *NRAS* mutations not being only the most frequent genetic alterations – arguing in favour of published data – also feature UVA- and UVB-induced damage to limited extent[11].

Figure 4 –adopted from Hodis et al. – summarizes the novel discoveries of exome sequencing providing definitive evidence for UV mutagenesis in melanoma pathogenesis[11].

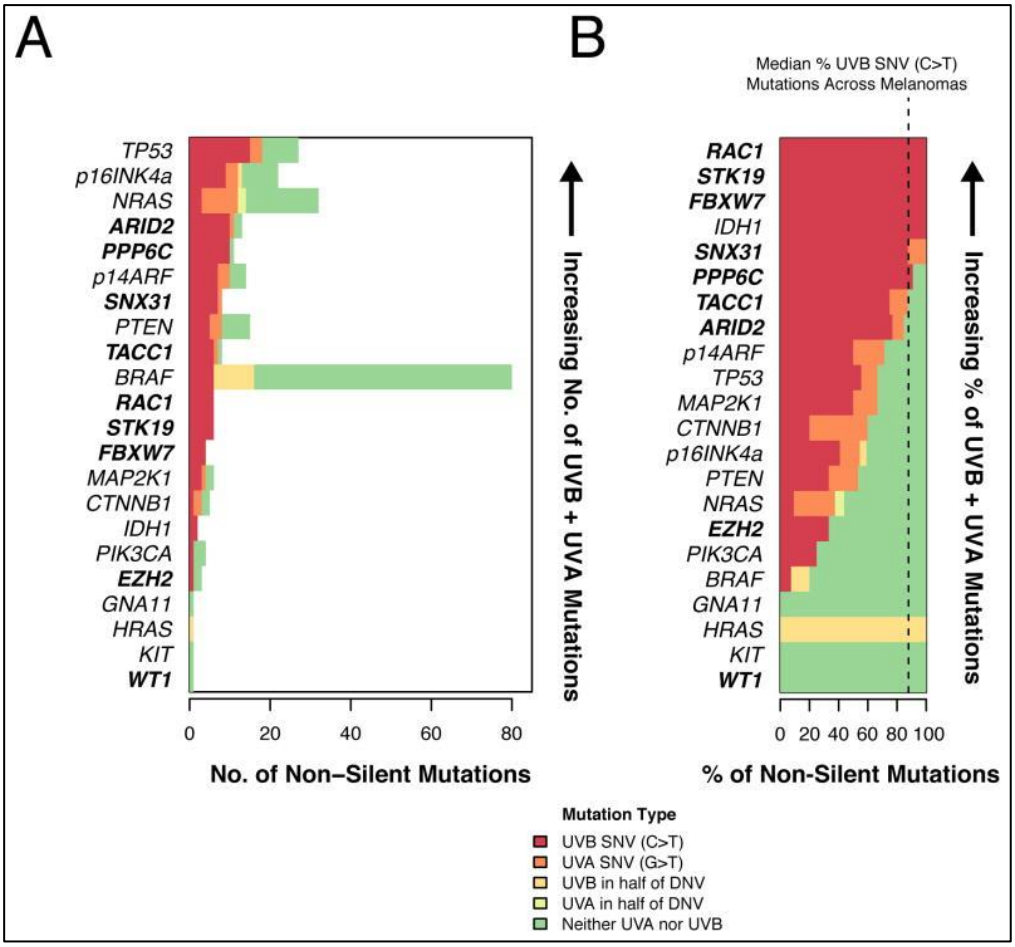

Figure 4 Signature of UV mutagenesis across driver mutations.

(A) *Total number and* ***(B)*** *% of driver mutations caused by UVB single nucleotide variant (SNV) (C>T), UVA SNV (G>T), UVB in half of dinucleotide variant (DNV) (NC>NT; CN>TN) and UVA in half of DNV (NG>NT; GN>TN) are indicated. Dotted line indicates exome-wide sample median % UVB SNV (C>T). The figure was published by Hodis et al. in 2012.*[11]

Objectives

In an effort to further advance our understanding of the relationship between primary malignant melanoma progression and the distinct forms of somatic DNA alterations including multiple epigenetic changes, copy number alterations and the well-known mutations such as *BRAF*^{V600E}, the specific objectives of the recent study were the followings:

1. **Investigating of transposable DNA methylation:**
   - to assess global DNA methylation status of a set of primary melanomas with different biologic behavior by investigating the methylation level on the 6 CpG sites of transposable *LINE 1* promoter sequences using Na-bisulphite pyrosequencing.
   - to correlate the global methylation pattern with the survival data of melanoma patients and the clinical-pathological parameters of primary tumours.

2. **Studying of regional methylation patterns over cancer related genes:**
   - to draw DNA methylation-based distinction among diverse melanoma subtypes using a Bead Assay specific for more than 800 cancer related genes.
   - to investigate the relationship between DNA methylation patterns and distinct types of somatic alterations, including the most frequent mutations and DNA copy number changes.

3. **Performing integrative genome approaches:**
   - to characterise genomic hotspots with functional relevance and define cis- and trans acting copy number alterations on a genome-wide scale that act in the establishment of disturbed gene expression pattern in primary melanomas.
   - to measure the correlation between gene expression and regional DNA methylation for genes that we had available DNA methylation profiling data.

Materials and Methods

Melanoma samples and nucleic acid extraction

Forty-six primary melanomas were involved in our studies altogether. Tumour tissues were obtained from the Department of Dermatology, University of Debrecen, Hungary. All human studies were conducted in accordance with principles outlined in the Declaration of Helsinki and were approved by the Regional and Institutional Ethics Committee of the University of Debrecen Medical and Health Science Centre and was conducted according to regulations (Protocol #2836-2008). Written informed consent was obtained from each patient. The clinicopathological data on primary melanoma specimens are summarised in Table 1 according to the new melanoma TNM staging system[95].

High-quality total RNA was prepared from primary melanoma tissues using the RNeasy Mini kit according to the protocol of the supplier (Qiagen, GmbH, Germany). The obtained RNA concentrations were measured using a NanoDrop ND-1000 UV-Vis Spectrophotometer (NanoDrop Technologies, Wilmington, Delaware, USA). RNA sample integrity was determined with the Agilent 2100 Bioanalyser using the RNA 6000 Nano Kit (Agilent Technologies, Palo Alto, CA, USA). All RNA samples exhibited a 28S/18S ribosomal RNA ratio greater than 1.5.

The G-spin™ Genomic DNA Extraction Kit (Intron, Korea) was used to isolate high molecular weight DNA samples from primary melanomas according to the protocol provided by the manufacturer. To determine the quantity of DNA obtained, we used a NanoDrop ND-1000 UV-Vis Spectrophotometer (NanoDrop Technologies, Wilmington, Delaware USA). DNA integrity was verified via 1.2% agarose gel electrophoresis.

Na-bisulphite treatment of genomic DNA samples

Bisulphite conversion involves the exposure of DNA to high temperature and as well as harsh pH conditions, which may result in heavy losses of the DNA by fragmentation and degradation[96]. Recently, multiple commercial kits provided improvements in terms of efficiency (over 99% conversion) and reduction of DNA degradation. In general, these kits are superior to the classical conversion protocols based on generic ingredients, providing greater consistency and lower overall degradation during the reaction[97].

Table 1 ***Clinicopathological data on primary melanoma specimens***

Variables	No. of tumours detected by applied approaches for:		
	Transposable DNA methylation	**Regional DNA methylation**	**Comparative Genome Hybridization**
All patients	**46***	**42**	**26**
Histological subtype			
Superficial spreading	30	26	15
Nodular	16	16	11
Gender			
Female	24	20	11
Male	22	22	15
Age (years)			
20-50	14	14	9
≥50	32	28	17
Breslow thickness (mm)[1]			
< 2	18	15	7
2 – 4	12	11	7
> 4	16	16	12
Location of primary tumour			
Extremity	25	21	11
Trunk	20	20	14
Head	1	1	1
Metastasis formation[2]			
Absent	24	20	13
Present	22	22	13
Patient's survival[3]			
Alive	24	21	17
Death	22	21	9
Ulceration			
Absent	24	20	8
Present	22	22	18
***BRAF*^{V600E} mutation[3]**			
mutant	12	12	11
wild type	24	24	12

**Altogether n=46 genomic DNA samples were involved in our studies. 42 out of the 46 samples took part in the "Regional DNA methylation analysis"; array CGH experiments were done in 26 out of the 46 specimens from which 17 overlapped with our previous gene expression studies.*
[1]thickness categories are based on the current staging system; [2]metastasis of the examined primary tumours; [3]patients with at least 5-year follow-up period were included; BRAF^{V600E} mutational status of primary melanomas were determined previously by our group (Lazar et. al. 2012.)

We applied the EZ DNA Methylation-Gold kit (Zymo Research) for bisulfite conversion of DNA samples prepared from primary melanoma samples. The conversion reactions were carried out according to manufacturer's protocol. Bisulphite conversion was carried out in a thermal cycler at 98 °C for 10 min and then at 64 °C for 2.5 hours. The remaining steps including binding, washing and desulphonation and elution were done according to the protocol of the manufacturer. Converted DNA samples were immediately used for Na-bisulphite pyrosequencing (see below).

Na-bisulphite pyrosequencing

Pyrosequencing is the first alternative to the conventional Sanger method for *de novo* DNA sequencing. Pyrosequencing technique is based on sequencing by synthesis and on the detection of released pyrophosphate (PPi) during DNA synthesis[98]. It employs a series of four enzymes to accurately detect nucleic acid sequences during the synthesis. In Pyrosequencing the sequencing primer is hybridized to a single-stranded DNA biotin-labeled template and mixed with the enzymes; DNA polymerase, ATP sulfurylase, luciferase, apyrase, and the substrates adenosine 5′ phosphosulfate (APS) and luciferin. Cycles of four deoxynucleotide-triphosphates (dNTPs) are separately added to the reaction mixture iteratively[99]. The cascade starts with a nucleic acid polymerization reaction in which inorganic PPi is released as a result of nucleotide incorporation by polymerase. Each nucleotide incorporation event is followed by release of inorganic pyrophosphate (PPi) in a quantity equimolar to the amount of incorporated nucleotide. The released PPi is quantitatively converted to ATP by ATP sulfurylase in the presence of APS. The generated ATP drives the luciferase-mediated conversion of luciferin to oxyluciferin, producing visible light in amounts that are proportional to the amount of ATPs. The light in the luciferase-catalyzed reaction with a maximum of 560 nanometer wavelength is then detected by a photon detection device such as a charge coupled device (CCD) camera or photomultiplier. Apyrase is a nucleotide-degrading enzyme, which continuously degrades ATP and non-incorporated dNTPs in the reaction mixture[98]. There is a certain time interval between each nucleotide dispensation to allow complete degradation. For this reason, dNTP addition is performed one at a time. Because the added nucleotide is known, the sequence of the template can be determined. The generated light is observed as a peak signal in the pyrogram (corresponding to electropherogram in dideoxy sequencing) proportional to the number of nucleotides incorporated[100].

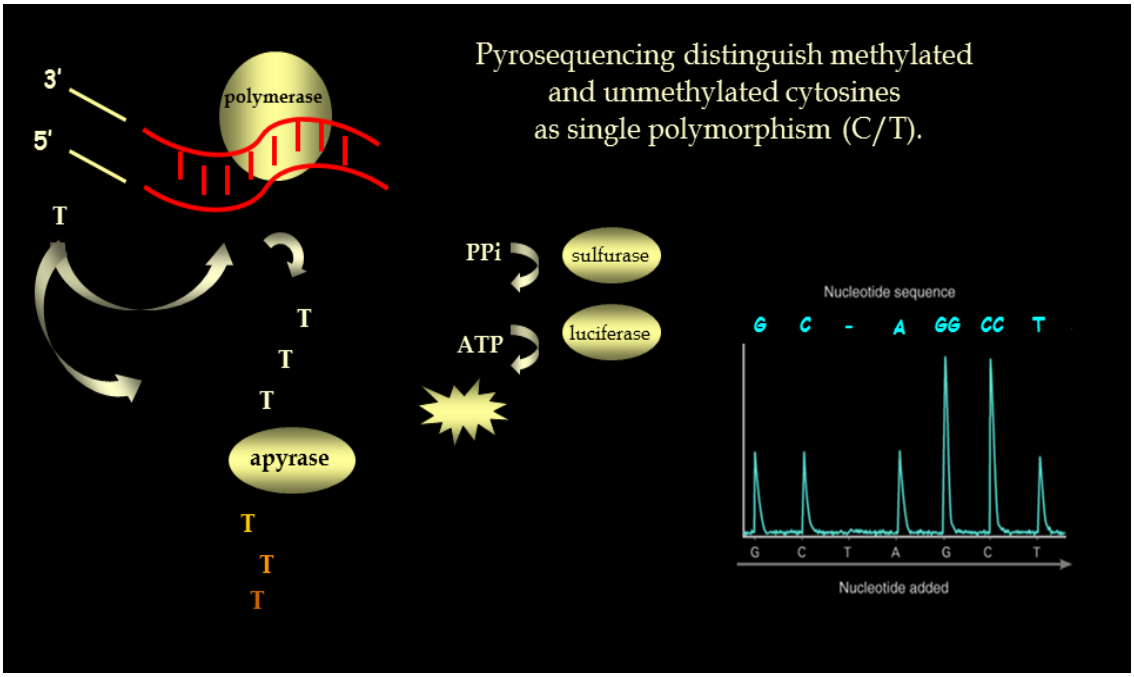

Figure 5 Schematic representation of pyrosequencing method (previously unpublished figure)

A schematic representation of pyrosequencing is shown in Figure 5. To quantify the percentage of methylated cytosine at 6 individual CpG sites of *LINE 1* promoter sequence, bisulphite-converted DNA was subsequently pyrosequenced using a pyrosequencing system (PSQ 96MA, Biotage). This method treats each individual CpG site as a C/T polymorphism and generates quantitative data for the relative proportion of the methylated versus the unmethylated allele. Hot-start PCR was performed using the HotStarTaq Master Mix Kit (Qiagen), and the pyrosequencing was carried out in accordance with the manufacturer's protocol (Biotage).

The following primers were applied:

- sense primer: 5'-BIOTIN-TAGGGAGTGTTAGATAGTGG
- antisense primer: 5'-AACTCCCTAACCCCTTAC
- sequencing primer: 5' AACTCCCTAACCCCTTAC.

The following sequence containing 6 unique CpG sites was analysed: 5'-**R**CCCTACTTC**R**ACTC**R**C**R**CAC**R**ATAC**R**.

The biotinylated strand of the target was captured on streptavidin-coated Sepharose beads, which are retained on the filter plate while the non-biotinylated strand is washed off under denaturing conditions. A sequencing primer is annealed to the template strand for the pyrosequencing reaction, in which the incorporation of nucleotides complementary to a template strand is monitored bioluminometrically. The intensity of the bioluminometric

responses are directly proportional to the amount of incorporated nucleotides and are termed as pyrograms, a representation of the complete synthesis reaction. The targeted CpGs for the *LINE1* are evaluated for individual sample by converting the resulting pyrograms to numerical values for peak heights using Q-CpG software (Biotage).

Bead Assay experiments

The quantitative methylation status of the 1,505 CpG sites corresponding to 807 cancer-related genes (mainly at the promoter regions) was determined using the Illumina GoldenGate Methylation Assay (Illumina, San Diego, CA, USA)[101] on bisulphite-treated DNA samples corresponding to 42 primary melanomas. Bisulphite treatment was performed as indicated before. This technology utilizes 3 μm silica beads which are replicated ~30 times on the array and has emerged as an attractive platform for genotyping, expression and methylation analysis[102]. The main steps of bead assay experiments are summarized in Figure 6.

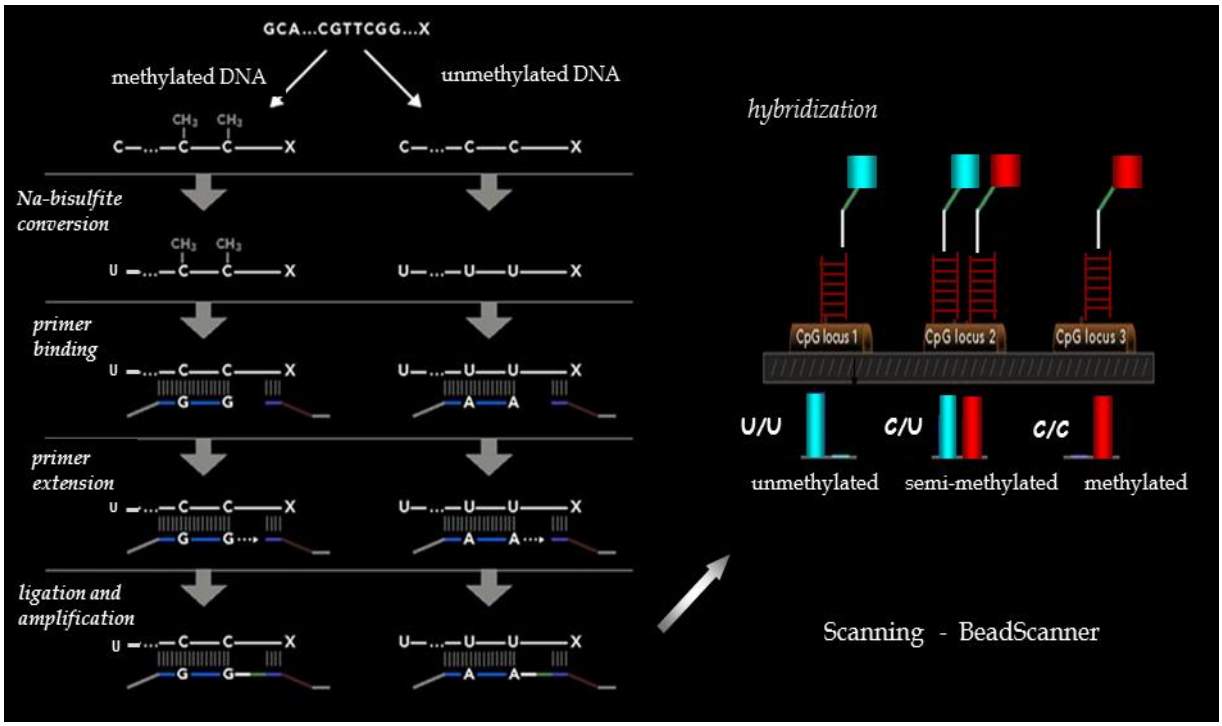

Figure 6 Schematic representation of Illumina Methylation Bead Assay
Na-bisulphite-treated genomic DNA is mixed with assay oligos (ASOs). Each ASO is complimentary to either the converted U (unmethylated site) or the protected C (methylated site). Following hybridization, primers are extended and ligated to the LSO creating a template for universal PCR. Labelled PCR primers are used to create a detectable product. Individual assays localize to specific bead types on the SAM by hybridization of address sequences. Source: www.illumina.com

Methylation levels in Illumina methylation assays are quantified by the signal values (*Avg-beta*) using the ratio of intensities between methylated (*M*) and unmethylated (*U*) alleles. BeadStudio v3.2 Software (Illumina, San Diego, CA, USA) was used to obtain the the Avg-Beta values[101].

In agreement with the literature, 83 probes corresponding to the sex chromosomes were excluded to avoid any sex-specific bias[34,101]. The probes with detection P values exceeding 0.01 in more than 10% of the specimens were removed from the analyses to exclude non-biological differences. Therefore, 895 CpG probes remained for further analyses and M-values, the logistically transformed Avg-Beta values were used for statistical approaches. Using the M-values was first introduced by Du et al. to overcome the heteroscedasticity observed in Avg-Beta values[103].

Two duplicate samples were included to measure inter-array reproducibility for quality control (Figure 7).

Subsequent statistical analyses were done by BRB Array Tools developed by Dr. Richard Simon and BRB-Array Tools Development Team. All applied statistical approached are detailed in 'Statistical analyses' section.

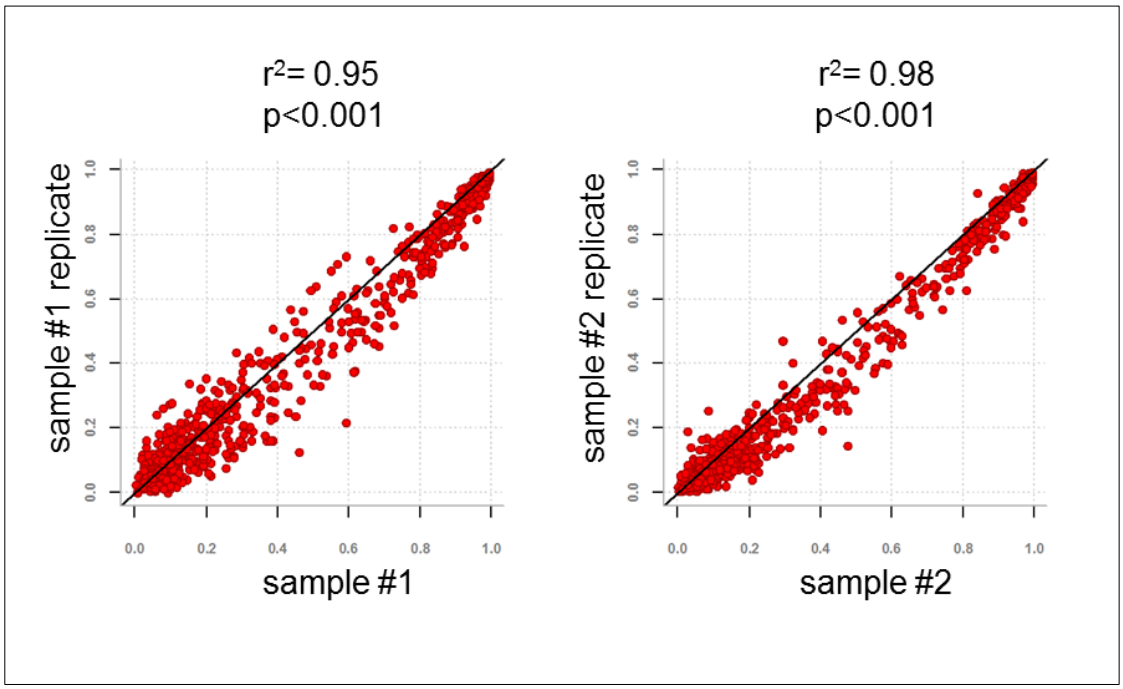

Figure 7 Pearson's correlation plots of technical replicates included among bead assay samples used for quality controls

Array Comparative Genome Hybridization

Tiling Array CGH (HG18 CGH 4x72K WG Tiling v2.0) experiments were done at Roche NimbleGen core facility, Reykjavik, Iceland. Data can be found under the following accession number: E-MTAB-947 at the Array Express Archive repository.

Array CGH results were analysed by Nexus 5.1 Copy Number Software (BioDiscovery, CA, USA). The GISTIC algorithm was used to identify regions containing a statistically high frequency of copy number aberrations compared to the "background" aberration frequency. This function is most appropriate for cancer samples, as it was designed using a cancer dataset. After the gain/loss aberrations were identified in each sample, a statistic (the G score) was calculated for each aberration. This G score is a measure of the frequency of occurrence of the aberration and the magnitude of the copy number change (log ratio intensity) at each location in the aggregate of all samples in the dataset[104]. Each location is scored separately for gains and losses. The locations in each sample are permuted, simulating data with random aberrations, and this random distribution is compared to the observed statistic to identify scores that are unlikely to occur by chance alone[104]. Figure 8 depicts the steps of array CGH technique.

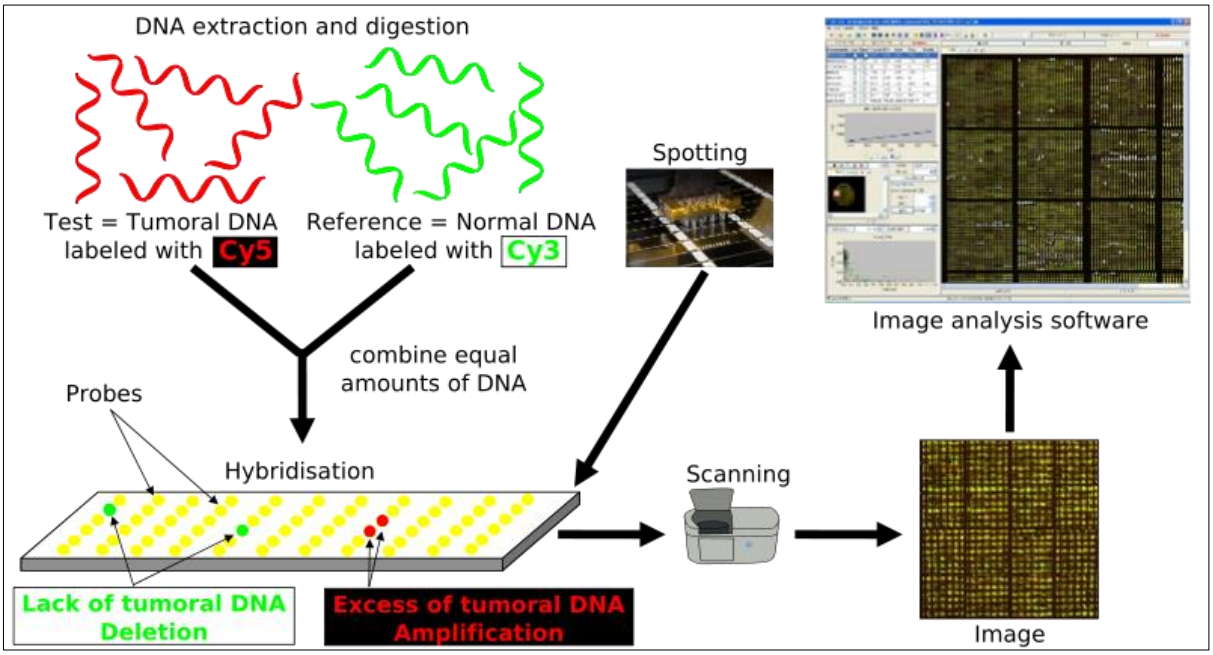

Figure 8 ***Representation of array Comparative Genome Hybridization workflow***
source:www.agilent.com

Fluorescence in situ hybridization and microscopic evaluation

FISH experiments were performed on touch preparations made from different subtypes of primary malignant melanoma samples. The tumours were mounted onto Superfrost Plus positively charged slides, submersed in 2x saline-sodium citrate (SSC) pH 7,00 at 37°C for 30 min and passed through graded ethanol and dried. Hybridization was performed using 3,5 ul of the multicolour FISH probe per slide at 37°C for 16-18h in an automated denaturation chamber according to the instructions of the manufacturer (Abbott Molecular Inc., USA). Multicolour FISH probe were specific for *RREB1* (Spectrum Red, red fluorescence) *MYB* (Spectrum Gold, yellow fluorescence) and *CCND1* genes (Spectrum Green, green fluorescence) and centromere region of chromosome 6 (Spectrum Aqua, blue fluorescence).
Slides were immersed in hybridization wash buffer at 45°C for 30 min, then placed in 2XSSC for 10 min at the same temperature, repeated the step before at room temperature for 10 min, rinsed in water for 10 min, dried and mounted with DAPI-free antifade solution.
Slides were evaluated with a Zeiss Axio Imager Confocal Microscope, equipped with Spectrum Red, Spectrum Gold, Spectrum Green and Spectrum Aqua single-band pass filter sets. A minimum of 30 cells were enumerated in different areas of the lesion. The lesion was considered positively if any of the following criteria were met:

i.) gain in 6p25 (*RREB1*) relative to CEP6 greater than 55%.
ii.) gain in 6p25 (*RREB1*) greater than 29%.
iii.) loss of 6q23 (*MYB*) relative to CEP6 greater than 40%.
iv.) gain in 11q13 (*CCND1*) greater than 38%.

Quantitative RT-PCR

The expression status of selected genes (FGFR3, MCAM and IL8) was measured using quantitative real-time PCR (QRT-PCR) with the ABI Prism® 7900HT Sequence Detection System (Applied Biosystems, Carlsbad, California, USA). Reverse transcription (RT) was carried out on total RNA (600 ng) using the High Capacity cDNA Archive Kit, according to the protocol of the supplier (Applied Biosystems, Carlsbad, California, USA). Predesigned TaqMan® Gene Expression Assays (Life Technologies Corporation, Carlsbad, CA, USA) were used to perform QRP-PCR for the abovementioned 3 genes. QRT-PCR data were analyzed using the Livak method ($2^{-\Delta\Delta Ct}$), with glyceraldehyde-3-phosphate dehydrogenase as the reference (endogenous control) gene and nevi collected from three different individuals and melanocyte as calibrator samples.

Statistical analyses

Analysis of transposable methylation pattern

To estimate the effect of the *LINE 1* methylation status on patient survival, the *LINE 1* methylation level represented by continuous variables was dichotomised at its cut-off value determined for each CpG site by the Receiver Operating Characteristic (ROC) curve analysis in which the true positive rate (Sensitivity) is plotted in function of the false positive rate (100-Specificity) for different cut-off points of a parameter. Each point on the ROC curve represents a sensitivity/specificity pair corresponding to a particular decision threshold[105]. The area under the ROC curve (AUC) is a measure of how well a parameter can distinguish between the hypomethylated and non-hypomethylated groups. As demonstrated in Figure 9, the threshold levels according to the ROC analysis were the following: CpG_1 (55.5), CpG_2 (63.1), CpG_3 (45.8), CpG_4 (55.8), CpG_5 (83.6) and CpG_6 (61.6).

Kaplan-Meier survival probability curve was constructed for the dichotomised clinical groups using the log-rank test to examine the difference in survival by *LINE 1* methylation level.

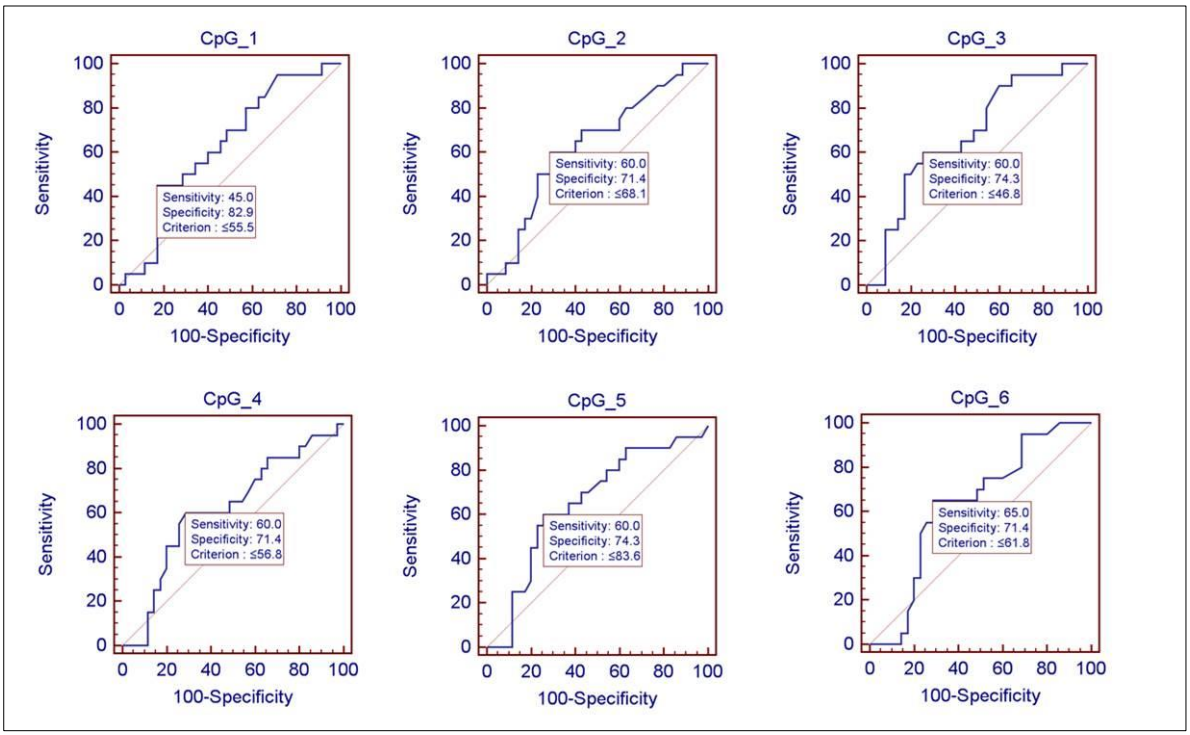

Figure 9 Threshold levels of LINE1 methylation values for each CpG was determined by ROC analysis

The clinical parameters including patient age and gender, Breslow thickness, Clark level, histological subtype, metastasis formation during the 5-year follow up period and tumour surface ulceration were examined by the Cox proportional hazards regression model, and the effect of hypomethylation on the survival was presented as hazard ratios (HR) with corresponding 95% confidence intervals (CI). To control for the above-noted additional confounders, a stepwise regression was applied to select variables.

As the initial D'Agostino and Pearson omnibus normality test revealed that *LINE 1* methylation values do not follow the Gaussian distribution, we used the nonparametric Mann Whitney and Kruskal-Wallis tests with Dunn's Multiple Comparison Post-test to establish a connection between the *LINE 1* methylation status and clinical parameters.

Analysis of regional methylation pattern

To compare the methylation patterns between primary melanoma groups detailed in Table 1, we applied random variance t-statistics on all the binary data classes such as Breslow thickness with the cut-off value of 4 mm; metastasis, ulceration and histologic subtype. Being continuous variable, Breslow thickness can be divided into more subgroups: according to the TNM system up to 5 groups can be created, however, due to the limitation of smaller samples, developing 3 groups based on the cut-off values of 2mm and 4mm were the most ideal. F-statistics was applied on the trichotomised Breslow groups for each CpG site.

CpG sites were considered differentially methylated when their p values based on univariate t-tests or f-tests were less than 0.01; in addition, given CpG sites were identified differentially methylated between the melanoma subgroups based on a multivariate permutation test providing 90% confidence that the false discovery rate was less than 20%. Volcano plots were applied to illustrate differential methylation patterns among clinical subgroups of melanomas (the clinicopathological characteristics of melanomas are summarized in Table 1). Volcano plots combine p-values of the t-tests for each CpG sites and ratios between the melanoma subgroups. Additionally, the trichotomised Breslow thickness groups were visualized by heatmap and compared by Principal Component Analysis (PCA).

For the aforementioned class comparisons, M-values, the logit transformations of signal intensities were used.

To evaluate the KEGG-based gene networks disturbed by DNA methylation, we applied the Efron-Tibshirani Gene Set Analysis that uses 'maxmean' statistics to identify gene sets expressed differentially among predefined classe. The threshold for determining significant gene sets was 0.01 in each approach.

The Cox proportional univariate approach was performed on each gene to test whether the methylation status of a particular gene significantly influences the survival at the $p< 0.05$ level. To control for covariates on survival and to predict the survival risk, the Supervised Principal Components method was used.

As normal tissues were not involved in or studies, we used external dataset from the study of Conway et al. involved 27 naevi to check the methylation status of a given gene in control tissues[26].

Remaining statistics were performed using SPSS 19.0 and GraphPad Prism 6.0 demo version. Venn diagram was made by VENNY, an interactive tool for comparing lists with Venn Diagrams developed by Oliveros, J.C. (2007). The tool is available at: http://bioinfogp.cnb.csic.es/tools/venny/index.html

Integrative genome analyses

To study the relationship between DNA copy number gains/losses and mRNA levels, we exported the median of the replicate probe $\log_2$ ratios and the expression values corresponding to the same genomic region for determining Pearson's correlation. The genelist generated through this analysis was imported to the Nexus 5.1 package (BioDiscovery, CA, USA). We assessed the genomic locations that exhibited significant copy number losses and concentrations of downregulated genes simultaneously. The statistics-generated P value was based on the number of deregulated transcripts located in significantly deleted genomic regions after multiple testing corrections.

In order to verify cis-acting and identify trans-acting CNVs, we performed an L1-constrained regression (Lasso-regression) on the important genes that was identified previously. This method assumes that the predictor variables are independent, so first we implemented a dimensionality reduction using the „CGHregions" R package[106]. This algorithm results in CNV regions, in which the clones are very much alike, with minimal information loss. The L1-constrained regression was performed with the „lol" R package using cross-validation optimizer. The resulted significant CNV regions were identified as cis-acting elements if they were on the same chromosome or were closer than 50 Mb to the investigated gene and as trans-acting elements otherwise. We assessed the score, which represents dependency of the response variable from the predictors, using the following equitation[106]:

$$score_i = -ln\left(\frac{\sigma^2_{with\ all}}{\sigma^2_{without\ all}}\right)$$

$$score_i^{cis} = -ln\left(\frac{\sigma^2_{with\ cis}}{\sigma^2_{without\ all}}\right)$$

$$score_i^{trans} = -ln\left(\frac{\sigma^2_{with\ cis} - \sigma^2_{with\ all}}{\sigma^2_{without\ all}}\right)$$

where:

$\sigma^2_{with\ all}$ represents the variance of the prediction residuals of the model with all significant predictors included

$\sigma^2_{with\ cis}$ represents the variance of the prediction residuals of the model with only the significant cis predictors included

$\sigma^2_{without\ all}$ represents the variance of the prediction residuals of the model without the significant predictors

To assess relation between gene expression and promoter methylation patterns, we applied Pearson's correlation for each of the 98 CpG sites corresponding to the 45 overlapping genes between the datasets.

We studied how DNA copy number changes and methylation pattern associated within the same genetic loci. For this purpose, the copy number and localised methylation data of the corresponding genomic regions were simultaneously analysed gene-by-gene using CGH Tools, and Pearson's correlation was performed with $p<0.01$ after correction for multiple testing. Additionally, Fisher's exact test was applied to identify the genome sequences where gene methylation occurs frequently.

Results

Transposable methylation patterns of primary melanomas

We quantitatively assessed the global DNA methylation patterns of 46 primary malignant melanomas with differing clinical characteristics (summarized in Table 1; Material and Methods) by measuring the methyl-cytosin content of the LINE 1 transposonal sequence. Six distinct CpG sites on the *LINE 1* transposonal DNA were measured by pyrosequencing. Not having demonstrated a Gaussian distribution by D'Agostino and Person omnibus normality test, the continuous variables of the *LINE 1* pyrosequencing results were dichotomised, and the binary groups were constructed using the threshold values determined by the ROC curve analysis demonstrated in Figure 10. The threshold levels were the following: CpG_1 (55.5), CpG_2 (63.1), CpG_3 (45.8), CpG_4 (55.8), CpG_5 (83.6) and CpG_6 (61.6).

The sample groups were defined as *LINE 1* hypomethylated (specimens with a *LINE 1* methylation <threshold value) and non-hypomethylated (samples with a *LINE 1* methylation ≥ threshold value).

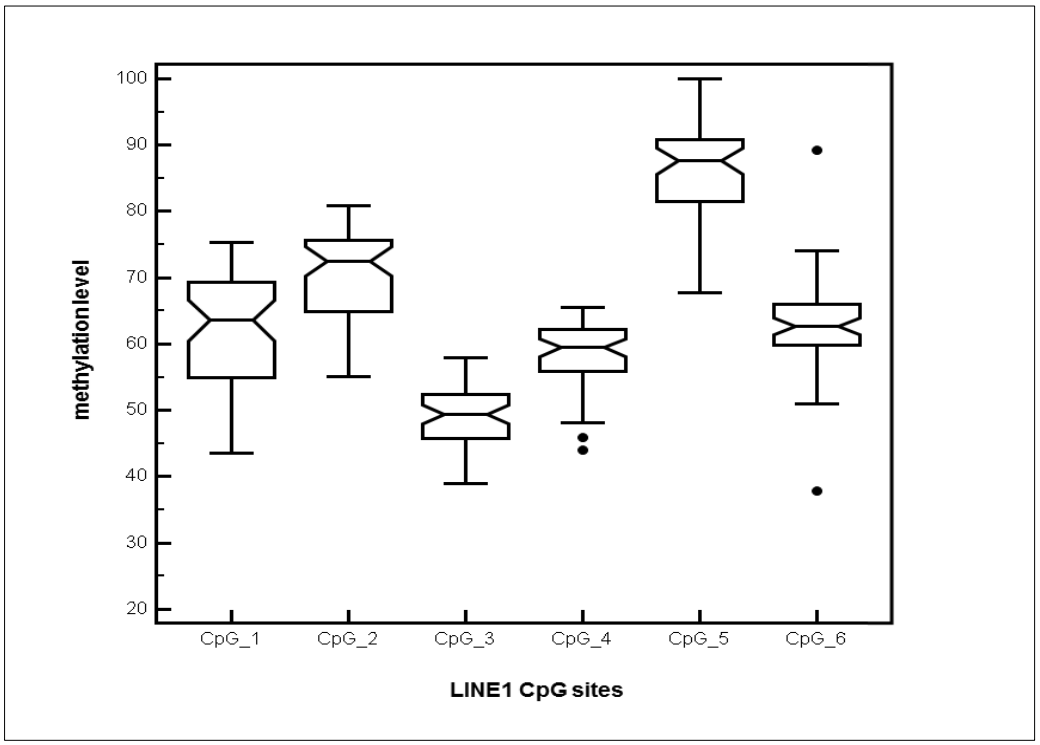

Figure 10 Distribution of LINE1 methylation values among CpG sites

Representative notched boxplots demonstrates the distribution of LINE methylation level for each CpG site measured by bisulphite-pyrosequencing.

A

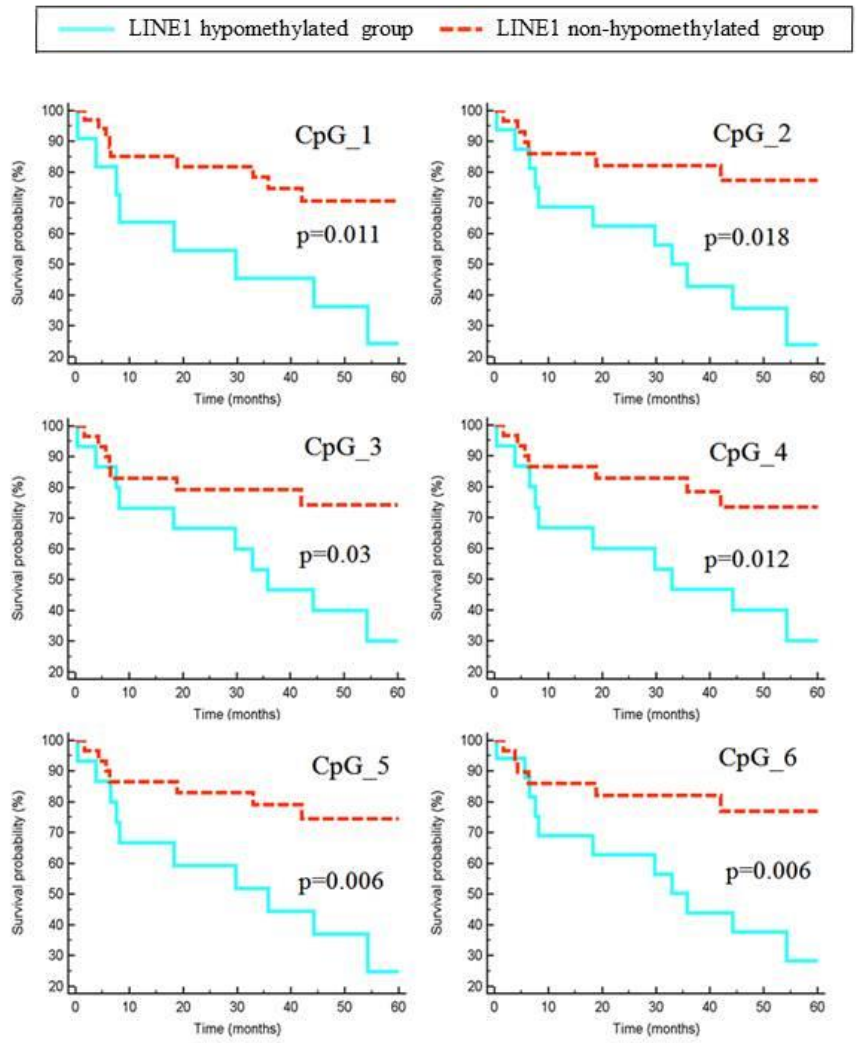

B

LINE1 CpG site	*CpG_1*	*CpG_2*	*CpG_3*	*CpG_4*	*CpG_5*	*CpG_6*
HR [1]	1.14	1.18	1.30	1.08	1.46	1.45
P value	0.78	0.74	0.62	0.88	0.45	0.48
95% CI [2]	0.42-3.12	0.43-3.26	0.44-3.84	0.38-3.04	0.53-4.03	0.51-4.15

Figure 11 Relationship between survival and LINE1 hypomethylation in primary melanomas
(A) *Kaplan-Meier analysis of primary melanoma (n=46) patients survival according to LINE 1 methylation levels which were measured by pyrosequencing at 6 CpG sites. Kaplan- Meyer function for Overall Survival rate (OS) was calculated for CM patients according to cut-off values (determined by ROC curves) of methylation of CpG_1 CpG_2, CpG_3, CpG_4, CpG_5 and CpG_6 sites of LINE 1, respectively. Dashed red line refers for patients with LINE 1 methylation above, whereas solid green line depicts LINE 1 methylation below the cut-off value, respectively. Cumulative survival by LINE1 methylation level was evaluated using the Log-Rank test and reported P values are two sided.* ***(B)*** *Clinical cofounders including age and gender of patients, Breslow thickness, Clark level, histological subtype, metastasis formation during the 5-year follow up period and tumour surface ulceration was examined by Cox proportional hazards regression model whereas the effect of hypomethylation on survival was presented as HR[1]: Hazard Ratios with corresponding 95% CI[2]: Confidence Intervals.*

As shown in Figure 11A, the Kaplan-Meier curve analysis revealed significant differences between the hypomethylated and non-hypomethylated patients, with a decreased overall survival (OS) rate for the hypomethylated group for each CpG site (CpG_1: p= 0.011; CpG_2: p= 0.018; CpG_3: p=0.03; CpG_4: p=0.012; CpG_5: p=0.006; and CpG_6: p=0.006). Notably, the hazard ratios (HR) were higher than 3.0 in each hypomethylated group for all six CpG sites.

The Cox proportional hazard regression model allowed for the control of additional clinical covariates as well as for the patient gender and age. As the stepwise regression method indicated metastatic potential (when primary melanomas develop metastasis during the five-year follow up period) that influences patient survival, this potential was included in the model, and the adjusted HR values were calculated. As demonstrated in Figure 11B, the adjusted HR values did not remain higher than 1.46 nor did the adjusted p-values remain significant.

As the stepwise method of Cox proportional hazard regression model suggested the direct relationship of the overall loss of 5-methylcytosine with metastatic potential, we built a logistic regression model with a stepwise selection for *LINE 1* hypomethylation and for the clinical parameters. Figure 12 demonstrates the association of metastatic capacity and global demethylation in primary melanomas. For each CpG site, we found high odds ratios (OR) for the hypomethylated sample groups; however, the OR remained significant for CpG1 (Figure 12B). The Mann-Whitney test confirmed that the global hypomethylation of all six CpGs was significantly associated with metastasis formation.

To increase the statistical power of the univariate test, primary melanomas with metastasis were divided into subgroups according to the number of metastases developed during the follow-up period, and the Kruskal-Wallis test with Dunn's Multiple Comparison Post-test was applied to measure the strength of the relationship. Figure 12A depicts significantly different levels of global methylation for most CpGs, except for CpG4, among tumours without metastasis and melanomas with more than one metastasis over 5years.

A

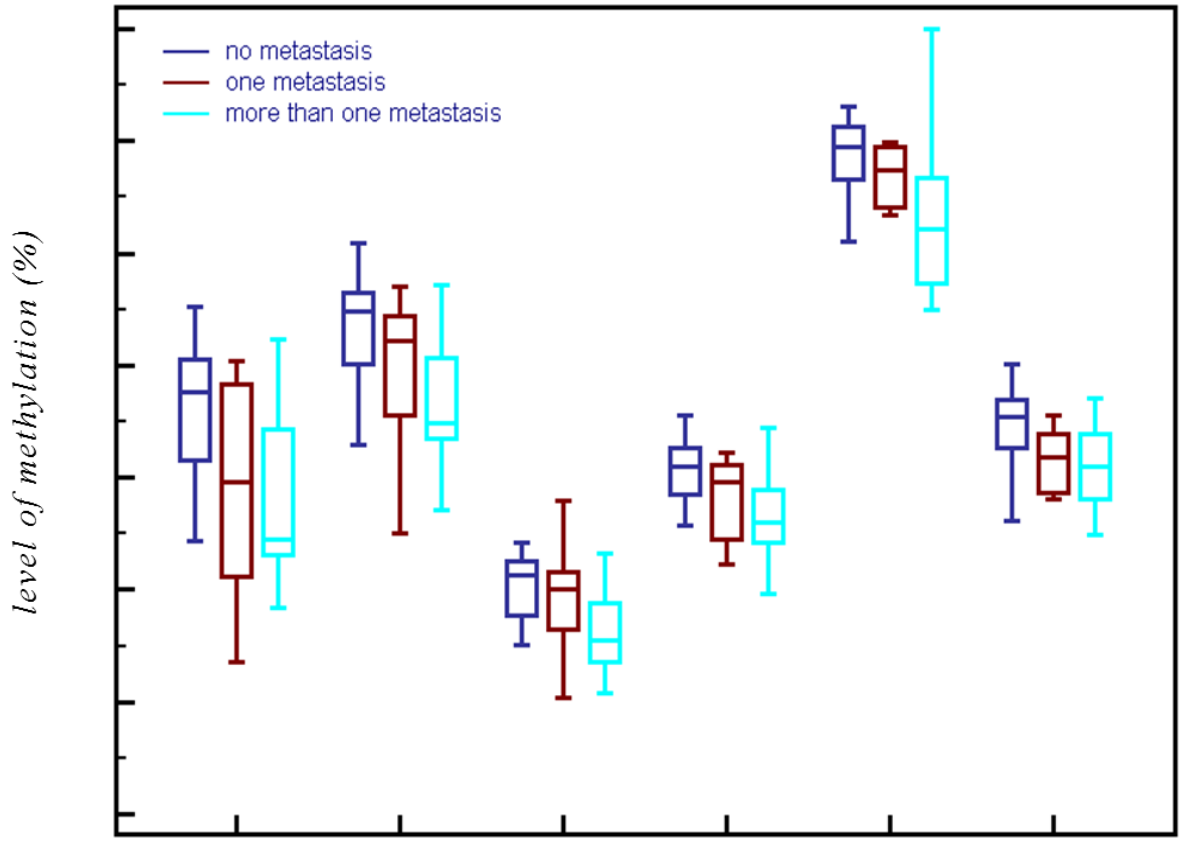

B

Line 1 CpG site	*CpG_1*	*CpG_2*	*CpG_3*	*CpG_4*	*CpG_5*	*CpG_6*
OR [1]	2.23	4.05	4.31	1.27	2.25	1.35
P value	< 0.01	0.15	0.20	0.40	0.20	0.30
95% CI [2]	2.12-2.30	0.59-17.59	1.55-7.80	0.90-3.77	1.34-6.90	0.72-4.30

Figure 12 Association between the number of metastasis and LINE1 hypomethylation

(A) *Primary melanomas that developed metastasis were divided into subgroups according to the number of metastasis formed during the follow-up period and Kruskall Wallis test with Dunn's Multiple Comparison Post-test was applied to study association of global hypomethylation and metastatic capacity which reached significant level in the majority of CpGs.* ***(B)*** *Logistic regression model for LINE1 hypomethylation and the clinical cofounders summarize the association of metastatic capacity and global demethylation in primary melanomas. For each CpGs high OR[1]: Odds Ratios was evaluated in the hypomethylated sample groups with corresponding 95% CI[2]: Confidence Intervals. Association reached significance for CpG_1.*

Regional methylation patterns of primary melanomas

Methylation changes of melanoma subgroups

We studied the methylation patterns of Na-bisulphite converted genomic DNA samples isolated from 42 primary melanomas. Samples were hybridized into Illumina Bead Assay GoldenGate Methylation Cancer Panel I which allowed us to measure 895 individual CpG sites at the same time. The CpG sites were predominantly specific for the promoter regions of the genes. After the initial filtering process, 895 CpG individual sites were available for further analyses and M-values, the logistically transformed Avg-Beta values, were used for statistical approaches which was done by BRB array Tools Software.

Our main goal was to investigate the relationship between the distinct biological types of melanomas and the promoter methylation levels. As the multivariate permutation test provides a tight probabilistic control on the proportion of false discoveries, this test was used for class comparison on each predefined subgroup (the clinical subgroups of primary melanomas are detailed in Table 1; Material and Methods part) according to the following criteria: CpG sites were considered differentially methylated when their p values were less than 0.01 and FDR rates were below the value of 0.2

Figure 13A demonstrates that relatively large number of CpG sites was found to be differentially methylated between melanoma subgroups. Interestingly, the majority of these CpGs were characterised by decreased DNA methylation levels in samples with poor prognosis (larger than 4 mm, metastatic, ulcerated and nodular primary melanomas). Histologic subtype exhibited a more disturbed methylation pattern involving high number of differentially methylated genes in both superficial and nodular subtype. As it can be seen in Figure 13A, some of the differentially methylated individual genes were represented by more than one significant CpG sites arguing in favour of the consistency of given alterations. Altogether, 111 differentially methylated genes were identified in the context of aforementioned clinical predictors: 43 individual genes were hypermethylated and 68 genes hypomethylated in melanomas with less favourable clinical outcome. The differentially methylated gene lists specific for the Breslow thickness, ulceration, metastatic capacity and histologic subtype are detailed in Supplementary Table 1. Venn diagrams (Figure 13B) indicate the common properties among genes with decreased and increased DNA methylation, respectively.

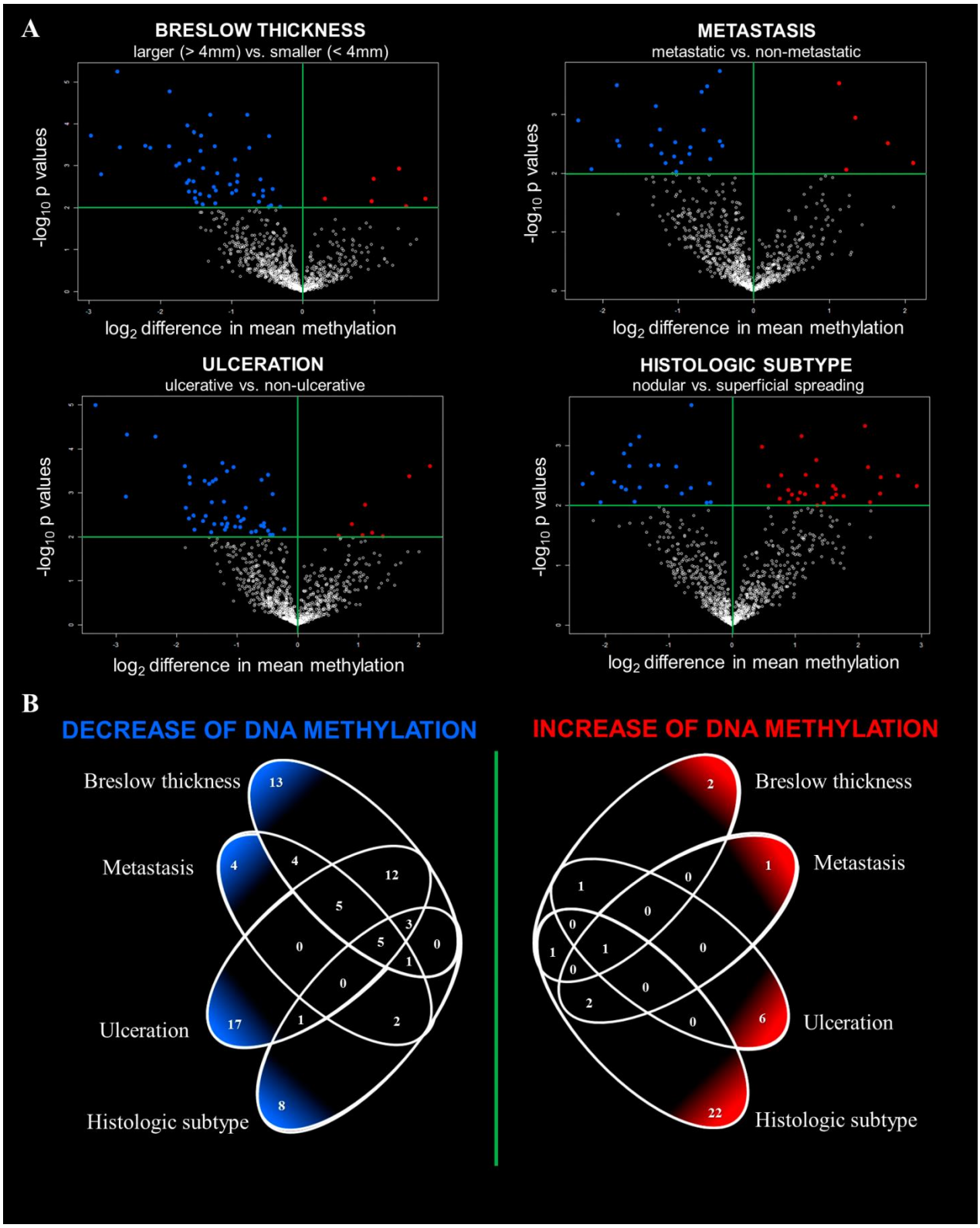

Figure 13 Methylation patterns of primary melanomas associated with known clinical predictors ***(A)*** *Volcano plots of differentially methylated genes associated with known predictors. Blue dots indicates decreased and red indicates increased methylation as follows: Breslow thickness: 51 hypomethylated probes (43 individual genes) and 5 hypermethylated probes (5 individual genes); metastatic capacity: 23 hypomethylated probes (21 individual genes) and 5 hypermethylated probes (4 individual genes), ulceration: 48 hypomethylated probes (43 individual genes) and 8 hypomethylated probes (8 individual genes), histologic subtype: 28 hypomethylated probes (26 individual genes) 23 hypermethylated probes (20 individual genes)* ***(B)*** *A Venn diagrams indicate the overlap of differentially methylated genes (in left: number of hypomethylated genes; in right: number of hypermethylated genes) for each clinical predictor class.*

Being a continuous variable, Breslow thickness allowed the most precise insight into how methylation pattern changes across melanoma stages. In Figure 14A, the heatmap horizontally shows the primary melanoma samples with distinct Breslow thicknesses. The intensive hypermethylation of 45 CpGs is marked with brown colour in the early stage tumours (Breslow thickness < 2mm), and this hypermethylation decreases during the medium and advanced stages. Low-level methylation values are represented with yellow colour. In other types of cancer, hypermethylation has been shown to be associated with tumour progression. Interestingly, the hypermethylation patterns of 45 CpGs, which are detected in the early stages of melanomas, gradually decrease in the medium stages and almost disappear in late stages of the disease. The Principal Component Analysis (Figure 14B) clearly demonstrated that, according to the pattern of the 45 hypermethylated CpGs, the melanoma groups were significantly separated.

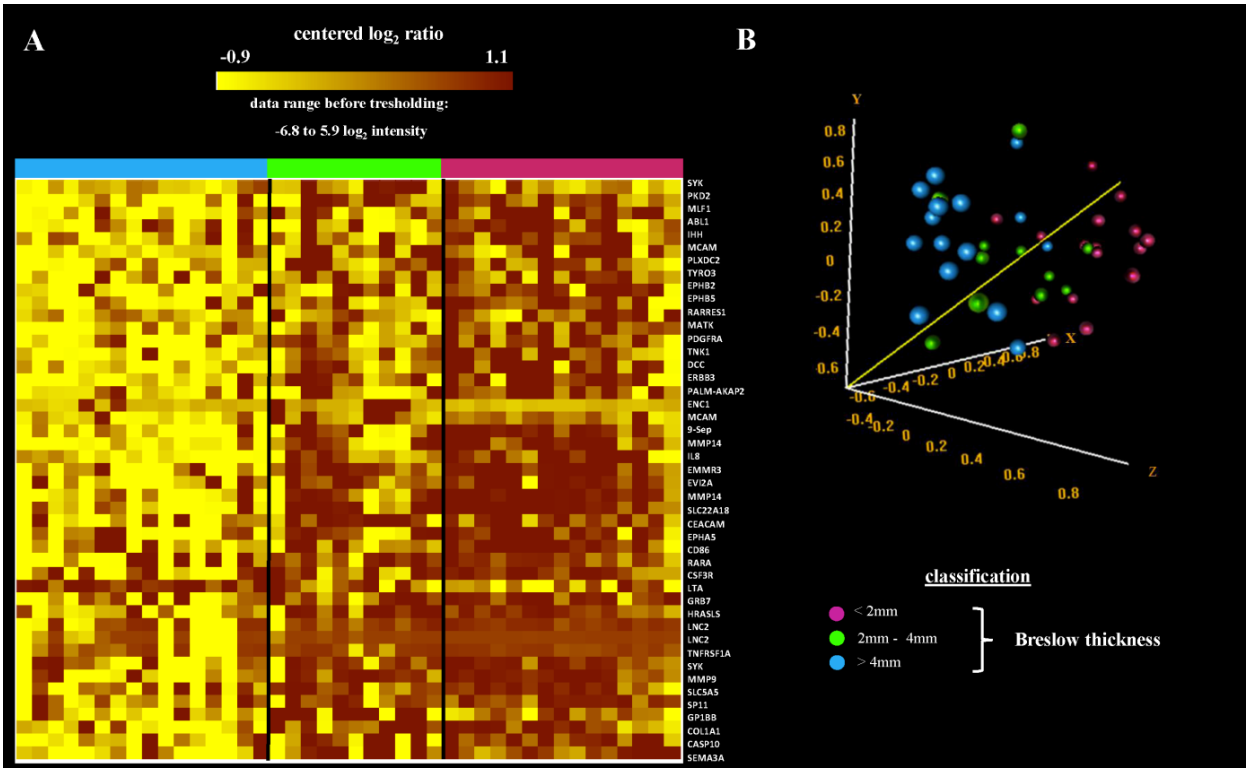

Figure 14 Hypermethylation is an early event in melanomas and decreases with tumour progression

(A) *The heatmap demonstrates the hypermethylation patterns (indicated in brown colour) of 45 CpGs, which can be detected in the early stages of melanomas (horizontal purple colour) but decrease from the medium stage (horizontal green colour) to the late stage (horizontal blue colour).* ***(B)*** *The principal component analysis for the distinction of the Breslow thickness the sample groups (large: blue dots; medium: green dots; and small melanoma samples: purple dots) based on the 45 differentially methylated CpGs. The analysis revealed that, according to the first three components, which covered the 56% of the total variance, the three groups were significantly different ($p < 0.05$)*

It is important to note that normal tissues were not used in our experiments. However, such datasets can be found in the literature, and we were therefore able to correct for the methylation status of normal naevi specimens (see Materials and Methods). These results thus argue that the hypermethylation of the 45 CpGs occurs early, in melanomas less than 2 mm, and then decreases during melanoma progression.

A

Characteristics	KEGG Pathway	Pathway description	No. of CpG probes	No. of individual genes	p-value (Efron-Tibshirani GSA test)
$BRAF^{V600E}$ mutation	hsa01430	Cell communication	28	19	< 0.005
	hsa04512	ECM-receptor interaction	20	15	0.005
Metastatic capacity	hsa04110	Cell cycle	26	24	< 0.005
Ulceration	hsa04670	Leukocyte transendothelial migration	22	17	0.005

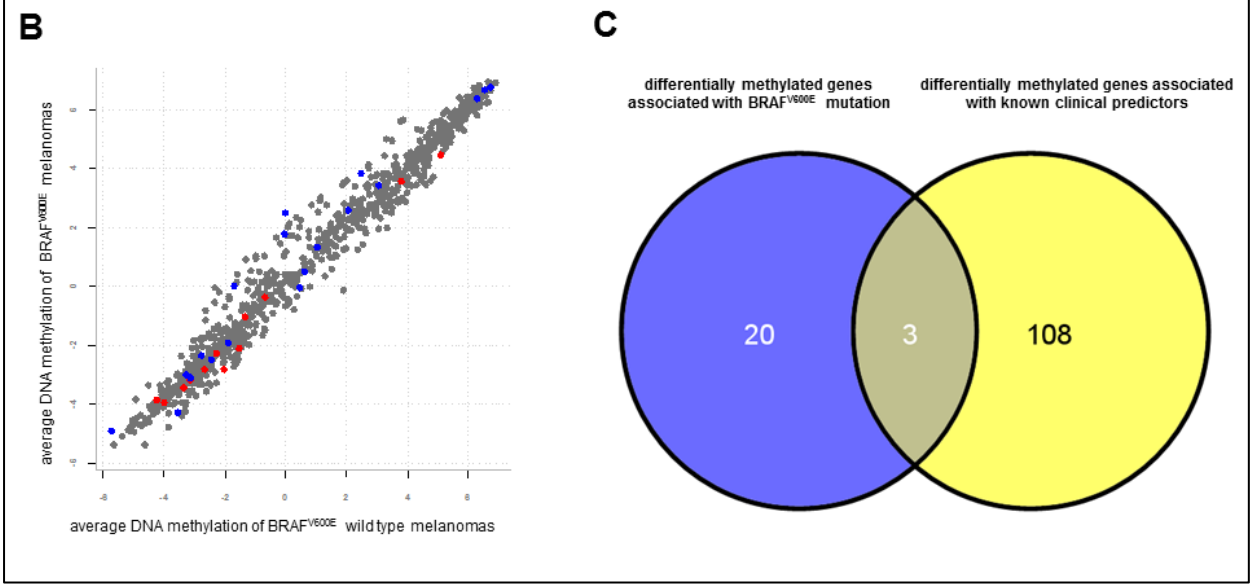

Figure 15 Differentially methylated gene sets between melanoma classes

(A) *Differentially methylated gene sets between $BRAF^{V600E}$ mutant and wild-type, metastatic and non-metastatic, ulcerated and non-ulcerated classes according to the Kyoto Encyclopaedia of Genes and Genomes.* ***(B)*** *Average log-ratios of methylation intensities in $BRAF^{V600E}$ mutant and wild-type melanomas. Red indicates significant genes associated with ECM-receptor interaction and blue depicts significant genes on Cell communication pathway. (Eleven genes overlap between the ECM-receptor interaction and Cell communication.)* ***(C)*** *Venn diagram shows lack of overlap between differentially methylated genes associated with $BRAF^{V600E}$ mutation and the known clinical predictors as Breslow thickness, metastatic capacity, ulceration and histologic subtype.*

In addition to individual gene signatures, we aimed to determine whether the perturbed KEGG-based gene networks are related to localised methylation patterns. We identified differentially methylated genes belongs to Cell cycle pathways in primary melanomas with metastatic capacity. Genes associated at Leukocyte signalling were also demonstrated to be differentially methylated in ulcerated samples (Figure 15A). Interestingly, Cell

communication and ECM-receptor interaction networks were found to be significant at the 0.01 level between *BRAF*^{V600E} mutant and wild type samples, notwithstanding the fact that, we were unable to find differentially methylated CpGs at the individual gene level (Figure 15A-B). The full list of CpG probes is given in Appendix 2. There was poor overlap (Figure 15C) between the differentially methylated genes associated with *BRAF*^{V600E} mutation and clinical subgroups discussed above.

We studied the possible relationship between the survival of patients and the methylation characteristics of the cancer related genes. We identified an association of six hypermethylated genes (*DSP, EPHB6, HCK, IL18, IRAK3* and *KIT*) on patients' 5-years survival. Four of the six genes (*DSP, HCK, IL18 and KIT*) exhibited significantly different Kaplan-Meier curves (Figure 16). However, when we included patient age, gender and *BRAF*^{V600E} mutation status in the survival risk prediction model, only the *KIT* gene remained significant.

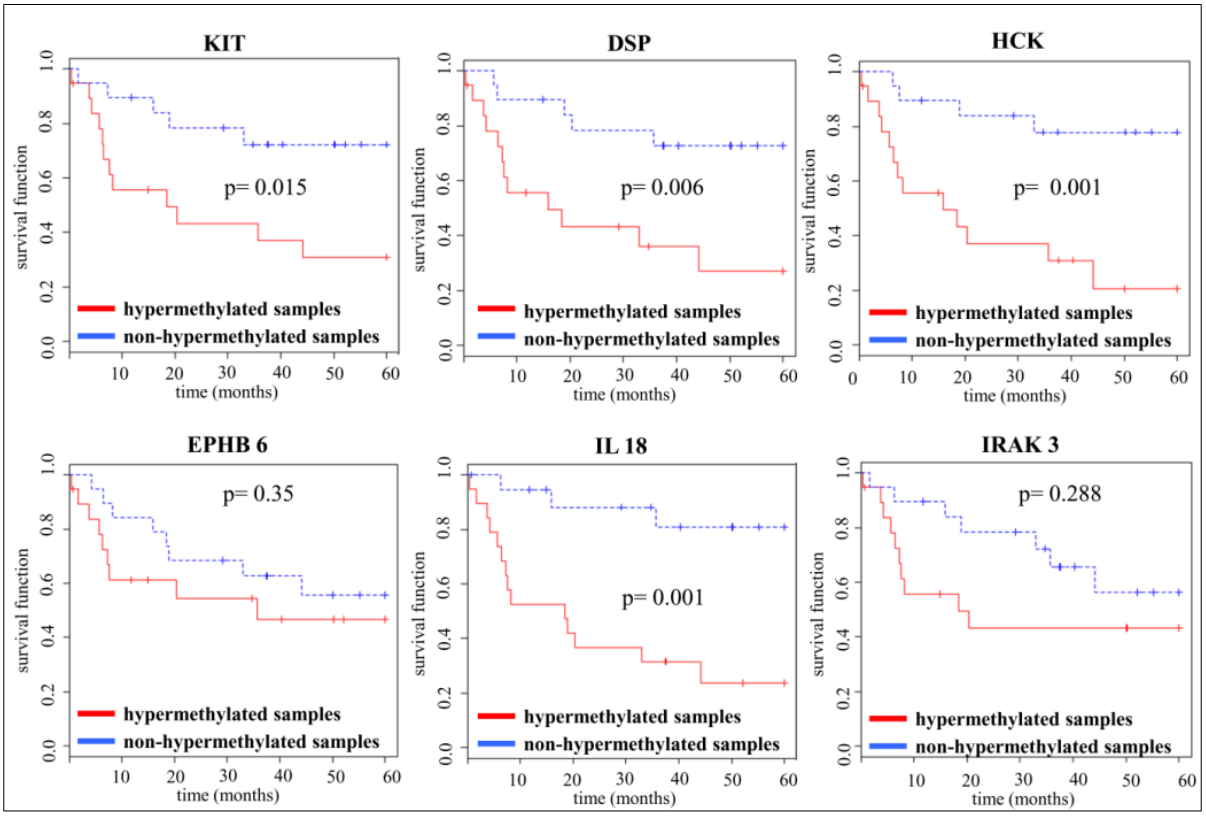

Figure 16 Hypermethylated genes associated with decreased survival rate in melanoma patients
The Kaplan-Meier curves for genes (DSP, EPHB6, HCK, IL18, IRAK3 and KIT) whose hypermethylation was associated with a lower overall survival rate(OS); the Cox proportional univariate approach was performed on each gene to test whether a methylation status of a particular gene significantly influences the survival at the $p < 0.05$ level.

Gene expression of differentially methylated genes

Three genes among the differentially methylated panel were chosen to measure mRNA expression levels by quantitative real-time PCR (FGFR3, MCAM and IL8) according to the following selection criteria: we exclusively focused on genes that had not been previously referred to as methylated in melanomas; furthermore, FGFR3 was chosen in the context of histologic subtype and MCAM of Breslow thickness, while IL8, being a commonly methylated gene among distinct clinical groups was measured across in all categories (Breslow thickness, histologic subtype, ulceration and metastatic capacity). As indicated in the 'Material and Methods' part, analysis was performed by the Livak method ($2^{-\Delta\Delta Ct}$), with glyceraldehyde-3-phosphate dehydrogenase as the reference gene and nevi collected from three different individuals as calibrator samples.

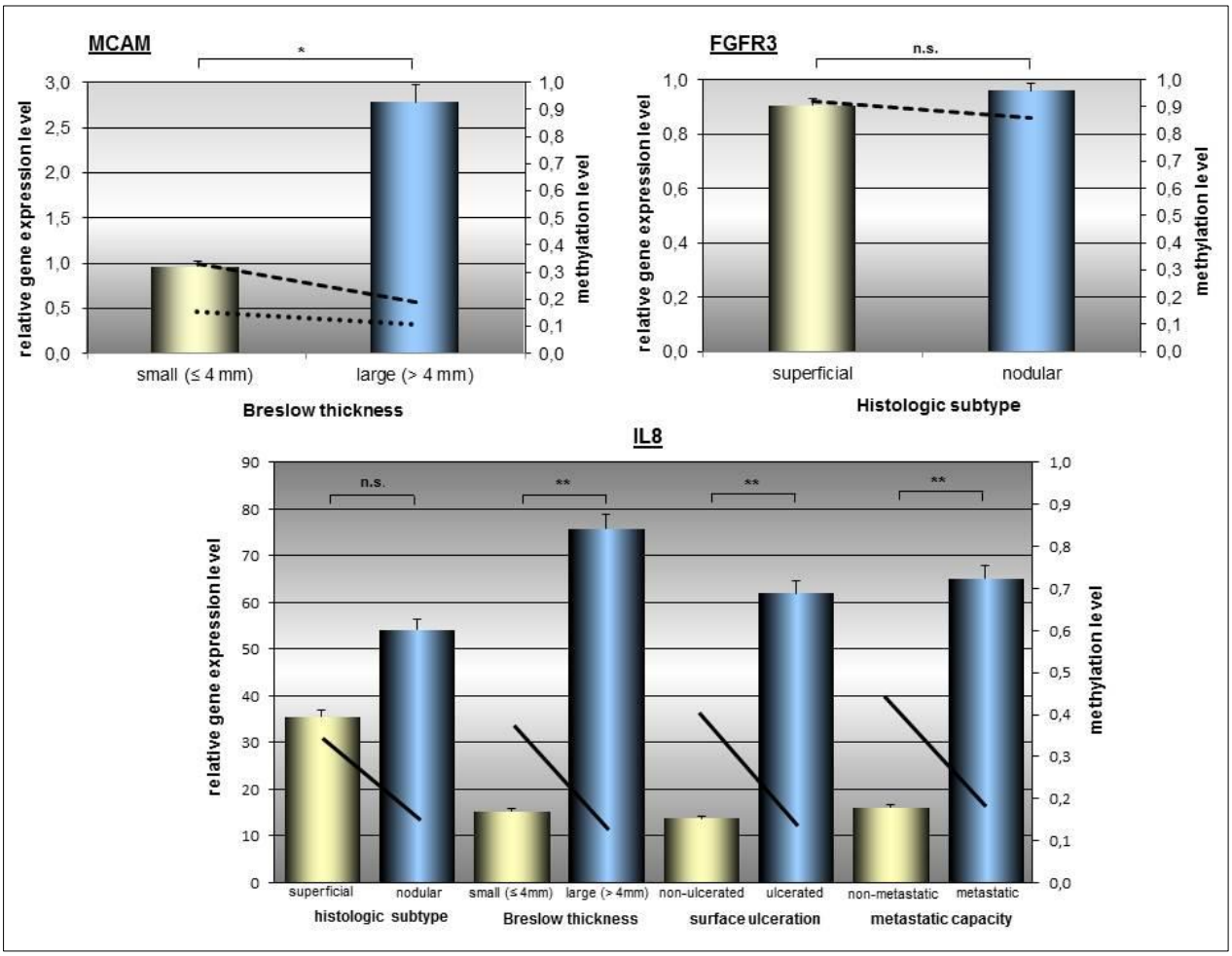

Figure 17 Relationship between gene expression and DNA methylation

The gene expressions of MCAM, FGFR3 and IL8 were measured by qRT-PCR and are presented as bars (fold change in left Y axis), and Avg-Beta methylation values are demonstrated as lines (shown in right Y axis). Methylation data was extracted from Illumina bead assay, with distinct probes represented as different lines. Gene expression differences among the groups were analysed using the Mann-Whitney test, which revealed significant differences for the MCAM and IL8 genes.

Inverse relationships were found between hypermethylation and mRNA expression regarding FGFR3, MCAM and IL8 as well, supporting the notion that the methylation pattern are functionally relevant to gene expression. Significant ($p<0.05$) MCAM mRNA expression level differences were revealed between smaller (Breslow thickness ≤ 4mm) and larger (Breslow thickness > 4mm) melanomas.

IL8 expression differed as well between sample distinct categories of Breslow thickness, melanoma surface ulceration and metastatic capacity. The qPCR and corresponding correlation results are summarised in Figure 17.

Integrative genome analysis of primary melanomas

Integration of copy number and methylation data with gene expression

We performed a detailed aCGH analysis on 26 primary melanomas and collected integrated array CGH and gene expression data from the same tumour (n=17) to characterise genetic alterations that might be associated with gene expression changes.

Table 2 Distribution of the most frequent copy number losses in melanomas

Cytoband Location	Region Length (bp)	*Frequency (%)	**P value	***Distribution of known CNV overlap (%)
4q28.3	470255	29	0.020	27
7q11.1	468074	29	< 0.001	94
9q12	179861	53	0.005	0
9q13	379778	53	0.005	72
11p11.2-p11.12	945190	35	< 0.001	5
15p11.1-q11.1	682823	29	< 0.001	0
15q11.1	463101	29	< 0.001	41
17q21.31	160872	29	0.007	0
20q11.1	691516	35	< 0.001	0

** Copy number loss frequency indicates the proportion of samples that exhibit the given genomic loss. ** P value has been determined by a multiple corrected Fisher's exact test. *** CNV overlap is the occurrence of copy number events that exist in healthy donors according to the Copy Number Project database (Wellcome Trust Sanger Institute).*

A genome-wide aCGH profiling analysis revealed numerous copy number alterations in the melanoma genome. Ulcerated melanomas displayed gains at 3p, 6p, 7p, 7q, 8q, 11p, 11q, 15q, 16p, 17q, 18q and 22q, with the smallest regions detected at 3p21.31-p21.2, 6p21.2-p21.1,

7p14.3, 7q36.2, 8q24.3, 11p15.5-p15.4, 11q13.3, 15q22.33-q23, 15q24.2, 16p13.3, 17q25.3, 18q21.1 and 22q12.3. Losses were found at 4q, 7q, 9q, 11p, 14q, 15p, 15q, 17q, 20q, 21p with the smallest regions observed at 4q28.3, 7q11.1, 9q12, 9q13, 11p11.2-p11.12, 14q11.1-q11.2, 15p11.1- q11.1, 17q21.31, 20q11.1, 21p11.2 ($p<0.05$).

As our previous study demonstrated the strong downregulated patterns in ulcerated melanomas, we focused mainly on copy number losses summarized in Table 2.

To determine the influence of copy number aberrations on the gene expression changes in primary melanomas, we sought to identify the genes whose expression was significantly correlated with copy number changes. By correlating the intensity of the aCGH ratios (median log2) with the expression levels of previously identified downregulated genes (987 genes), we identified 150 genes whose expression was significantly and positively correlated with copy number changes in ulcerated melanomas ($p<0.05$). The gene list generated through this analysis was significantly enriched in genes mapping to chromosomes 6q and 10q. Figure 18 shows the frequency distribution of copy number losses in ulcerated (red line) and non-ulcerated (green line) melanomas. We found more narrow regions that were deleted on the long arm of chromosome 6 (6q14.1-q14.2, 6q16.3-q21, 6q22.31-q22.32, 6q23.3 and 6q24.2), consisting of 9 deregulated genes (*ELOV4*, *ME1*, *TPBG*, *AIM1*, *TPD52L1*, *IL20RA*, *HEPB2*, *PERP* and *UTRN*).

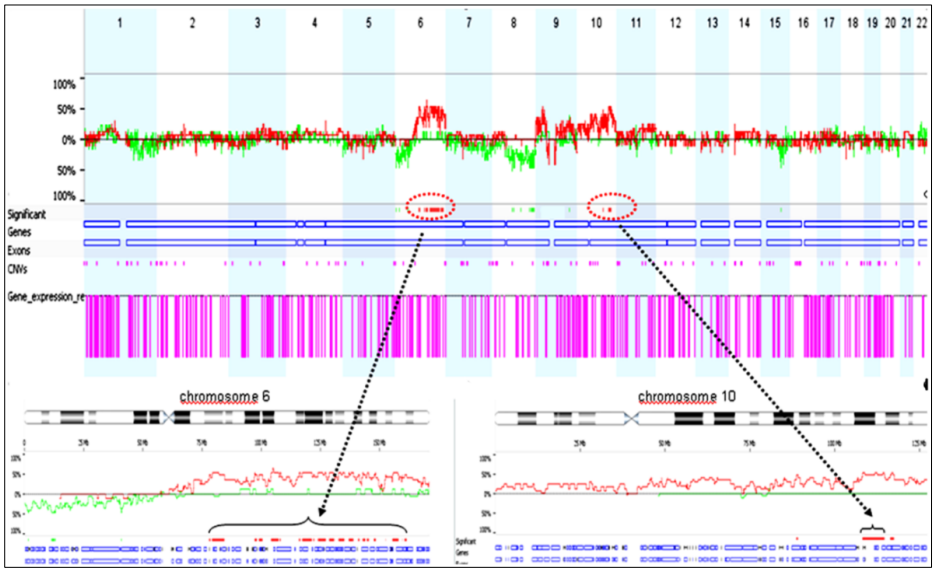

Figure 18 Correlation of copy number alterations (CNAs) and gene expression

Chromosomes 6 and 10 shows significantly different copy number losses that are highly correlated with gene downregulation based on comparison of CNAs in the ulcerated vs. non-ulcerated tumour subgroups. The differences in CNAs (red indicates CNA losses, and green indicates CNA gains) were obtained by subtracting the alterations in the ulcerated group (above the baseline) from the alterations in the non-ulcerated group (below the baseline) using Fisher's exact test corrected for multiple testing. Five narrowed deleted regions were found on chromosome 6 and one deleted region was detected on chromosome 10q that was also downregulated.

A significant association between genomic losses and the downregulation of genes on chromosome 10 was only observed for one gene (*ABLIM1*, localised to 10q25).

Lasso regression, performed by lol R-package, identified both copy number gains (Figure 19 B) and losses (Figure 19 A) as top scoring ($Score_{trans} \geq 0.5$) trans- acting somatic DNA aberrations accompanied by transcriptomic alterations. Interestingly, even trans- acting copy number gains were accompanied by transcriptomic silencing, there was no association between gains and gene upregulation revealed.

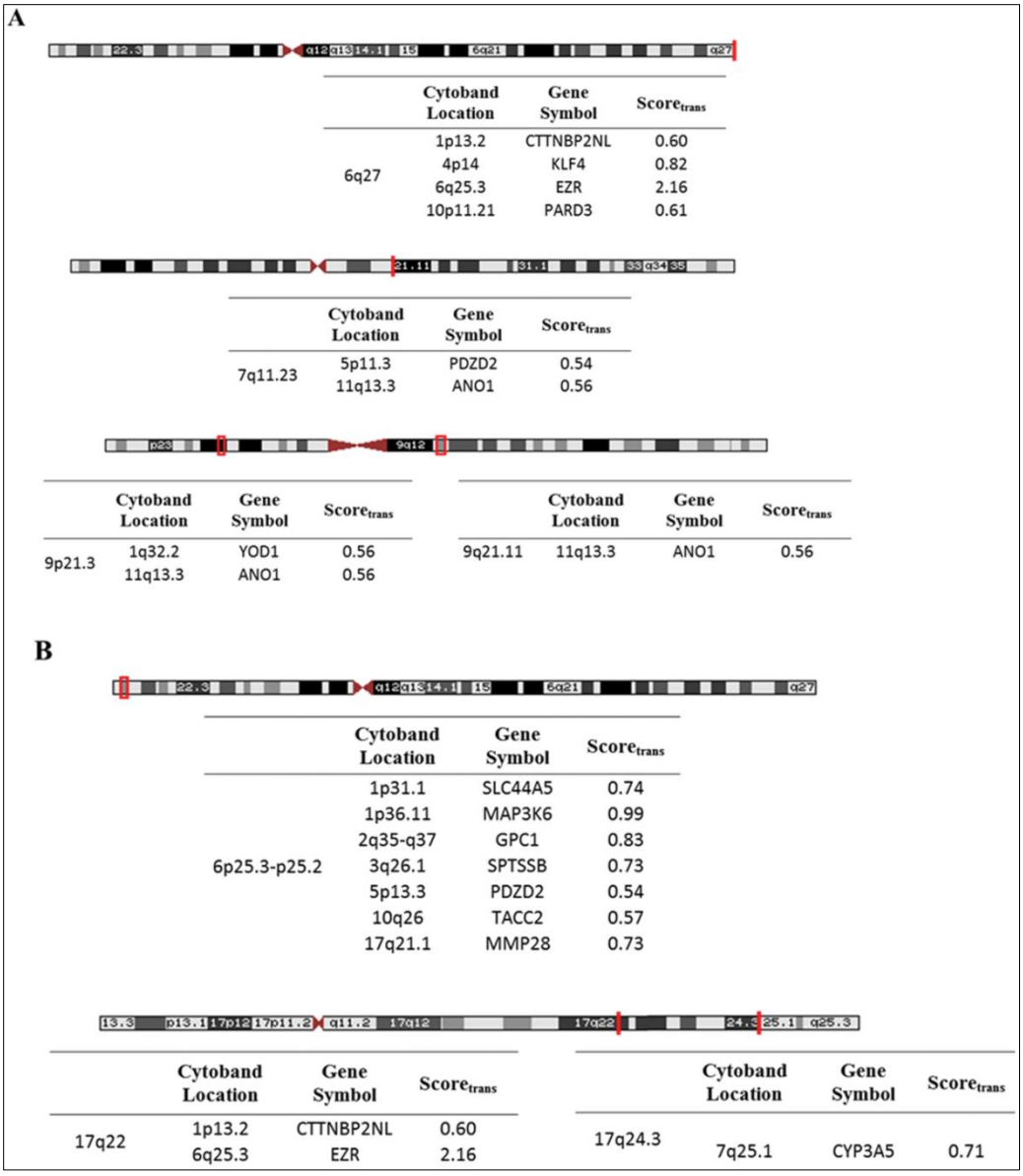

	Cytoband Location	Gene Symbol	$Score_{trans}$
6q27	1p13.2	CTTNBP2NL	0.60
	4p14	KLF4	0.82
	6q25.3	EZR	2.16
	10p11.21	PARD3	0.61

	Cytoband Location	Gene Symbol	$Score_{trans}$
7q11.23	5p11.3	PDZD2	0.54
	11q13.3	ANO1	0.56

	Cytoband Location	Gene Symbol	$Score_{trans}$
9p21.3	1q32.2	YOD1	0.56
	11q13.3	ANO1	0.56

	Cytoband Location	Gene Symbol	$Score_{trans}$
9q21.11	11q13.3	ANO1	0.56

	Cytoband Location	Gene Symbol	$Score_{trans}$
6p25.3-p25.2	1p31.1	SLC44A5	0.74
	1p36.11	MAP3K6	0.99
	2q35-q37	GPC1	0.83
	3q26.1	SPTSSB	0.73
	5p13.3	PDZD2	0.54
	10q26	TACC2	0.57
	17q21.1	MMP28	0.73

	Cytoband Location	Gene Symbol	$Score_{trans}$
17q22	1p13.2	CTTNBP2NL	0.60
	6q25.3	EZR	2.16

	Cytoband Location	Gene Symbol	$Score_{trans}$
17q24.3	7q25.1	CYP3A5	0.71

Figure 19 Trans-acting copy number alterations

*Lasso regression was performed on the previously identified 1080 differentially expressed genes to assess trans- acting copy number alterations on mRNA expression. Cytoband locations were mapped by UCSC Genome Browser and the tables below represent the genes whose expression can possibly be affected by CN losses **(A)** and gains **(B)** at trans-acting CN elements. The $score_{trans}$ represents the strength of the relationship between trans-acting elements and mRNA expression*

Three distinct copy number losses (9p21.3, 9q21.11 and 7q11.23) were related to the downregulation of Anoctamin1 (*ANO1*), whereas Ezrin (*EZR*) deregulation was probably caused by the copy number loss of 6q27 (Figure 18 A) and the copy number gain of 17q22 (Figure 19 B). Cis- affecting copy number losses given in Table 2 were verified by Lasso-regression as we revealed $Score_{cis}$ values more than 0.5 for each region.

To define the influence of the epigenetic alterations on melanoma ulceration, we estimated if the 98 overlapping CpG sites were methylated differently by univariate t- tests for each genes. Figure 20A plots a clustered heat map showing the lack of differences between the sample groups with an exception of *JAK2* and *IL1RN* genes (Figure 20B), however, significant differences did not remained after adjustment of multiple comparison (Figure 20C).

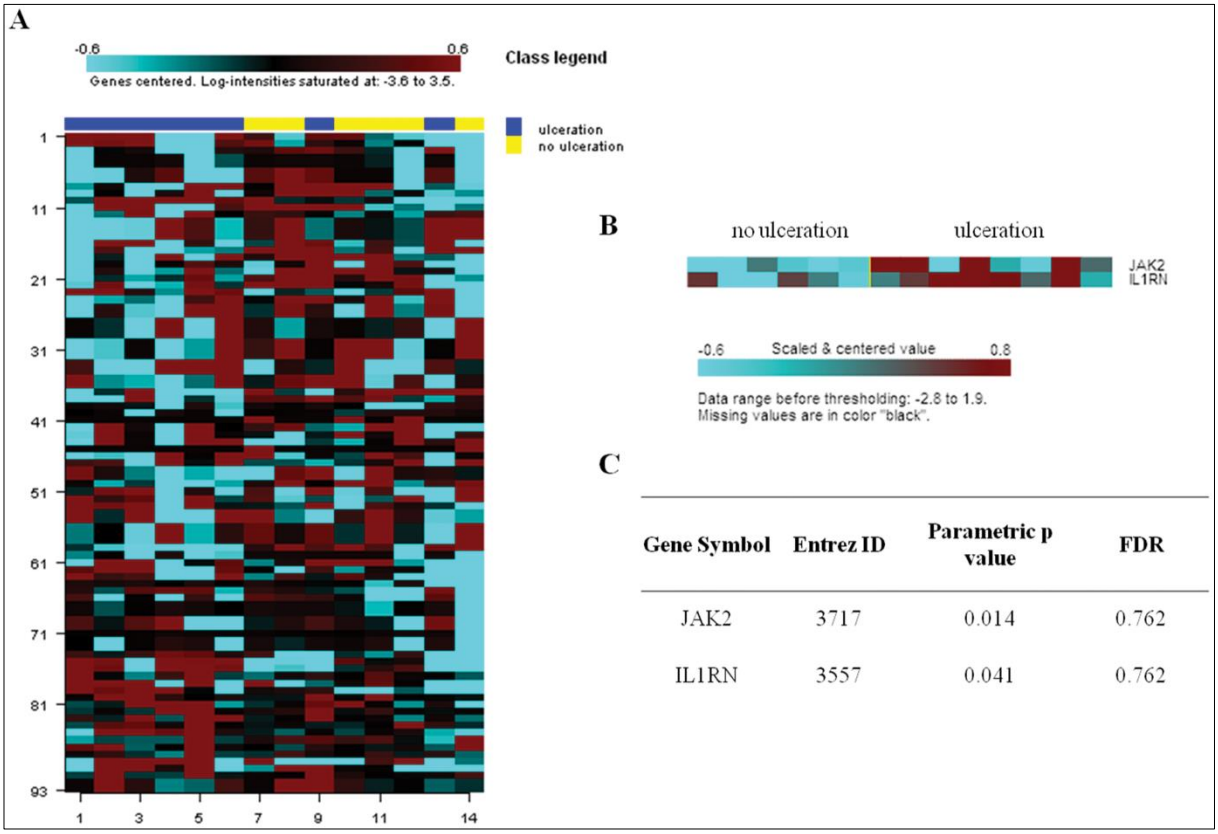

Gene Symbol	Entrez ID	Parametric p value	FDR
JAK2	3717	0.014	0.762
IL1RN	3557	0.041	0.762

Figure 20 Relationship between DNA methylation and melanoma ulceration
Clustered heatmap, performed to demonstrate promoter methylation patterns, shows lack of differences between ulcerated and non- ulcerated sample groups. The heatmap is based on the univariate t-tests performed for each sites (specific for 45 independent genes) that overlapped with the gene expression results. Two genes (IL1RN and JAK2) demonstrated increased methylation for the ulcerated sample group; however, significant differences did not remain after adjustment for multiple comparisons.

Furthermore, we correlated the gene expression data with the observed epigenetic changes (Illumina Golden Gate Cancer Panel 1) in the same tumour. Of the 987 downregulated genes identified using the Affymetrix microarray; we found 45 common genes represented by 98 different CpGs on the methylation array platform. A strong or medium inverse correlation (a medium inverse correlation was assessed if $r \leq -0.30$ and a strong inverse correlation if $r \leq -0.50$ by Pearson's correlation) between gene expression and methylation levels was detected in the case of 11 genes corresponding to 17 different CpG sites. Detailed list of these genes are shown in Table 3.

Table 3 ***Genomic regions enriched with downregulated genes affected by promoter hypermethylation***

Gene Symbol	**Cytogenetic Location**	**Probe ID**	**Pearson's *r***
EPHB3	3q27.1	EPHB3_E0_F	-0.56
		EPHB3_P569_R	-0.39
FGFR3	4p16.3	FGFR3_E297_R	-0.44
		FGFR3_P1152_R	-0.11
ITGA2	5q11.1	ITGA2_E120_F	-0.60
		ITGA2_P26_R	-0.40
DST	6p12.1	DST_E31_F	-0.38
		DST_P262_R	-0.41
EPHB6	7q34	EPHB6_P827_R	-0.34
PTGS1	9q33.3	PTGS1_E80_F	-0.45
		PTGS1_P2_F	-0.25
FGFR2	10q26.13	FGFR2_P266_R	-0.37
		FGFR2_P460_R	-0.29
CDH13	16q23.3	CDH13_E102_F	-0.50
		CDH13_P88_F	-0.37
JAG1	20p12.2	JAG1_P66_F	-0.47
TIAM1	21q22.11	TIAM1_P117_F	-0.34
		TIAM1_P188_R	-0.20
ETS2	21q22.2	ETS2_P684_F	-0.69
		ETS2_P835_F	-0.33

Coincidence of localised methylation and copy number alterations

We determined the frequent copy number gains and losses associated with the *BRAF*^{V600E} mutation (Figure 21A-C) and Breslow thickness are shown Appendix 3 in primary melanomas. As expected, a set of marked copy number alterations was associated with both the *BRAF*^{V600E} mutation and Breslow thickness categories.

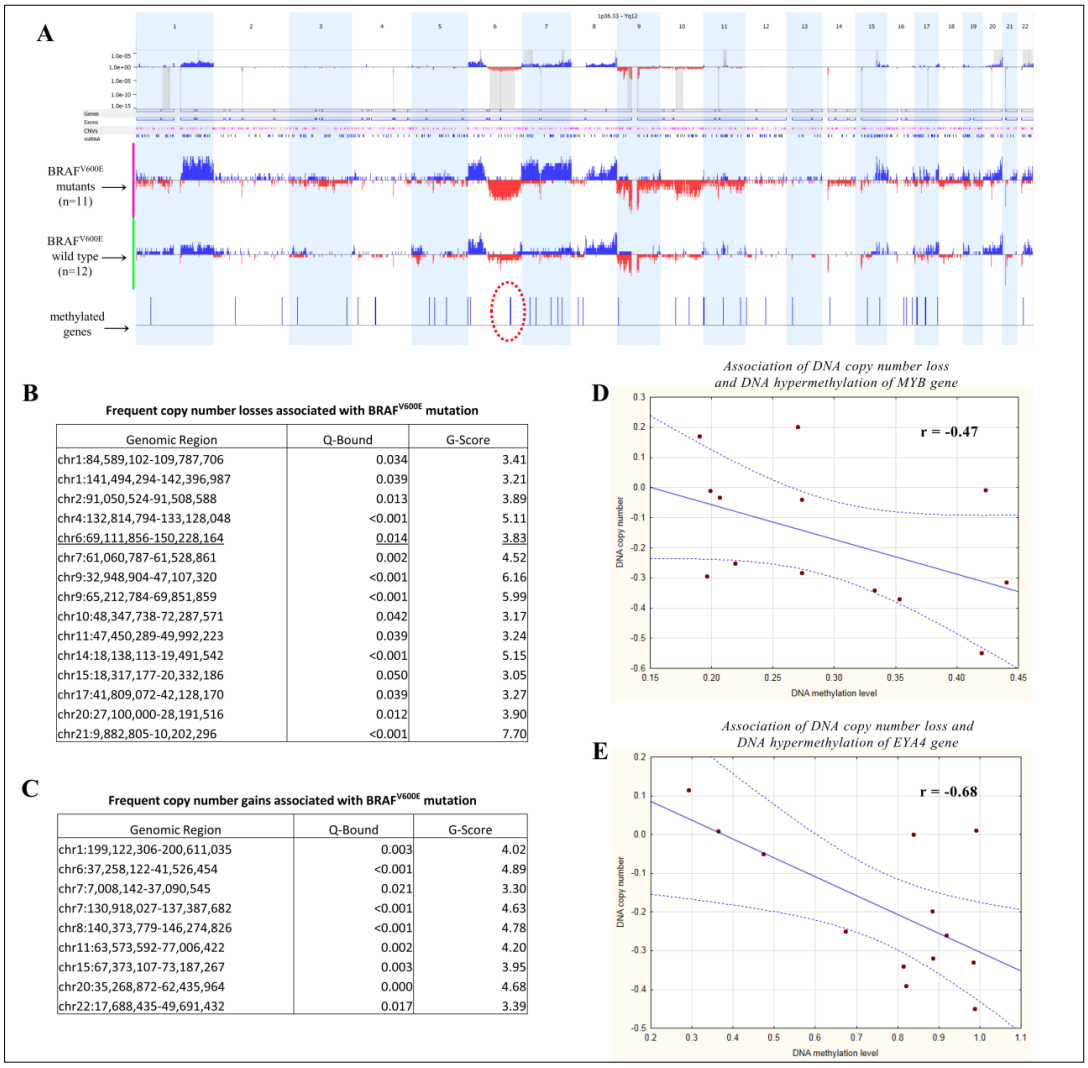

Genomic Region	Q-Bound	G-Score
chr1:84,589,102-109,787,706	0.034	3.41
chr1:141,494,294-142,396,987	0.039	3.21
chr2:91,050,524-91,508,588	0.013	3.89
chr4:132,814,794-133,128,048	<0.001	5.11
chr6:69,111,856-150,228,164	0.014	3.83
chr7:61,060,787-61,528,861	0.002	4.52
chr9:32,948,904-47,107,320	<0.001	6.16
chr9:65,212,784-69,851,859	<0.001	5.99
chr10:48,347,738-72,287,571	0.042	3.17
chr11:47,450,289-49,992,223	0.039	3.24
chr14:18,138,113-19,491,542	<0.001	5.15
chr15:18,317,177-20,332,186	0.050	3.05
chr17:41,809,072-42,128,170	0.039	3.27
chr20:27,100,000-28,191,516	0.012	3.90
chr21:9,882,805-10,202,296	<0.001	7.70

Genomic Region	Q-Bound	G-Score
chr1:199,122,306-200,611,035	0.003	4.02
chr6:37,258,122-41,526,454	<0.001	4.89
chr7:7,008,142-37,090,545	0.021	3.30
chr7:130,918,027-137,387,682	<0.001	4.63
chr8:140,373,779-146,274,826	<0.001	4.78
chr11:63,573,592-77,006,422	0.002	4.20
chr15:67,373,107-73,187,267	0.003	3.95
chr20:35,268,872-62,435,964	0.000	4.68
chr22:17,688,435-49,691,432	0.017	3.39

Figure 21 Coincidence of DNA copy number (CN) alterations and hypermethylation

(A) *The distribution of CN aberrations (red indicates CN losses and blue indicates CN gains on the frequency plot) specific for the BRAF*^{V600E} *mutant (purple line on the left) and BRAF*^{V600E} *wild-type (green line on the left) primary melanomas. The methylated genes are shown as blue lines in the lower part of the figure, and the red dotted circle highlights 6q23 as the only region where a coincidence was revealed. The significant CN alterations are highlighted in grey in the upper part of the figure. Frequent CN losses* ***(B)*** *and CN gains* ***(C)*** *are given based on the G-score, which is a measure of the frequency of occurrence of the aberration and the magnitude of the CN alteration at each location in the aggregate of all samples in the dataset. The locations of the alterations in each sample are permuted, simulating data with random aberrations, and the significance is represented as Q-Bounds. Panel* ***(C)*** *depicts the correlation plot for CN alterations and DNA methylation regarding the MYB gene and* ***(D)*** *the EYA4 gene.*

In the *BRAF*^{V600E} mutant samples, significant CN losses (Figure 22B) were found at in the 1p, 1q, 2p, 4q, 6q, 7p, 9p, 9q, 10p, 10q, 11p, 14p, 15p, 17p, 20p and 21p regions, whereas CN gains (Figure 21C) were detected across chromosomes 1q, 6p, 7p, 7q, 8q, 11q, 15q, 20q and 22q.

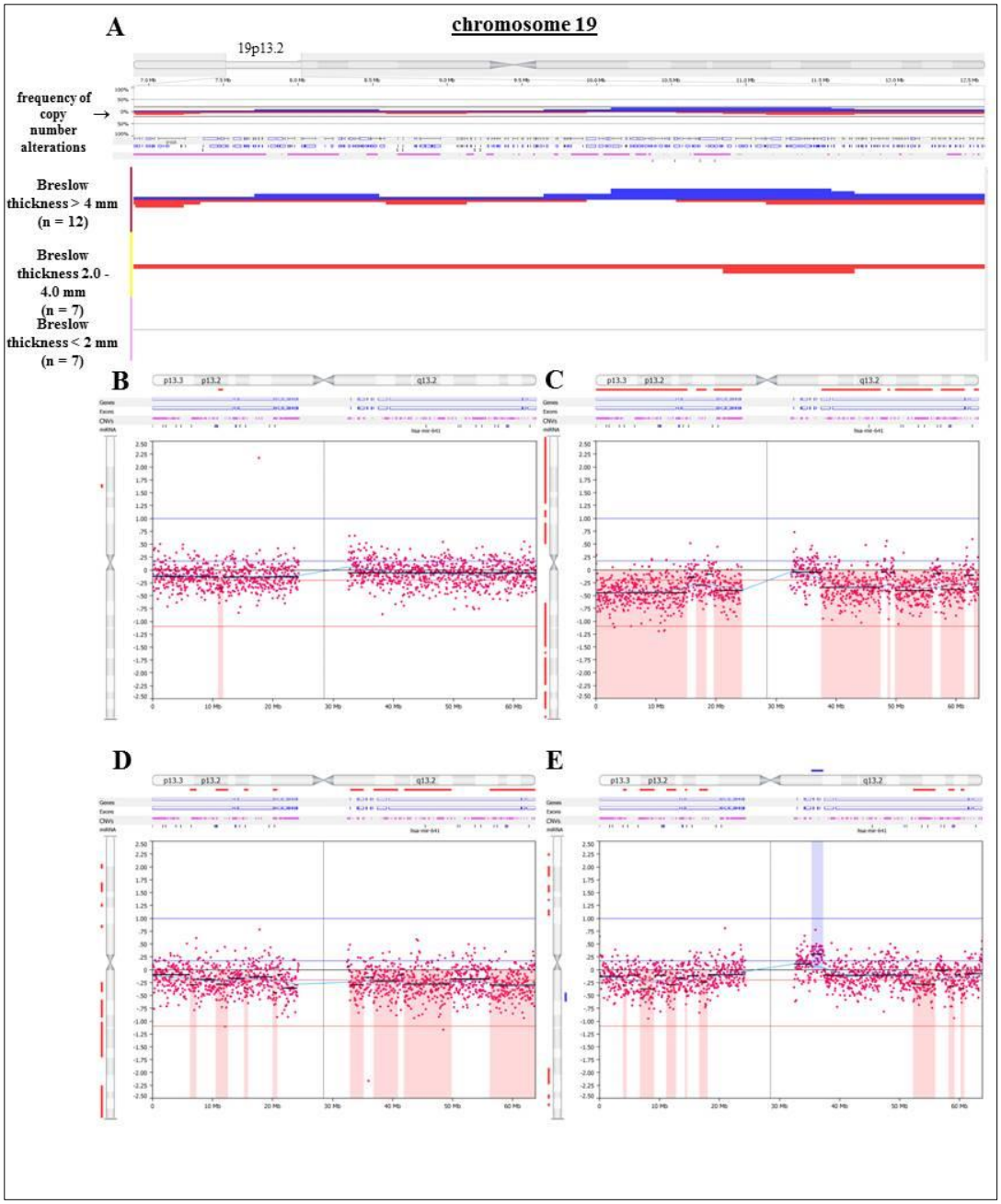

Figure 22 Copy number alteration of chromosome 19 in Breslow thickness > 4 mm melanomas
(A) *The Tiling Array CGH revealed characteristic CN differences among the three sample groups (pink line on the left: Breslow thickness < 2mm; yellow line: Breslow thickness 2 – 4 mm; red line: Breslow thickness > 4 mm) regarding the CN alterations of chromosome 19. The CN-altered regions involve 19p13.2 harbouring the Methyltransferase-1 gene (DNMT1). Panels* ***(B-E)*** *depict representative figures of CN losses revealed exclusively in medium- or advanced-stage (according to Breslow thickness) primary melanomas.*

In the late stages of primary melanomas (Breslow thickness > 4mm), significant CN losses were observed more frequently and comprised deletions of 1p, 4q, 7p, 9p, 14p and 21p, whereas CN gains were only observed in the 11q region, as summarised in Appendix 3. Despite not reaching a significant level, it is worth noting that the CN losses in 19p12 (harbouring the DNA Methyltransferase-1 gene) were exclusively associated with more advanced stages (Breslow thickness > 2mm; Figure 22A). However, among the late-stage samples (Breslow thickness > 4mm), CN gains were also found with CN losses in some samples. Figure 22B-D represents late-stage melanomas that exhibited CN losses in 19p12.

In addition to the general mapping of the CN-altered genomic regions, we quantitatively assessed the coincidence of CN alteration and methylation patterns gene by gene. Similar to other studies, we established gene level measurements by averaging the methylation states within gene-specific regions. As significantly and positively correlated genes were revealed at the levels of methylation and CN alteration, the correlations cannot possibly represent coordinated allele loss and hypermethylation; nevertheless, these results do not remain significant after the multiple correction procedure. Moreover, direct correlation often involves genome parts that are positively correlated at the level of methylation and CN without detected CN changes or altered methylation. Therefore, we applied an alternative approach based on the frequency of methylated genes harbouring significant CN alterations to test Knudson's two-hit hypothesis. As indicated in Figure 21A, 6q12-6q25.1 comprises a relatively large, significant CN loss and two hypermethylated genes, namely, *EYA4* (6q23) and *MYB* (6q22-q23). When measured quantitatively, a significant inverse correlation was observed between CN loss and DNA hypermethylation (Figure 21 D-E).
Array CGH results were further confirmed by four colour FISH experiments specific for 11q13 (specific for *CCND1* gene), 6p25 (specific for *RREB1* gene), 6q23 (specific for *MYB* gene) and centromere 6 on 27 primary melanomas (Figure 23).

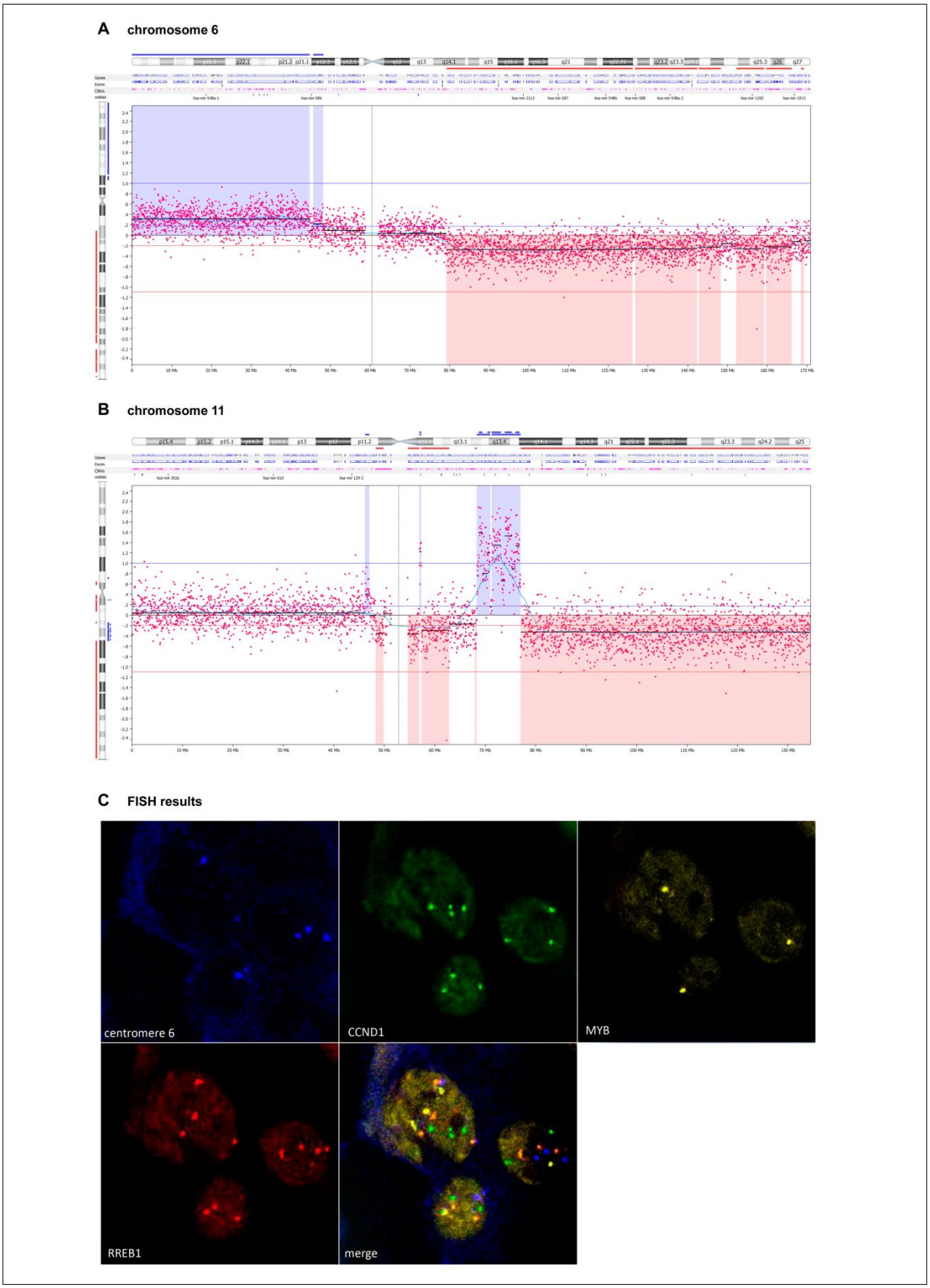

Figure 23 FISH analysis to confirm array CGH results

CN alteration at specific regions of a representative BRAF^{V600E} mutant primary melanoma: ***(A)*** *CN gains were revealed at chromosome 6p while CN losses occurred at chromosome 6q in BRAF^{V600E} samples.* ***(B)*** *High level CN gain was seen at the region of 11q13-q14.* ***(C)*** *Four colour FISH was performed to verify the CN altered genomic regions: green fluorescence (gain of CCND1 gene on 11q13), yellow fluorescence (loss of MYB gene on 6q23), red fluorescence (gain of RREB1 gene on 6p25), whereas blue fluorescence indicates centromere 6.*

Discussion

Melanoma is an aggressive, rapidly fatal, therapy-resistant malignancy of the melanocytes. The incidence of this disease has been increasing worldwide, resulting in a growing public health problem. Although the steadily increasing incidence of melanoma is not in parallel with mortality, due to the dissemination of the disease, in the United States nearly 9,000, in Hungary 3-400 melanoma death can be assumed yearly[107]. Although there are several ongoing clinical trials to explore the effectiveness of distinct therapeutic agents in malignant melanoma; currently, vemurafenib is the solely registered molecular targeted therapy that results an objective response and significantly prolonged survival in the majority of melanoma patients, notwithstanding the fact that melanomas rapidly develop resistance against the vemurafenib[108]. Therefore, early diagnosis remains the key to improved survival for all affected individuals. To develop treatments for advanced melanoma and to increase the survival of patients with metastatic melanoma, it is important to characterise both genetic and epigenetic patterns along with gene expression changes leading to each progressive step of the disease.

DNA methylation, covalent histone posttranslational modifications, chromatin remodelling and micro-RNA gene interference, represent different utilities in the integrated apparatus of epigenetic mechanisms[96]. In addition to playing a role in several physiological processes, epigenetic mechanisms have been described as key factors in modifying the accessibility of DNA to transcription factors and, therefore, in altering the gene expression patterns of several cancer types[109]. The best factor that is described in melanoma epigenetics is DNA methylation, a covalent modification of mainly cytosines which itself features a diverse presence[110]. In addition to the most recently described 5-hydroxymethylcytosine, it is important to distinguish between genome-wide hypomethylation and localised hypermethylation[41]. The former is related to the overall loss of 5-methylcytosine, which is believed to correspond to the methylcytosines of repetitive transposable elements (*LINE and SINE* sequences) having integrated into the human genome during evolution and gained protection from transcription due to their higher levels of 5-methylcytosine[38]. Considering that repetitive transposable elements constitute 40% of the human genome, it is clear why the literature generalises the transposable demethylation of the whole genome as global hypomethylation.

Data from other types of neoplasms such as ovarian and colon cancer have established a relationship between shortened survival and global demethylation[111,112]. Additionally,

Hoshimoto et al. described the shortened relapse-free survival of demethylated melanomas[113]. Sigalotti et al. conducted a valuable study aimed at estimating the *LINE 1* methylation status of 42 short-term cultures from surgically removed cutaneous melanomas that were exclusively representative for stage III[42]. Surprisingly, among the three *LINE 1* CpG sites, the hypomethylation of two CpG sites was associated with prolonged patient survival[42].

Although some authors claim that *LINE1* demethylation in tumours represents a valuable target for early diagnosis, furthermore, rapid and systematic screenings of *LINE1* methylation are already available[114]; results taken from the literature are still controversial. Therefore, we conducted a detailed study which comprised 46 primary melanomas, and measured at 6 *LINE1* CpG sites using quantitative pyrosequencing. In contrast to Sigalotti's research group[42], we demonstrated a shortened relapse-free survival in *LINE 1* hypomethylation patients in all six CpG sites using the log-rank test. More importantly, using the same statistical approach as Sigalotti's group, the metastatic capacity was significantly associated with global hypomethylation for any of the 6 CpGs. When the primary melanomas with metastasis were divided into subgroups based on the number of metastases formed during the 5-year follow-up period, significantly different levels of global methylation were observed between the groups for the majority of CpGs. Our results contrast with the findings of Sigalotti's group. However, their study comprised cell cultures derived from homogeneous staged specimens, whereas our experiments were performed using primary melanomas characteristic of distinct clinical behaviour.

According to our results the *LINE1* hypomethylation status strongly predicts the metastatic capacity of primary melanomas suggesting the role of transposonal hypomethylation in the progression of primary melanomas.

In contrast to the transposable widespread hypomethylation, DNA hypermethylation (known also as localized or regional hypermethylation) is usually strictly localised to the transcriptionally active gene regions and promoters and directly inhibits gene expression. In the field of malignant melanoma epigenetics, there are substantial amounts of data available regarding gene silencing associated with the localised CpG hypermethylation of a specific gene promoter, which were recently reviewed by several groups [29,36,50].

In addition to the rapid progress that has been made in studying promoter hypermethylation at the single-gene level, only two groups have attempted to conduct array-based experiments to identify the methylation pattern of thousands of gene promoters[26]. Regrettably, one group has focused only on comparing the methylation level of primary invasive melanomas with

benign melanocytes and has clearly identified a group of genes in a statistically powerful interpretation that can be used to discriminate naevi from melanomas based on their methylation signature. Another group has examined the short-term cultures of homogeneous stage III specimens[115].

As no data are currently available regarding the methylation markers of diverse melanomas with different clinical behaviours, we performed a systematic comparison of localised methylation patterns among 42 primary melanomas using the Illumina Golden Gate Cancer Panel Bead Assay. We found 111 differentially methylated CpGs altogether among melanoma subgroups and the majority of CpG sites were hypermethylated in melanomas that represent more favourable prognoses including a non-ulcerated tumour surface, superficial spreading histological subtype, non-metastatic subgroup and smaller tumour thickness (Breslow thickness < 2 mm). Regarding more advanced-stage specimens, the hypermethylome detected in melanomas that represents better prognoses markedly decreased. The decrease in the methylation levels occurred gradually, as the continuous Breslow thickness variables allowed us to distinguish more than two groups among primary melanomas and to map the progress of demethylation during distinct stages (Breslow thickness < 2 mm; Breslow thickness 2 - 4 mm; Breslow thickness > 4 mm). The genes involved in demethylation partially overlap among clinical subgroups: five genes (*EMR3*, *SEPT9*, *IL8*, *MMP14* and *SLC22A18*) were found to be commonly demethylated in large (Breslow thickness > 4 mm), nodular subtype, ulcerated and metastatic melanomas. The *SEPT9* gene is an ovarian tumour suppressor playing a role in cell cycle control; IL8 gene expression is elevated in metastatic melanomas and can increase the level of *MMP2*; *SLC22A18* has been reported to be down-regulated due to promoter hypermethylation in gliomas; *MMP14* has not been found to play a role in melanoma progression thus far. Among the aforementioned clinical groups, the largest similarity (27 overlapping genes) has been detected between the demethylated genes associated with Breslow thickness and ulceration. The histologic subtype represents the most unique methylation pattern, comprising 30 differentially methylated genes between superficial and nodular melanomas.

Our results contrast those of studies describing hypermethylation patterns of specific genes as tumour progression-related markers based on single gene approaches[29,50]. We have rather seen the loss of methylation related to progression steps, suggesting a more complexity and dynamics of DNA methylation events. Similarly, Conway et al. supported the claim that a covalent change from cytosine to 5-methylcytosine in the promoter region occurs as an early aberration event in melanomas[26]. Notwithstanding, their results highlighted not only the

hypermethylated but also the large extent of demethylated genes in heterogeneous melanomas compared to naevi. Taking a global view of how DNA methylation is associated with the distinct progression steps, it seems that methylation changes play more important role in the initiation of melanoma and accompany the earlier stages of melanomas.

Apart from the clinicopathological characteristics of melanomas, *BRAF*^{V600E} mutation was found to be individually associated with the CpG methylation changes of 23 genes that are related to Cell Communication and ECM-receptor interaction networks. We detected mainly the hypermethylation pattern in these genes with lack of overlap with those genes that are altered during the progression steps. A similar association between the *BRAF*^{V600E} mutation and DNA methylation was described in colon cancer[116,117], as methylated samples convincingly represented a distinct subset encompassing almost all cases of tumours with the *BRAF*^{V600E} mutation. Previously, a single group published two independent studies regarding *in vitro* data that demonstrated how the *BRAF*^{V600E} mutation causes widespread alterations in DNA methylation. A remarkable study performed by Roon et al. revealed the *BRAF*^{V600E} mutation-specific hypermethylation of CpG regions in colon cancer samples by Differential Methylation Hybridization on high-density oligonucleotide microarrays. Interestingly, the authors identified several cancer-related pathways, including the PI3 kinase and Wnt signaling pathways being differentially methylated between *BRAF*^{V600E} mutant and wild type samples. Additionally, the group found the silencing of *FOXD3* hypermethylated manner. Based on these studies, authors suggest that a specific epigenetic pattern can contribute to a favorable context for the acquisition of *BRAF*^{V600E} mutations. However, further studies are warranted to further clarify the relationship between the mutation and DNA methylation.

With regard to the effects of DNA hypermethylation on melanoma patients' survival, correcting for clinical cofounders, only the *KIT* gene was associated with a lower overall survival rate. Considering the oncogenic status of the *KIT* gene that is targeted by imatinib therapy, our results are hard to interpret. Our contradictory result can possibly be due to another epigenetic mechanism discovered in 2009 and known as 5-hydroxy-methyl-cytosin (5-hm-C), the sixth base of the DNA. Compared to 5-methyl-cytosin (5-m-C), 5-hm-C adversely affects and enhances the gene expression[118].

Although the precise mechanism of action and regulation of 5-hm-C is being investigated; the presence of a new base in melanomas has also been demonstrated. Since detection methods used 2-3 years ago cannot distinguish between the two different types of methylation, the *KIT* gene hydroxymethylation was possibly detected, which can cause gene upregulation. The

novel type of DNA methylation indicates the partial limitation of our results as well as all the experiments done before 2012 in melanoma[14]. In the future, the extent of the *KIT* gene 5-hm-C should be investigated along with a revised survival analysis.

Overall, we detected 131 differentially methylated genes: 111 genes associate with the clinicopathological parameters and 23 methylated genes accompany *BRAF*^{V600E} mutation, while – as it was given in Figure 15 at the "Results" part – 3 genes overlapped.

Taking a global view of the available published data (as shown in Figure 24), the genes that were previously reported [36]and reviewed by several groups to be hypermethylated based on single gene approaches[29], show a lack of a lack of similarity – involving only two genes, namely, *RUNX3* and *SYK* – with the single Bead Assay study conducted by Conway et al. and compared heterogeneous melanomas with benign naevi samples[26].

Broad agreement has not been revealed between our data and the results of other groups which might be due to the fact that our samples represent solely the primary tumours with differing biological properties.

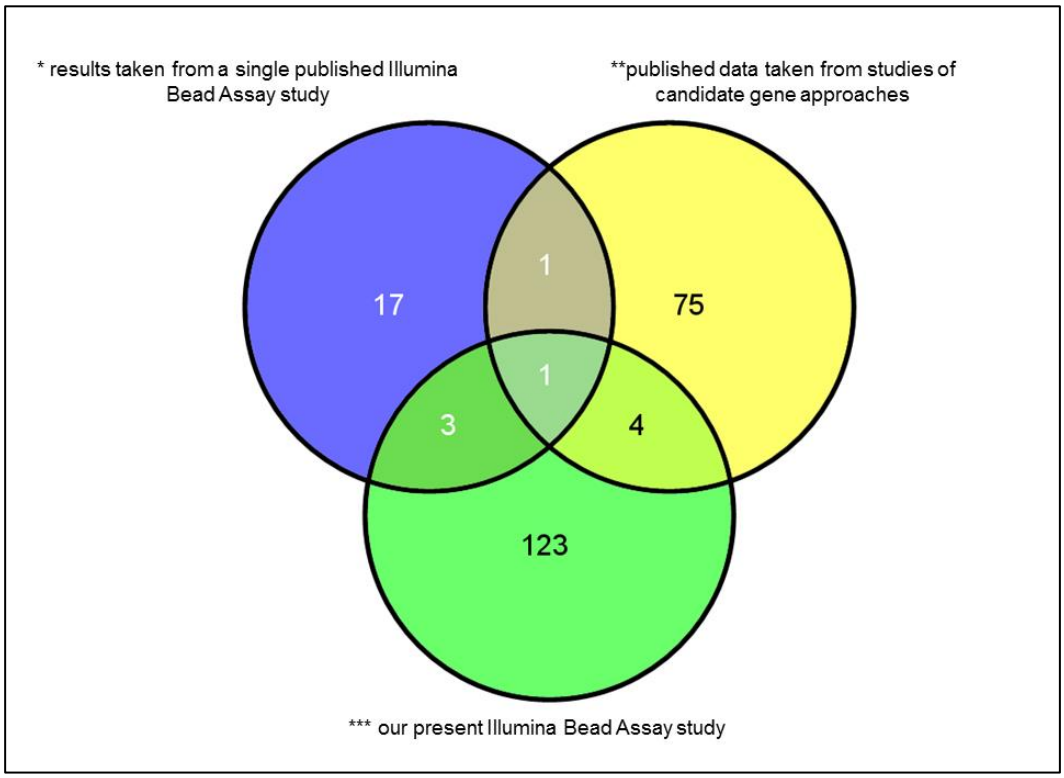

Figure 24 ***Overlap between the published data and our present study***

** a single study was published using the same Illumina Methylation Bead Assay method by Conway et al.[26], the study focused on comparing primary melanomas versus benign naevi samples; ** to date more than 80 genes have been reported to be differentially methylated based on candidate gene approaches[29,36,50]; *** our present study reported 129 differentially methylated genes corresponding to clinical variables and BRAF*^{V600E} *mutation)*

In addition to the common mutations, specific patterns of CN alterations have been reported in melanomas characteristic of unfavourable clinical outcomes. Furthermore, it has become obvious that *BRAF*^{V600E} mutated melanomas display distinct patterns for CN changes, providing the first line of evidence in support of Knudson's two-hit hypothesis[93,119-121]. However, none of the published studies attempted to evaluate the relationship between CN alterations and DNA methylation in melanomas. Our group performed a Tiling Array CGH, and, apart from highlighting common CN losses and amplification in the subgroups of primary melanomas, we demonstrated that 6q12-6q25.1 comprises a remarkable CN loss, harbouring two hypermethylated genes on 6q23, *EYA4* and *MYB1*. This result was measured and verified quantitatively and provides evidence for Knudson's two-hit hypothesis at the level of CN loss and DNA hypermethylation. Notably, *MYB1* is an important discriminator between melanomas and naevi, as validated by FISH in 123 melanomas and 110 naevi. The copy number deletion of *MYB1* is currently used in the diagnosis of melanoma.

Our Tiling Array CGH experiments showed another important feature: the CN alterations of chromosome 19 were only detected in advanced staged primary melanomas. Notably, the altered genomic regions encompass 19p13.2, which harbours the *DNMT1* gene (DNA Methyltransferase-1), which plays a role in the establishment and regulation of tissue-specific patterns of methylated cytosine residues. The DNA CN alterations of *DNMT1* in advanced stages primary melanomas raise crucial questions: Is demethylation, contributing to clinical outcomes, only a passive consequence of CN loss? Or do CN alterations – as was demonstrated in the context of epigenetic mechanisms and the *BRAF*^{V600E} mutation – directly control the DNA methylation changes to influence the gene expression patterns of given molecules? Similar findings were only published in mesotheliomas[122].

Regardless of the reason for changes in methylation, we obtained better insight into how gene expression levels are regulated by DNA methylation: demethylation was associated with increased mRNA levels, whereas hypermethylation was associated with decreased levels.

Summarizing our DNA methylation studies, we demonstrated the strong influence of DNA methylation changes on melanoma progression. However, hypermethylation, which has been greatly emphasised in the literature, appears to represent more complexity both in melanoma initiation and progression. Additionally, the inhibition of promoter hypermethylation might represent the most promising therapeutic target for the treatment of melanoma, and several types of DNMT inhibitors are currently being developed. Considering the dual role of DNA methylation, further efforts are needed to investigate the importance of such drugs in melanoma treatment. Future studies are warranted in investigating the role of DNA

methylation in the melanoma tumourigenesis; it is also crucial to describe the characteristics of DNA methylation triggered by environmental factors such as UV exposure.

Further studies on the extent and functional consequence of *DNMT1* deletion might be important for the controversial issues of therapeutic interventions that target directly the *DNMT1*. *DNMT1* deletion can result in disrupted methylation maintenance in a subgroup of melanomas, and hence, targeting a non-functional enzyme might be less preferable.

The phenotype of malignant melanoma is the result of a constellation of somatic alterations[87,93]. Integrative genomic approaches have recently afforded the opportunity to profile multiple types of alterations on a genome-wide scale in the context of gene expression and function.

Array CGH is currently the best tool for searching for non-random DNA copy number alterations in cancer genomes and finding new genes that harbour copy number gains or losses with prognostic relevance. As a result of improved resolution, there is currently an abundance of CGH data available in both large genomic regions and for uniquely affected genes. However, these studies focused little on elucidating the genomic alterations that contribute to gene regulation. Valseria et al. were the first to highlight SCNA (somatic copy number alteration) genes[123]. The downregulation and upregulation of these genes is accompanied by genomic losses or gains in melanoma. Because the experiments were based on a metastatic cell line, the aforementioned authors failed to find any progression-related clinical effects associated with these SNCA genes[123].

For obtaining a more generalized insights into the molecular mechanisms that might be responsible for the aggressive phenotype associated with the observed gene expression signature of ulcerated melanomas, we performed an extensive genome analysis by integrating DNA copy number and methylation results with the gene expression changes revealed in ulcerated vs. non-ulcerated melanomas.

The main purpose of this part of the present study was to give functional relevance to the copy number events by providing a statistically powerful integrated interpretation of gene expression changes and copy number alterations. Based on our aCGH analyses, we found more regions on chromosome 6q and only one region on chromosome 10q that showed significantly different loss of copy numbers between the two clinical subgroups. It is important to note that these regions were enriched for the downregulated transcripts and significantly correlated with our previously defined gene expression results. There are a total of 36 genes in these two regions, among which we identified 10 downregulated transcripts

using the Affymetrix microarray. It is important to note that these genes include *TPBG, PERP* and *UTRN*, which are involved in cell-cell and cell-matrix adhesion. *PERP* also functions as a p53-induced apoptosis effector molecule. Furthermore, *TPD52L1* participates in apoptosis followed by nuclear fragmentation. According to the literature, *IL20RA* is a tissue-specific Interleukin Receptor that is highly expressed in normal skin[124]. The remaining 5 genes could not be directly associated with carcinogenesis; however, a detailed, functional analysis is needed to precisely define the role of each of the new genes we have identified. It is worth noting that previous high-resolution aCGH experiments have also provided convincing evidence of the importance of copy number alterations at 6q, as this region often experiences hemizygous deletion, with *MYB1* being the only gene specified on 6q23[92,125]. These experiments also suggest that copy number alterations in *MYB1* are an important discriminator between melanomas and nevi, as validated by FISH in 123 melanomas and 110 nevi[126]. This study supports the assumption that 6q23 can assist in the diagnosis of melanoma. In agreement with previous findings, we further support the idea that the deletion of 6q23 is an important alteration in melanoma progression. However, it should also be pointed out those additional new genes (*IL20RA, HEPB2 and PERP*) that are located in this region and are downregulated might make significant contributions to melanoma progression. In addition to 6q23, we found a significant association between the tendency towards gene deregulation and DNA sequence deletions at 6q14, 6q16, 6q22, 6q24 and 6q25. Somatic copy number alterations at 10q were characterised in many cases, but particularly attributed to the *PTEN* tumour suppressor gene.

While systematic correlation analysis among the copy number events and the corresponding genes captures cis- effects it is also important to measure trans- acting copy number alterations which occur at a given genomic loci and can affect the mRNA expressions of distant genes[106].

For the latter purpose we used „lol" R package which was introduced by Yuan et al., and provided an appropriate method for validating the cis- acting elements as well[106].

Regarding the trans- regulatory copy number elements, the top scoring ($Score_{trans}$) alterations included copy number gains and losses, however, both types of alterations were associated with transcriptomic deregulation. The week immunostaning of EZR protein in the majority of melanomas was mentioned by a single study; however, this phenomenon was not associated with ulceration[127]. In our study, we showed that *EZR* (6q25.3) deregulation was related to the copy number loss of 6q27 and the copy number gain of 17q22 suggesting the trans-regulatory effects of these copy number alterations. Frequent loss of 9p21 region is a well characterized

copy number aberration in melanomas[128,129]; however, it has not been mentioned as a trans-regulatory element for Anoctamin 1 gene (11q13.3) so far. As our results demonstrated, the transcriptomic regulation of this gene can be possibly disturbed also by copy number loss of 9q21.11 and 7q11.23 regions.

By correlating 45 overlapping genes between the gene expression dataset and the methylation assays, we identified 11 genes that exhibited inverse relationships. Two of the 11 genes (*EPHB3, EPHB6)* are members of the erythropoietin-producing hepatocyte kinase B (*EPHB*) receptor family. Both of these genes play a suggested role in tumour suppression via regulating cell adhesion and migration. In addition, these genes have downstream effects on several members of the kallikrein family, which we also found to be downregulated in ulcerated melanomas in line with other groups[82]. Based on our data, we assumed that the downregulation of 2 fibroblast growth factor receptors (*FGFR2, FGFR3*) probably resulted from promoter hypermethylation of the coding genes. In the literature, downregulation of the remaining genes (*CDH13, DST, ETS2, JAG1, ITGA2, PTGS1, TIAM1*) have not been mentioned due to promoter hypermethylation so far.

Even with no detection of direct relationship of ulceration and promoter methylation, the above mentioned inverse correlations support the claim that similarly to copy number variation; promoter hypermethylation also plays an important role in transcriptomic silencing. Notably, it was suggested in the literature that Knudson's two-hit hypothesis is often achieved through a combination of DNA methylation and copy number alteration to the same gene[122,130]. Due to limitation of our studies, parallel detection of both types of somatic alterations was not achieved in primary melanomas. Nevertheless, the inverse relation between gene expression and methylation of the corresponding genes, together with global presence of copy number alteration should be taken into consideration, which suggests that somatic aberrations do not act separately but represent different utility in an integrated apparatus that acts together and develops transcriptomic silencing in ulcerated melanomas.

In summary, this study has provided evidence that the gene expression signatures of primary melanomas are suitable for distinguishing patients with poor and favourable prognoses. We have also shown that different patterns of genetic and epigenetic aberrations associated with distinct molecular subtypes of the disease contribute to the specific transcriptomic profiles of these genes. We believe that our systematic correlation of gene regulation, methylation pattern and the DNA copy number alteration data in the same cohort of primary melanomas will be useful for finding new genes and will allow further functional utilisation of those genes. This study has important implications as we continue to develop a better understanding

of melanoma progression, which will allow us to identify specific genes for use as prognostic markers in future studies.

Summary

The main purpose of the doctoral thesis was to provide a comprehensive genetic and epigenetic study to define somatic DNA alterations that contribute to the aggressive biological behavior of human primary melanomas.

1. **Investigating genome-wide (transposable) DNA methylation:**
   - We demonstrated the strong influence of *LINE1* transposable demethylation in the metastatic formation of primary melanomas during the follow-up period.
2. **Studying regional (localized) DNA methylation:**
   - The methylome, presenting in early stage samples and associated with the *BRAF*^{V600E} mutation, decreased in the more advanced stages of the disease.
   - Local coordinated allele loss and DNA hypermethylation was shown at the region of 6q22-q23 that encodes the *MYB1* and *EYA4* genes.
   - We revealed that the 19p13.2 genomic region harboring *DNMT1* gene (DNA methyltransferase-1 responsible for the maintenance of methylation patterns during DNA replication) often suffers from DNA copy number loss in melanomas thicker than 4 mm.
   - The DNA methylation changes of the *KIT* gene was significantly associated with shortened relapse-free survival in melanoma patients.
3. **Integrative genomic analysis:**
   - A set of genes with copy number loss were defined in ulcerated malignant melanomas, which were significantly enriched on chromosome 6q and 10q. Most of the genes were involved in cell-cell and cell-matrix adhesion or apoptosis.
   - The first evidence for trans-acting copy number changes was given in melanomas.
   - The expression and methylation patterns of additional genes exhibited an inverse correlation, suggesting that transcriptional silencing of these genes is driven by epigenetic events.

In conclusion, we demonstrated the strong influence of genome-wide as well as regional DNA methylation changes on melanoma progression. Methylation pattern was demonstrated to be a part of an integrated apparatus of somatic DNA alterations. We identified functionally relevant molecular hotspots characterised by copy number losses and promoter hypermethylation that might indicate a poor clinical outcome of melanoma.

Összefoglalás

A doktori disszertáció egyik fő célja volt, hogy átfogó képet alkosson a primer malignus melanoma agresszív biológiai viselkedésével összefüggő genetikai és epigenetikai változásokról.

1. **Genom szintű (transzpozonális) DNS metilációs analízis:**
   - Eredményeink alapján a *LINE1* transzpozon szekvencia hipometilációja kapcsolatba hozható a primer melanomák áttétképző képességével.
2. **Regionális (lokalizált) DNS metilációs vizsgálatok:**
   - A *BRAF*^{V600E} mutációt hordozó mintákat, továbbá a korai stádiumú melanomákat egyedi hipermetilációs mintázat jellemzi, mely csökken a daganat progressziója során.
   - Lokális, összehangolt kópiaszám csökkenést és DNS hipermetilációt figyeltünk meg a *MYB1 és EYA4* géneket kódoló 6q22-q23 kromoszóma szakaszon.
   - A *DNMT1* gént (fenntartó metiltranszferáz, mely a kialakult metilációs mintázat örökítéséért felel a DNS replikáció során) kódoló szakasz gyakran szenved deléciót a 4 mm-nél vastagabb daganatokban.
   - Megállapítottuk, hogy a *KIT* gén hipermetilációja a melanomás betegek csökkent 5 éves túlélésével társul.
3. **Integrált genom analízis:**
   - A kifekélyesedő felszínű melanomákban számos kópiaszám csökkenést detektáltunk, melyeket a 6q és 10q kromoszóma szakaszokon láttunk. A gének többsége a sejt-sejt, sejt-mártrix és az apoptózisban részt vevő fehérjéket kódolnak.
   - Elsőként mutattunk ki a melanomákban transz-irányba ható kópiaszám változásokat.
   - Megfigyeltük a génexpressziós és DNS metiláció inverz korrelációját, mely jelenség az epigenetikai mechanizmusok transzkripciós szabályozását erősítik melanoma progresszió során.

Eddigi eredményeink alapján mind a genom szintű, mind a regionális metilációs változások hozzájárulnak a melanoma progressziójához. Kimutattuk, hogy a DNS metilációs változások a kópiaszám eltérésekkel együtt működve járulnak hozzá a melanoma megváltozott fenotípusához. Integrált genom analízisünk segítségével ún. genomi forrópontokat azonosítottunk, továbbá a kópiaszám változások hatását távolabbi génekre is kimutattuk.

References

1. Godar, D.E. Worldwide increasing incidences of cutaneous malignant melanoma. *J Skin Cancer* **2011**, 858425 (2011).
2. Braeuer, R.R. et al. Why is melanoma so metastatic? *Pigment Cell Melanoma Res* **27**, 19-36 (2014).
3. Balk, S.J. Ultraviolet radiation: a hazard to children and adolescents. *Pediatrics* **127**, e791-817 (2011).
4. Herlyn, M., Berking, C., Li, G. & Satyamoorthy, K. Lessons from melanocyte development for understanding the biological events in naevus and melanoma formation. *Melanoma Res* **10**, 303-12 (2000).
5. Guitera, P. et al. Melanoma histological Breslow thickness predicted by 75-MHz ultrasonography. *Br J Dermatol* **159**, 364-9 (2008).
6. Fisher, N.M., Schaffer, J.V., Berwick, M. & Bolognia, J.L. Breslow depth of cutaneous melanoma: impact of factors related to surveillance of the skin, including prior skin biopsies and family history of melanoma. *J Am Acad Dermatol* **53**, 393-406 (2005).
7. Balch, C.M. et al. The prognostic significance of ulceration of cutaneous melanoma. *Cancer* **45**, 3012-7 (1980).
8. Grande Sarpa, H. et al. Prognostic significance of extent of ulceration in primary cutaneous melanoma. *Am J Surg Pathol* **30**, 1396-400 (2006).
9. Marghoob, A.A., Koenig, K., Bittencourt, F.V., Kopf, A.W. & Bart, R.S. Breslow thickness and clark level in melanoma: support for including level in pathology reports and in American Joint Committee on Cancer Staging. *Cancer* **88**, 589-95 (2000).
10. Roberts, D.L. et al. U.K. guidelines for the management of cutaneous melanoma. *Br J Dermatol* **146**, 7-17 (2002).
11. Hodis, E. et al. A landscape of driver mutations in melanoma. *Cell* **150**, 251-63 (2012).
12. Krauthammer, M. et al. Exome sequencing identifies recurrent somatic RAC1 mutations in melanoma. *Nat Genet* **44**, 1006-14 (2012).
13. Rothhammer, T. & Bosserhoff, A.K. Epigenetic events in malignant melanoma. *Pigment Cell Res* **20**, 92-111 (2007).
14. Lian, C.G. et al. Loss of 5-hydroxymethylcytosine is an epigenetic hallmark of melanoma. *Cell* **150**, 1135-46 (2012).
15. Sawan, C., Vaissiere, T., Murr, R. & Herceg, Z. Epigenetic drivers and genetic passengers on the road to cancer. *Mutat Res* **642**, 1-13 (2008).
16. Herceg, Z. & Vaissiere, T. Epigenetic mechanisms and cancer: an interface between the environment and the genome. *Epigenetics* **6**, 804-19 (2011).
17. Richards, H.W. & Medrano, E.E. Epigenetic marks in melanoma. *Pigment Cell Melanoma Res* **22**, 14-29 (2009).
18. Sigalotti, L., Fratta, E., Parisi, G., Coral, S. & Maio, M. Epigenetic markers of prognosis in melanoma. *Methods Mol Biol* **1102**, 481-99 (2014).
19. Herceg, Z. Epigenetics and cancer: towards an evaluation of the impact of environmental and dietary factors. *Mutagenesis* **22**, 91-103 (2007).
20. Herceg, Z. & Hainaut, P. Genetic and epigenetic alterations as biomarkers for cancer detection, diagnosis and prognosis. *Mol Oncol* **1**, 26-41 (2007).
21. El-Osta, A. DNMT cooperativity--the developing links between methylation, chromatin structure and cancer. *Bioessays* **25**, 1071-84 (2003).

22. Cheng, X. & Blumenthal, R.M. Mammalian DNA methyltransferases: a structural perspective. *Structure* **16**, 341-50 (2008).
23. Guryanova, O. & Levine, R. DNMT3A and stem cell function: new insights into old pathways. *Haematologica* **97**, 324 (2012).
24. Esteller, M. Cancer epigenetics: DNA methylation and chromatin alterations in human cancer. *Adv Exp Med Biol* **532**, 39-49 (2003).
25. Figueiredo, L.M., Cross, G.A. & Janzen, C.J. Epigenetic regulation in African trypanosomes: a new kid on the block. *Nat Rev Microbiol* **7**, 504-13 (2009).
26. Conway, K. et al. DNA-methylation profiling distinguishes malignant melanomas from benign nevi. *Pigment Cell Melanoma Res* **24**, 352-60 (2011).
27. Furuta, J. et al. Promoter methylation profiling of 30 genes in human malignant melanoma. *Cancer Sci* **95**, 962-8 (2004).
28. Marini, A. et al. Epigenetic inactivation of tumor suppressor genes in serum of patients with cutaneous melanoma. *J Invest Dermatol* **126**, 422-31 (2006).
29. Sigalotti, L. et al. Epigenetics of human cutaneous melanoma: setting the stage for new therapeutic strategies. *J Transl Med* **8**, 56 (2010).
30. Schraml, P. et al. Predictive value of the MGMT promoter methylation status in metastatic melanoma patients receiving first-line temozolomide plus bevacizumab in the trial SAKK 50/07. *Oncol Rep* **28**, 654-8 (2012).
31. Liu, S., Ren, S., Howell, P., Fodstad, O. & Riker, A.I. Identification of novel epigenetically modified genes in human melanoma via promoter methylation gene profiling. *Pigment Cell Melanoma Res* **21**, 545-58 (2008).
32. Lahtz, C., Stranzenbach, R., Fiedler, E., Helmbold, P. & Dammann, R.H. Methylation of PTEN as a prognostic factor in malignant melanoma of the skin. *J Invest Dermatol* **130**, 620-2 (2010).
33. Fan, J.B. et al. Illumina universal bead arrays. *Methods Enzymol* **410**, 57-73 (2006).
34. Hernandez-Vargas, H. et al. Hepatocellular carcinoma displays distinct DNA methylation signatures with potential as clinical predictors. *PLoS One* **5**, e9749 (2010).
35. Hernandez-Vargas, H. et al. Methylome analysis reveals Jak-STAT pathway deregulation in putative breast cancer stem cells. *Epigenetics* **6**, 428-39 (2011).
36. Howell, P.M., Jr. et al. Epigenetics in human melanoma. *Cancer Control* **16**, 200-18 (2009).
37. James, S.J. et al. Mechanisms of DNA damage, DNA hypomethylation, and tumor progression in the folate/methyl-deficient rat model of hepatocarcinogenesis. *J Nutr* **133**, 3740S-3747S (2003).
38. Wild, L. & Flanagan, J.M. Genome-wide hypomethylation in cancer may be a passive consequence of transformation. *Biochim Biophys Acta* **1806**, 50-7 (2010).
39. Metivier, R. et al. Cyclical DNA methylation of a transcriptionally active promoter. *Nature* **452**, 45-50 (2008).
40. Tellez, C.S. et al. CpG island methylation profiling in human melanoma cell lines. *Melanoma Res* **19**, 146-55 (2009).
41. Hyland, P.L. et al. LINE-1 methylation in peripheral blood and the risk of melanoma in melanoma-prone families with and without CDKN2A mutations. *Melanoma Res* **23**, 55-60 (2013).
42. Sigalotti, L. et al. Methylation levels of the "long interspersed nucleotide element-1" repetitive sequences predict survival of melanoma patients. *J Transl Med* **9**, 78 (2011).
43. Grunau, C. et al. BAGE hypomethylation, a new epigenetic biomarker for colon cancer detection. *Cancer Epidemiol Biomarkers Prev* **17**, 1374-9 (2008).

44. Luo, J., Li, Y.N., Wang, F., Zhang, W.M. & Geng, X. S-adenosylmethionine inhibits the growth of cancer cells by reversing the hypomethylation status of c-myc and H-ras in human gastric cancer and colon cancer. *Int J Biol Sci* **6**, 784-95 (2010).
45. Son, K.S. et al. Hypomethylation of the interleukin-10 gene in breast cancer tissues. *Breast* **19**, 484-488 (2010).
46. Kong, L.M. et al. Promoter hypomethylation up-regulates CD147 expression through increasing Sp1 binding and associates with poor prognosis in human hepatocellular carcinoma. *J Cell Mol Med* **15**, 1415-28 (2011).
47. Kaneko, Y. et al. Hypomethylation of c-myc and epidermal growth factor receptor genes in human hepatocellular carcinoma and fetal liver. *Jpn J Cancer Res* **76**, 1136-40 (1985).
48. Feinberg, A.P., Ohlsson, R. & Henikoff, S. The epigenetic progenitor origin of human cancer. *Nat Rev Genet* **7**, 21-33 (2006).
49. Levati, L. et al. Altered expression of selected microRNAs in melanoma: antiproliferative and proapoptotic activity of miRNA-155. *Int J Oncol* **35**, 393-400 (2009).
50. Burgess, D.J. Epigenetics: Melanoma insights written in the DNA. *Nat Rev Cancer* **12**, 738-9 (2012).
51. van den Hurk, K. et al. Genetics and epigenetics of cutaneous malignant melanoma: a concert out of tune. *Biochim Biophys Acta* **1826**, 89-102 (2012).
52. Penn, N.W., Suwalski, R., O'Riley, C., Bojanowski, K. & Yura, R. The presence of 5-hydroxymethylcytosine in animal deoxyribonucleic acid. *Biochem J* **126**, 781-90 (1972).
53. Tahiliani, M. et al. Conversion of 5-methylcytosine to 5-hydroxymethylcytosine in mammalian DNA by MLL partner TET1. *Science* **324**, 930-5 (2009).
54. Kriaucionis, S. & Heintz, N. The nuclear DNA base 5-hydroxymethylcytosine is present in Purkinje neurons and the brain. *Science* **324**, 929-30 (2009).
55. Koh, K.P. et al. Tet1 and Tet2 regulate 5-hydroxymethylcytosine production and cell lineage specification in mouse embryonic stem cells. *Cell Stem Cell* **8**, 200-13 (2011).
56. Pfeifer, G.P., Kadam, S. & Jin, S.G. 5-hydroxymethylcytosine and its potential roles in development and cancer. *Epigenetics Chromatin* **6**, 10 (2013).
57. Yamaguchi, S. et al. Dynamics of 5-methylcytosine and 5-hydroxymethylcytosine during germ cell reprogramming. *Cell Res* **23**, 329-39 (2013).
58. Palii, S.S., Van Emburgh, B.O., Sankpal, U.T., Brown, K.D. & Robertson, K.D. DNA methylation inhibitor 5-Aza-2'-deoxycytidine induces reversible genome-wide DNA damage that is distinctly influenced by DNA methyltransferases 1 and 3B. *Mol Cell Biol* **28**, 752-71 (2008).
59. Kaminskas, E., Farrell, A.T., Wang, Y.C., Sridhara, R. & Pazdur, R. FDA drug approval summary: azacitidine (5-azacytidine, Vidaza) for injectable suspension. *Oncologist* **10**, 176-82 (2005).
60. Rudek, M.A. et al. Pharmacokinetics of 5-azacitidine administered with phenylbutyrate in patients with refractory solid tumors or hematologic malignancies. *J Clin Oncol* **23**, 3906-11 (2005).
61. Schwabe, M. & Lubbert, M. Epigenetic lesions in malignant melanoma. *Curr Pharm Biotechnol* **8**, 382-7 (2007).
62. Yoo, C.B., Cheng, J.C. & Jones, P.A. Zebularine: a new drug for epigenetic therapy. *Biochem Soc Trans* **32**, 910-2 (2004).
63. Marquez, V.E. et al. Zebularine: a unique molecule for an epigenetically based strategy in cancer chemotherapy. *Ann N Y Acad Sci* **1058**, 246-54 (2005).

64. Herranz, M. et al. The novel DNA methylation inhibitor zebularine is effective against the development of murine T-cell lymphoma. *Blood* **107**, 1174-7 (2006).
65. Yang, P.M. et al. Zebularine inhibits tumorigenesis and stemness of colorectal cancer via p53-dependent endoplasmic reticulum stress. *Sci Rep* **3**, 3219 (2013).
66. Singh, V., Sharma, P. & Capalash, N. DNA methyltransferase-1 inhibitors as epigenetic therapy for cancer. *Curr Cancer Drug Targets* **13**, 379-99 (2013).
67. Jung, Y. et al. Potential advantages of DNA methyltransferase 1 (DNMT1)-targeted inhibition for cancer therapy. *J Mol Med (Berl)* **85**, 1137-48 (2007).
68. Amato, R.J. Inhibition of DNA methylation by antisense oligonucleotide MG98 as cancer therapy. *Clin Genitourin Cancer* **5**, 422-6 (2007).
69. Vanden Berghe, W. Epigenetic impact of dietary polyphenols in cancer chemoprevention: lifelong remodeling of our epigenomes. *Pharmacol Res* **65**, 565-76 (2012).
70. Hauser, A.T. & Jung, M. Targeting epigenetic mechanisms: potential of natural products in cancer chemoprevention. *Planta Med* **74**, 1593-601 (2008).
71. Gerhauser, C. Epigenetic impact of dietary isothiocyanates in cancer chemoprevention. *Curr Opin Clin Nutr Metab Care* **16**, 405-10 (2013).
72. Fini, L. et al. Chemopreventive properties of pinoresinol-rich olive oil involve a selective activation of the ATM-p53 cascade in colon cancer cell lines. *Carcinogenesis* **29**, 139-46 (2008).
73. Lecumberri, E., Dupertuis, Y.M., Miralbell, R. & Pichard, C. Green tea polyphenol epigallocatechin-3-gallate (EGCG) as adjuvant in cancer therapy. *Clin Nutr* **32**, 894-903 (2013).
74. Paliwal, A., Vaissiere, T. & Herceg, Z. Quantitative detection of DNA methylation states in minute amounts of DNA from body fluids. *Methods* **52**, 242-7 (2010).
75. Mirmohammadsadegh, A. et al. Epigenetic silencing of the PTEN gene in melanoma. *Cancer Res* **66**, 6546-52 (2006).
76. Bittner, M. et al. Molecular classification of cutaneous malignant melanoma by gene expression profiling. *Nature* **406**, 536-40 (2000).
77. Winnepenninckx, V. et al. Gene expression profiling of primary cutaneous melanoma and clinical outcome. *J Natl Cancer Inst* **98**, 472-82 (2006).
78. Jeffs, A.R. et al. A gene expression signature of invasive potential in metastatic melanoma cells. *PLoS One* **4**, e8461 (2009).
79. Timar, J., Gyorffy, B. & Raso, E. Gene signature of the metastatic potential of cutaneous melanoma: too much for too little? *Clin Exp Metastasis* **27**, 371-87 (2010).
80. Alonso, S.R. et al. A high-throughput study in melanoma identifies epithelial-mesenchymal transition as a major determinant of metastasis. *Cancer Res* **67**, 3450-60 (2007).
81. Jaeger, J. et al. Gene expression signatures for tumor progression, tumor subtype, and tumor thickness in laser-microdissected melanoma tissues. *Clin Cancer Res* **13**, 806-15 (2007).
82. Martins, W.K. et al. Gene network analyses point to the importance of human tissue kallikreins in melanoma progression. *BMC Med Genomics* **4**, 76 (2011).
83. Berger, M.F. et al. Integrative analysis of the melanoma transcriptome. *Genome Research* **20**, 413-27 (2010).
84. Kabbarah, O. et al. Integrative genome comparison of primary and metastatic melanomas. *PLoS One* **5**, e10770 (2010).
85. Ghosh, P. & Chin, L. Genetics and genomics of melanoma. *Expert Rev Dermatol* **4**, 131 (2009).

86. Curtin, J.A. et al. Distinct sets of genetic alterations in melanoma. *N Engl J Med* **353**, 2135-47 (2005).
87. Vizkeleti, L. et al. The role of CCND1 alterations during the progression of cutaneous malignant melanoma. *Tumour Biol* **33**, 2189-99 (2012).
88. Lazar, V. et al. Characterization of candidate gene copy number alterations in the 11q13 region along with BRAF and NRAS mutations in human melanoma. *Mod Pathol* **22**, 1367-78 (2009).
89. Garraway, L.A. et al. Integrative genomic analyses identify MITF as a lineage survival oncogene amplified in malignant melanoma. *Nature* **436**, 117-22 (2005).
90. Hoek, K.S. et al. Novel MITF targets identified using a two-step DNA microarray strategy. *Pigment Cell Melanoma Res* **21**, 665-76 (2008).
91. Cronin, J.C. et al. Frequent mutations in the MITF pathway in melanoma. *Pigment Cell Melanoma Res* **22**, 435-44 (2009).
92. Gast, A. et al. Somatic alterations in the melanoma genome: a high-resolution array-based comparative genomic hybridization study. *Genes Chromosomes Cancer* **49**, 733-45 (2010).
93. Lazar, V. et al. Marked genetic differences between BRAF and NRAS mutated primary melanomas as revealed by array comparative genomic hybridization. *Melanoma Res* **22**, 202-14 (2012).
94. Kim, M. et al. Comparative oncogenomics identifies NEDD9 as a melanoma metastasis gene. *Cell* **125**, 1269-81 (2006).
95. Plotar, V., Liszkay, G., Ladanyi, A. & Toth, E. [New TNM classification (AJCC 2009) and the pathological significance of sentinel lymph node biopsy in malignant melanoma]. *Magy Onkol* **57**, 68-72 (2013).
96. Fraga, M.F. & Esteller, M. DNA methylation: a profile of methods and applications. *Biotechniques* **33**, 632, 634, 636-49 (2002).
97. El-Maarri, O. Methods: DNA methylation. *Adv Exp Med Biol* **544**, 197-204 (2003).
98. Nilsson, T.K. & Johansson, C.A. A novel method for diagnosis of adult hypolactasia by genotyping of the -13910 C/T polymorphism with Pyrosequencing technology. *Scand J Gastroenterol* **39**, 287-90 (2004).
99. King, C.R. & Scott-Horton, T. Pyrosequencing: a simple method for accurate genotyping. *Methods Mol Biol* **373**, 39-56 (2007).
100. Vaissiere, T. et al. Quantitative analysis of DNA methylation after whole bisulfitome amplification of a minute amount of DNA from body fluids. *Epigenetics* **4**, 221-30 (2009).
101. Bibikova, M. & Fan, J.B. GoldenGate assay for DNA methylation profiling. *Methods Mol Biol* **507**, 149-63 (2009).
102. Bibikova, M. et al. High-throughput DNA methylation profiling using universal bead arrays. *Genome Research* **16**, 383-93 (2006).
103. Du, P. et al. Comparison of Beta-value and M-value methods for quantifying methylation levels by microarray analysis. *BMC Bioinformatics* **11**, 587 (2010).
104. Beroukhim, R. et al. Assessing the significance of chromosomal aberrations in cancer: methodology and application to glioma. *Proc Natl Acad Sci U S A* **104**, 20007-12 (2007).
105. Greenfield, S., Cretin, S., Worthman, L.G. & Dorey, F. The use of an ROC curve to express quality of care results. *Med Decis Making* **2**, 23-31 (1982).
106. Yuan, Y., Curtis, C., Caldas, C. & Markowetz, F. A sparse regulatory network of copy-number driven gene expression reveals putative breast cancer oncogenes. *IEEE/ACM Trans Comput Biol Bioinform* **9**, 947-54 (2012).

107. Balatoni, T., Liszkay, G., Miklos, Z. & Kasler, M. [Epidemiology of malignant melanoma (Clinical experience at the National Institute of Oncology in Hungary)]. *Orv Hetil* **152**, 1000-6 (2011).
108. Liszkay, G. [Vemurafenib (Zelboraf) in the therapy of melanoma]. *Magy Onkol* **57**, 110-3 (2013).
109. Carmona, F.J. & Esteller, M. DNA methylation in early neoplasia. *Cancer Biomark* **9**, 101-11 (2010).
110. Heyn, H. et al. DNA methylation contributes to natural human variation. *Genome Research* **23**, 1363-72 (2013).
111. Choi, J.Y. et al. Association between global DNA hypomethylation in leukocytes and risk of breast cancer. *Carcinogenesis* **30**, 1889-97 (2009).
112. Sunami, E., de Maat, M., Vu, A., Turner, R.R. & Hoon, D.S. LINE-1 hypomethylation during primary colon cancer progression. *PLoS One* **6**, e18884 (2011).
113. Hoshimoto, S. et al. AIM1 and LINE-1 epigenetic aberrations in tumor and serum relate to melanoma progression and disease outcome. *J Invest Dermatol* **132**, 1689-97 (2012).
114. Szekvolgyi, L. et al. Chip-on-beads: flow-cytometric evaluation of chromatin immunoprecipitation. *Cytometry A* **69**, 1086-91 (2006).
115. Sigalotti, L. et al. Whole genome methylation profiles as independent markers of survival in stage IIIC melanoma patients. *J Transl Med* **10**, 185 (2012).
116. Arain, M.A. et al. CIMP status of interval colon cancers: another piece to the puzzle. *Am J Gastroenterol* **105**, 1189-95 (2010).
117. Curtin, K., Slattery, M.L. & Samowitz, W.S. CpG island methylation in colorectal cancer: past, present and future. *Patholog Res Int* **2011**, 902674 (2011).
118. Munzel, M., Globisch, D. & Carell, T. 5-Hydroxymethylcytosine, the sixth base of the genome. *Angew Chem Int Ed Engl* **50**, 6460-8 (2011).
119. Gorden, A. et al. Analysis of BRAF and N-RAS mutations in metastatic melanoma tissues. *Cancer Res* **63**, 3955-7 (2003).
120. Johansson, P., Pavey, S. & Hayward, N. Confirmation of a BRAF mutation-associated gene expression signature in melanoma. *Pigment Cell Res* **20**, 216-21 (2007).
121. Sakaizawa, K. et al. Mutation analysis of BRAF and KIT in circulating melanoma cells at the single cell level. *Br J Cancer* **106**, 939-46 (2012).
122. Christensen, B.C. et al. Integrated profiling reveals a global correlation between epigenetic and genetic alterations in mesothelioma. *Cancer Res* **70**, 5686-94 (2010).
123. Freedman, J.A., Tyler, D.S., Nevins, J.R. & Augustine, C.K. Use of gene expression and pathway signatures to characterize the complexity of human melanoma. *Am J Pathol* **178**, 2513-22 (2011).
124. Blumberg, H. et al. Interleukin 20: discovery, receptor identification, and role in epidermal function. *Cell* **104**, 9-19 (2001).
125. Stark, M. & Hayward, N. Genome-wide loss of heterozygosity and copy number analysis in melanoma using high-density single-nucleotide polymorphism arrays. *Cancer Res* **67**, 2632-42 (2007).
126. Palmieri, D. et al. Analyses of resected human brain metastases of breast cancer reveal the association between up-regulation of hexokinase 2 and poor prognosis. *Mol Cancer Res* **7**, 1438-45 (2009).
127. Ilmonen, S., Vaheri, A., Asko-Seljavaara, S. & Carpen, O. Ezrin in primary cutaneous melanoma. *Mod Pathol* **18**, 503-10 (2005).
128. Rakosy, Z. et al. Characterization of 9p21 copy number alterations in human melanoma by fluorescence in situ hybridization. *Cancer Genet Cytogenet* **182**, 116-21 (2008).

129. Conway, C. et al. Deletion at chromosome arm 9p in relation to BRAF/NRAS mutations and prognostic significance for primary melanoma. *Genes Chromosomes Cancer* **49**, 425-38 (2010).
130. Christensen, B.C. et al. Epigenetic profiles distinguish pleural mesothelioma from normal pleura and predict lung asbestos burden and clinical outcome. *Cancer Res* **69**, 227-34 (2009).

Publications

UNIVERSITY OF DEBRECEN
UNIVERSITY AND NATIONAL LIBRARY
PUBLICATIONS

Register number: DEENKÉTK/85/2014.
Item number:
Subject: Ph.D. List of Publications

Candidate: Szilvia Ecsedi

Neptun ID: ZWZDQM

Doctoral School: Doctoral School of Health Sciences

Mtmt ID: 10020957

List of publications related to the dissertation

1. **Ecsedi, S.I.**, Hernandez-Vargas, H., Lima, S.C., Vízkeleti, L., Tóth, R., Lázár, V., Koroknai, V., Kiss, T., Emri, G., Herceg, Z., Ádány, R., Balázs, M.: DNA methylation characteristics of primary melanomas with distinct biological behaviour.
PloS One. "accepted by publisher", 2014.
IF:3.73 (2012)

2. **Ecsedi, S.I.**, Hernandez-Vargas, H., Lima, S.C., Herceg, Z., Ádány, R., Balázs, M.: Transposable hypomethylation is associated with metastatic capacity of primary melanomas.
Int. J. Clin. Exp. Pathol. 6 (12), 2343-2348, 2013.
IF:2.242 (2012)

3. Rákosy, Z., **Ecsedi, S.**, Tóth, R., Vízkeleti, L., Hernandez-Vargas, H., Lázár, V., Emri, G., Szatmári, I., Herceg, Z., Ádány, R., Balázs, M.: Integrative genomics identifies gene signature associated with melanoma ulceration.
PLoS One. 8 (1), e54958, 2013.
DOI: http://dx.doi.org/10.1371/journal.pone.0054958
IF:3.73 (2012)

4. Balázs, M., **Ecsedi, S.**, Vízkeleti, L., Bégány, Á.: Genomics of human malignant melanoma.
In: Breakthroughs in Melanoma Research. Ed.: Yohei Tanaka, InTech, Rijeka, 237-263, 2011.

List of other publications

5. **Ecsedi, S.**, Tóth, L., Balázs, M.: Array CGH analysis of the rare laryngeal basaloid squamous cell carcinoma: A case report.
Int. J. Clin. Exp. Pathol. 5 (8), 834-839, 2012.
IF:2.242

6. Lázár, V., **Ecsedi, S.**, Vízkeleti, L., Rákosy, Z., Boross, G., Szappanos, B., Bégány, Á., Emri, G., Ádány, R., Balázs, M.: Marked genetic differences between BRAF and NRAS mutated primary melanomas as revealed by array comparative genomic hybridization.
Melanoma Res. 22 (3), 202-214, 2012.
DOI: http://dx.doi.org/10.1097/CMR.0b013e328352dbc8
IF:2.518

7. Vízkeleti, L., **Ecsedi, S.**, Rákosy, Z., Bégány, Á., Emri, G., Tóth, R., Orosz, A., Szöllősi, A., Méhes, G., Ádány, R., Balázs, M.: Prognostic relevance of the expressions of CAV1 and TES genes on 7q31 in melanoma.
Front Biosci (Elite Ed). E4 (1), 1802-1812, 2012.
DOI: http://dx.doi.org/10.2741/501

8. Vízkeleti, L., **Ecsedi, S.**, Rákosy, Z., Orosz, A., Lázár, V., Emri, G., Koroknai, V., Kiss, T., Ádány, R., Balázs, M.: The role of CCND1 alterations during the progression of cutaneous malignant melanoma.
Tumor Biol. 33 (6), 2189-2199, 2012.
DOI: http://dx.doi.org/10.1007/s13277-012-0480-6
IF:2.518

9. Juhász, A., Sziklai, I., Rákosy, Z., **Ecsedi, S.**, Ádány, R., Balázs, M.: Elevated level of tenascin and matrix metalloproteinase 9 correlates with the bone destruction capacity of cholesteatomas.
Otol. Neurotol. 30 (4), 559-565, 2009.
DOI: http://dx.doi.org/10.1097/MAO.0b013e31819fe6ed
IF:1.435

10. Lázár, V., **Ecsedi, S.**, Szöllősi, A., Tóth, R., Vízkeleti, L., Rákosy, Z., Bégány, Á., Ádány, R., Balázs, M.: Characterization of candidate gene copy number alterations in the 11q13 region along with BRAF and NRAS mutations in human melanoma.
Mod. Pathol. 22 (10), 1367-1378, 2009.
DOI: http://dx.doi.org/10.1038/modpathol.2009.109
IF:4.406

11. **Ecsedi, S.**, Rákosy, Z., Vízkeleti, L., Juhász, A., Sziklai, I., Ádány, R., Balázs, M.: Chromosomal imbalances are associated with increased proliferation and might contribute to bone destruction in cholesteatoma.
Otolaryngol. Head Neck Surg. 139 (5), 635-640, 2008.
DOI: http://dx.doi.org/10.1016/j.otohns.2008.07.019
IF:1.409

12. Rákosy, Z., Vízkeleti, L., **Ecsedi, S.**, Bégány, Á., Emri, G., Ádány, R., Balázs, M.: Characterization of the 9p21 copy number alterations in human melanoma by fluorescence in situ hybridization.
Cancer Genet. Cytogenet. 182 (2), 116-121, 2008.
DOI: http://dx.doi.org/10.1016/j.cancergencyto.2008.01.008
IF:1.482

13. Rákosy, Z., Vízkeleti, L., **Ecsedi, S.**, Vokó, Z., Bégány, Á., Barok, M., Krekk, Z., Gallai, M., Szentirmay, Z., Ádány, R., Balázs, M.: EGFR gene copy number alterations in primary cutaneous malignant melanomas are associated with poor prognosis.
Int. J. Cancer. 121 (8), 1729-1737, 2007.
DOI: http://dx.doi.org/10.1002/ijc.22928
IF:4.555

Total IF of journals (all publications): 30.267

Total IF of journals (publications related to the dissertation): 9.702

The Candidate's publication data submitted to the Publication Database of the University of Debrecen have been validated by Kenezy Life Sciences Library on the basis of Web of Science, Scopus and Journal Citation Report (Impact Factor) databases.

22 April, 2014

International presentations related to the dissertation

Ecsedi S, Hernandez-Vargas H, Lima SC, Vizkeleti L, Toth R, Lazar V, Herceg Z, Adany R, Balazs M. Global hypomethylation and promoter related demethylation are associated with copy number loss of *DNMT1* gene and unfavourable clinical outcome in primary melanomas. 38th FEBS Congress, 6-11 July, 2013, Saint Petersburg, Russia

Ecsedi S, Lazar V, Vizkeleti L, Emri G, Rakosy Z, Adany R, Balazs M. Copy number variation and promoter methylation contribute to transcriptomic profiles associated with malignant melanoma progression. The 4th EMBO Meeting, 22-25 Sept, 2012, Nice, France

Ecsedi S, Vizkeleti L, Lima SC, Hernandez-Vargas H, Rakosy Z, Herceg Z, Adany R, Balazs M. DNA methylation pattern of malignant melanoma at wide panel of cancer related genes. The 2nd EMBO Meeting, 4-7 Sept, 2010, Barcelona, Spain

National presentations related to the dissertation

Ecsedi S, Hernandez-Vargas H, Herceg Z, Adany R, Balazs M. A daganat genom alterációi: epigenetikai és strukturális változások. VII. Conference of the Hungarian Association of Public Health Schools (NKE), 4-6 Sept, 2013, Kaposvár, Hungary

Ecsedi S, Vizkeleti L, Hernandez-Vargas H, Lima SC, Toth R, Lazar V, Herceg Z, Adany R, Balazs M. Transposonal hypomethylation and local demethylation of primary melanomas are associated with copy number loss of *DNMT1* and unfavourable clinical outcome. Hungarian Molecular Life Sciences 2013 Conference. 5-7 Apr, 2013, Siófok, Hungary

Ecsedi S, Vizkeleti L, Lima SC, Hernandez-Vargas H, Herceg Z, Adany R, Balazs M. Hypo- és hypermetilációs epigenetikai mintázatok humán malignus melanomákban. VI. Conference of the Hungarian Association of Public Health Schools (NKE), 5-7 Sept, 2012, Budapest, Hungary

Ecsedi S, Lima SC, Hernandez-Vargas H, Lazar V, Vizkeleti L, Rakosy Zs, Herceg Z, Adany R, Balazs M. Kópiaszám variabilitás és epigenetika változások primer melanomákban. V. Conference of the Hungarian Association of Public Health Schools (NKE), 31 Aug - 2 Sept, 2011, Szeged, Hungary

Other presentations

Ecsedi S, Vizkeleti L, Kiss T, Koroknai V, Rakosy Z, Emri G, Begany A, Adany R, Balazs M. Alterations of osteopontin protein (SPP1) expression in malignant melanoma. VIII. Hungarian Genetics Congress and XV. Cell and Developmental Biology Conference, 17-19 Apr, 2009, Nyíregyháza, Hungary

Ecsedi S, Vizkeleti L, Rakosy Z, Juhasz A, Adany R, Balazs M. Cytogenetically analysis of cholesteatomas with different biological behaviour. V. Hungarian Cell Analytical Conference; 4-6 May, 2006, Budapest, Hungary

Ecsedi S, Vizkeleti L, Rakosy Z, Juhasz A, Adány R, Balazs M. Analysis of chromosomal alterations in interphase cells in cholesteatomas. Hungarian Cancer Society XXVI. Congress 10-12 Nov, 2005; Budapest, Hungary

Vizkeleti L, **Ecsedi S,** Emri G, Kiss T, Koroknai V, Adany R, Balazs M. Combined gene copy number and gene expression profiling of matched primary and metastatic melanomas. The 5th EMBO Meeting, 21-24 Sept, 2013, Amsterdam, the Netherlands

Kiss T, Koroknai V, **Ecsedi S,** Vizkeleti L, Adany R, Balazs M. Osteopontin expression in malignant melanoma. VII. Conference of the Hungarian Association of Public Health Schools (NKE), 4-6 Sept, 2013, Kaposvár, Hungary

Szasz I, Koroknai V, Kiss T, **Ecsedi S,** Vizkeleti L, Adany R, Balazs M. Genetic and gene expression changes are associated with drug resistance in melanoma cell lines. VII. Conference of the Hungarian Association of Public Health Schools (NKE), 4-6 Sept, 2013, Kaposvár, Hungary

Vizkeleti L, **Ecsedi S,** Adany R, Balazs M. Combined gene copy number and gene expression profiling of matched primary and metastatic melanomas. Hungarian Molecular Life Sciences 2013 Conference. 5-7 Apr, 2013, Siófok, Hungary

Kiss T, Koroknai V, **Ecsedi S,** Vizkeleti L, Emri G, Adany R, Balazs M. The role of osteopontin expression in melanoma progression. Hungarian Molecular Life Sciences 2013 Conference. 5-7 Apr, 2013, Siófok, Hungary

Koroknai V, Kiss T, Vizkeleti L, **Ecsedi S,** Szasz I, Adany R, Balazs M. Investigation of molecular alterations associated with the invasion of melanoma cell lines. Hungarian Molecular Life Sciences 2013 Conference. 5-7 Apr, 2013, Siófok, Hungary

Vizkeleti L, **Ecsedi S,** Rakosy Z, Orosz A, Lazar V, Emri G, Koroknai V, Kiss T, Adany R, Balazs M. CCND1 as a potential prognostic marker of cutaneous melanomas? CYTO 2012, XXVII Congress of the International Society for Advancement of Cytometry, 23-27 June, 2012, Leipzig, Germany

Balazs M, **Ecsedi S,** Vizkeleti L, Lazar V, Emri G, Adany R. A melanoma genom eltérései. (NKE), 5-7 Sept, 2012, Budapest, Hungary

Vizkeleti L, **Ecsedi S,** Emri G, Toth R, Koroknai V, Kiss T, Adany R, Balazs M. Genetikai eltérések szerepe humán melanomák progressziójában. VI. Conference of the Hungarian Association of Public Health Schools (NKE), 5-7 Sept, 2012, Budapest, Hungary

Koroknai V, Kiss T, Vizkeleti L, **Ecsedi S,** Adany R, Balazs M. Investigation of molecular alterations associated with melanoma invasion. VI. Conference of the Hungarian Association of Public Health Schools (NKE), 5-7 Sept, 2012, Budapest, Hungary

Kiss T, Koroknai V, **Ecsedi S,** Vizkeleti L, Emri G, Adany R, Balazs M. The role of osteopontin in melanoma progression. VI. Conference of the Hungarian Association of Public Health Schools (NKE), 5-7 Sept, 2012, Budapest, Hungary

Vizkeleti L, **Ecsedi S,** Orosz A, Lazar V, Rakosy Zs, Koroknai V, Kiss T, Emri G, Adany R, Balazs M. Ciklin D1 szerepe malignus melanomák progressziójában. V. Conference of the Hungarian Association of Public Health Schools (NKE), 31 Aug - 2 Sept, 2011, Szeged, Hungary

Kiss T, Koroknai V, **Ecsedi S,** Vizkeleti L, Mehes G, Nagy B, Begany A. Emri G, Adany R, Balazs M. Osteopontin: a candidate molecule for melanoma progression. V. Conference of the Hungarian Association of Public Health Schools (NKE), 31 Aug - 2 Sept, 2011, Szeged, Hungary

Koroknai V, Kiss T, Vizkeleti L, **Ecsedi S,** Emri G, Balazs M, Adany R. The role of simultaneous genetic alterations in the progression of malignant melanoma. V. Conference of the Hungarian Association of Public Health Schools (NKE), 31 Aug - 2 Sept, 2011, Szeged, Hungary

Vizkeleti L, **Ecsedi S,** Rakosy Z, Begany A, Emri G, Adany R, Balazs M. Genetic and gene expression alterations of the 7q31 locus in human melanomas. IV. Conference of the Hungarian Association of Public Health Schools (NKE), 2-4 Sept, 2010, Szombathely, Hungary

Balazs M, **Ecsedi S,** Vizkeleti L, Lazar V, Rakosy Z, Begany A, Emri G, Adany R. Heterogeneity of the melanoma genome, the role of gene amplifications in *tumour* progression. Hungarian Cancer Society XXVIII. Congress, 12-14 Nov, 2009, Budapest, Hungary

Vizkeleti L, **Ecsedi S,** Rakosy Z, Szollosi A, Emri G, Begany A, Mehes G, Adany R, Balazs M. Expression alterations of genes located on the 7q31 region in human malignant melanomas. ECCO 15 - 34th ESMO Multidisciplinary Congress, 20-24 Sept, 2009, Berlin, Germany

Balazs M, **Ecsedi S,** Vizkeleti L, Lazar V, Rakosy Z, Begany A, Emri G, Adany R. Diversity of the human melanoma genom. VIII. Hungarian Genetics Congress and XV. Cell and Developmental Biology Conference, 17-19 Apr, 2009, Nyíregyháza, Hungary

Lazar V, **Ecsedi S,** Rakosy Z, Toth R, Szollosi A, Emri G, Adany R, Balazs M. of Cyclin D1 and other candidate gene amplification in the 11q13 region in human primary cutaneous melanoma. ISAC XXIV. International Congress. Cytometry in the Age of Systems Biology, 17-21 May, 2008, Budapest, Hungary

Vizkeleti L, Szollosi A, **Ecsedi S,** Rakosy Z, Begany A, Adany R, Balazs M. Altered gene expressions on FRA7G fragile site in hamun malignant melanoma. ISAC XXIV. International Congress. Cytometry in the Age of Systems Biology, 17-21 May, 2008, Budapest, Hungary

Rakosy Z, Begany A, Emri G, Vizkeleti L, **Ecsedi S,** Adany R, Balazs M. Role of EGFR gene amplification in melanoma progression. 80. Conference of Hungarian Society of Dermatology, 13-15 Dec, 2007, Budapest, Hungary

Vizkeleti L, Lazar V, **Ecsedi S,** Rakosy Z, Begany A, Adany R, Balazs M. Array Comparative Genomic hybridization Analysis of Cutaneous Melanoma; Marie Curie - Genome Architecture in Relation to Disease. Array techniques to identify copy number variations. Workshop 1, 11 – 15 Sept, 2007, Helsinki, Finland

Balazs M, Lazar V, Rakosy Z, Vizkeleti L, **Ecsedi S,** Begany A, Emri G, Adany R. Array CGH and fluorescence in situ hybridization analyses reveal new genomic alterations in malignant melanoma. MAF10 10th Conference on Methods and Applications of Fluorescence, 9-12 Sept, 2007, Salzburg, Austria

Vizkeleti L, **Ecsedi S,** Rakosy Z, Begany A, Adany R, Balazs M. Alterations of 7q31 locus in human malignant melanomas; V. Hungarian Cell Analytical Conference. 4-6 May, 2006, Budapest, Hungary

Rakosy Z, Vizkeleti L, **Ecsedi S,** Begany A, Adany R, Balazs M. Analysis of gene expression pattern of primary malignant melanomas using microarray technique. V. Hungarian Cell Analytical Conference; 4-6 May, 2006, Budapest, Hungary

Keywords

primary melanoma

tumour progression

copy number amplification

copy number deletions

cis-acting copy number alteration

trans-acting copy number alteration

epigenetics

DNA methylation

DNA methyltransferase

transposable / global hypomethylation

promoter hypermethylation

Tárgyszavak

primer melanoma

daganat progresszió

kópiaszám növekedés

kópiaszám csökkenés

transz-hatású kópiaszám változás

epigenetika

DNA metiláció

DNS metiltranszferáz

transzpozon/globális hipometiláció

promoter hipermetiláció

Acknowledgements

It is with a humble heart that I acknowledge the breadth of perspective and knowledge I have gained both professionally and personally at the Institute of Preventive Medicine since 2004 when I entered as an undergraduate student.

I am grateful to *Professor Róza Ádány* for making my studies in this institute possible.

I express my profound gratitude to my advisor, *Professor Margit Balázs* for introducing me into the world of cancer genetics, her exemplary guidance, wisdom and constant encouragement throughout my PhD studies.

My sincere appreciation is extended to *Professor Zdenko Herceg* for his invaluable support and advice on epigenetic research. Furthermore, I am grateful *to Dr. Sheila Soires-Coelho Lima, Dr. Hector Hernandez-Vargas, Dr. Anastas Gospodinov* and *Cyrille Cuenin* for their graciousness during my studies at the International Agency for Research on Cancer, in Lyon, France.

I express a deep sense of gratitude to *Professor Tsuyoshi Takami* for his cordial support. It was my greatest privilege to be able to work alongside such dedicated researcher at Gifu University, in Gifu, Japan.

I am indebted to *Dr. Zsuzsa Rákosy* for being inexhaustible source of support.

I express my sincere gratitude *to Dr. Réka Tóth* for helping me constantly in advanced statistics and stimulating my interest in the field of bioinformatics. I am especially grateful for *Dr. Laura Vízkeleti and Dr. Viktória Lázár* for their aimed comments and suggestions.

I convey thanks to *Dr. Helga Bárdos* for introducing me into confocal microscopy.

I am obliged to *Dr. Ágnes Bégány* and *Dr. Gabriella* Emri for the valuable information provided by them in their respective fields.

I am appreciative of all my colleagues, especially of *Viktória Koroknai, Tímea Kiss, István Szász, Karolina Rigó, Andrea Lukács, Orsolya Papp, Györgyné Kovács,* Attila Nagy and Tibor Gáll for their friendship and generous help.

Lastly, I thank almighty *my Family* for their constant supports on me in completing my doctoral thesis.

This research was supported by the Hungarian National Research Fund (OTKA K75191), the Hungarian Academy of Sciences (grant number 2011 TKI 473), by the TÁMOP 4.2.1/B-09/1/KONV-2010-0007 and TÁMOP-4.2.2.A-11/1/KONV-2012-0031 projects; the TÁMOP projects are co-financed by the European Union and the European Social Fund.

„This research was realized in the frames of TÁMOP 4.2.4. A/2-11-1-2012-0001 „National Excellence Program – Elaborating and operating an inland student and researcher personal support system convergence program" The project was subsidized by the European Union and co-financed by the European Social Fund."

Appendices

Appendix 1

Differentially methylated gene sets associated with clinical characteristics of primary melanomas.
Red indicates increased and blue indicates decreased DNA metthylation leveli in samples with less favourable outcome. Results are based on t-tests and FDR corrections.

BRESLOW THICKNESS						
No.	Parametric p-value	Geom mean of ratios in melanomas larger than 4mm	Geom mean of ratios in melanomas smaller than 4mm	Relative difference	UniqueID	Gene Symbol
1	5.60E-06	1.33	8.06	0.16	EMR3_E61_F	
2	1.72E-05	0.16	0.6	0.27	MMP14_P208_R	MMP14
3	5.99E-05	0.1	0.26	0.4	ERBB3_P870_R	ERBB3
4	6.22E-05	0.14	0.23	0.58	PKD2_P336_R	PKD2
5	0.0001106	1.27	3.92	0.33	CEACAM1_P44_R	CEACAM1
6	0.0001527	0.12	0.34	0.35	TNK1_P41_R	TNK1
7	0.0001669	0.046	0.13	0.35	CEACAM1_E57_R	CEACAM1
8	0.0001875	0.66	5.19	0.13	SLC22A18_P216_R	SLC22A18
9	0.000196	2.94	7.95	0.37	MMP9_P189_F	MMP9
10	0.0002019	0.041	0.057	0.72	EPHB2_E297_F	EPHB2
11	0.0003331	16.21	74.74	0.22	LCN2_P141_R	LCN2
12	0.0003372	0.031	0.072	0.42	TYRO3_P501_F	TYRO3
13	0.0003498	0.17	0.61	0.27	IL8_E118_R	IL8
14	0.0003665	0.7	3.1	0.23	MMP14_P13_F	MMP14
15	0.0003691	0.19	1.11	0.17	SEPT9_P374_F	SEPT9
16	0.0003782	0.081	0.14	0.59	PLXDC2_E337_F	PLXDC2
17	0.0004501	0.049	0.13	0.37	PDGFRA_P1429_F	PDGFRA
18	0.0007143	0.077	0.15	0.52	MATK_P64_F	MATK
19	0.0007559	3.14	9.38	0.33	HRASLS_P353_R	HRASLS
20	0.0009196	15.76	52.53	0.3	SLC22A18_P472_R	SLC22A18
21	0.0010254	0.54	1.83	0.29	COL1A1_P5_F	COL1A1
22	0.0011234	19.69	52.01	0.38	GABRG3_E123_R	GABRG3
23	0.0015297	0.037	0.086	0.43	RAB32_E314_R	RAB32
24	0.0015674	0.82	5.83	0.14	EVI2A_P94_R	EVI2A
25	0.0017022	0.11	0.21	0.53	MLF1_E243_F	MLF1
26	0.0020598	28.12	14.09	2	MMP19_P306_F	MMP19
27	0.0021244	0.11	0.17	0.66	MCAM_P169_R	MCAM
28	0.0022682	1.08	3.27	0.33	HLA-DPA1_P205_R	HLA-DPA1

29	0.0023415	0.076	0.22	0.34	TUSC3_E29_R	TUSC3
30	0.0024948	2.68	5.07	0.53	SPI1_E205_F	SPI1
31	0.0026561	24.02	74.02	0.32	PI3_P274_R	PI3
32	0.0028823	3.49	7.12	0.49	SLC5A5_E60_F	SLC5A5
33	0.0032837	0.2	0.48	0.42	MCAM_P265_R	MCAM
34	0.0036087	0.064	0.085	0.75	EPHA5_E158_R	EPHA5
35	0.003825	0.12	0.27	0.43	DCC_P471_R	DCC
36	0.003945	0.1	0.19	0.52	IHH_P246_R	IHH
37	0.0040188	73.06	107.76	0.68	HSPA2_P162_R	HSPA2
38	0.0042101	4.55	12.98	0.35	SYK_P584_F	SYK
39	0.0042284	7.29	22.19	0.33	LCN2_P86_R	LCN2
40	0.0046446	5.39	10.8	0.5	CSF3R_P472_F	CSF3R
41	0.0046965	22.19	60.1	0.37	HLA-DPA1_E35_R	HLA-DPA1
42	0.004927	1.3	2.09	0.62	EPHA5_P66_F	EPHA5
43	0.0052947	0.6	1.5	0.4	SEMA3A_P658_R	SEMA3A
44	0.005457	0.057	0.084	0.68	PTPRG_P476_F	PTPRG
45	0.0061376	2.35	6.75	0.35	GRB7_E71_R	GRB7
46	0.0062312	30.23	9.21	3.28	LTA_E28_R	LTA
47	0.0062593	95.86	77.32	1.24	ASB4_P52_R	ASB4
48	0.0070871	0.48	0.25	1.96	GPX1_P194_F	GPX1
49	0.0073372	0.16	0.25	0.65	DCC_P177_F	DCC
50	0.0074906	0.37	1.05	0.36	GP1BB_E23_F	GP1BB
51	0.0080037	15.87	37.33	0.43	AGXT_P180_F	AGXT
52	0.0083799	0.018	0.046	0.38	ADAMTS12_P250_R	ADAMTS12
53	0.0092646	0.048	0.066	0.73	CDK10_E74_F	CDK10
54	0.0094254	13.47	4.89	2.76	NBL1_P24_F	NBL1
55	0.0097887	0.23	0.29	0.8	KRAS_P651_F	KRAS
56	0.0099619	0.043	0.06	0.72	CDKN1A_E101_F	CDKN1A
METASTASIS						
No.	**Parametric p-value**	**Geom mean of ratios in metastatic melanomas**	**Geom mean of ratios in non-metastatic**	**Relative difference**	**UniqueID**	**Symbol**
1	0.0001791	0.07	0.096	0.73	IRF7_P277_R	IRF7
2	0.0002887	27.04	12.38	2.18	MMP19_P306_F	MMP19
3	0.0003099	0.2	0.7	0.29	IL8_E118_R	IL8
4	0.0003334	0.056	0.086	0.65	FGFR1_E317_F	FGFR1
5	0.0004125	0.15	0.24	0.62	PKD2_P336_R	PKD2
6	0.0007175	3.46	8.52	0.41	MMP9_P189_F	MMP9
7	0.001095	60.72	23.96	2.53	AATK_E63_R	AATK
8	0.0012575	0.25	1.25	0.2	SEPT9_P374_F	SEPT9
9	0.0017848	1.6	3.8	0.42	KRAS_E82_F	KRAS
10	0.0018301	0.089	0.14	0.63	PLXDC2_E337_F	PLXDC2
11	0.0027612	2.14	7.49	0.29	EMR3_E61_F	EMR3
12	0.0028547	0.35	0.48	0.74	FGF9_P1404_F	FGF9

13	0.0029845	0.036	0.074	0.49	TYRO3_P501_F	TYRO3
14	0.003026	21.93	6.44	3.4	AATK_P709_R	AATK
15	0.0033631	0.94	3.24	0.29	MMP14_P13_F	MMP14
16	0.0033876	3.67	9.37	0.39	GABRG3_P75_F	GABRG3
17	0.003388	0.066	0.088	0.75	EPHA5_E158_R	EPHA5
18	0.0035554	0.11	0.19	0.56	MMP9_P237_R	MMP9
19	0.0045843	25.29	59.43	0.43	SPI1_P48_F	SPI1
20	0.0046431	2.96	5.34	0.55	SPI1_E205_F	SPI1
21	0.0052326	0.043	0.09	0.48	RAB32_E314_R	RAB32
22	0.0058127	0.064	0.095	0.67	RASGRF1_E16_F	RASGRF1
23	0.0064959	6.23	1.45	4.3	WNT10B_P823_R	WNT10B
24	0.0066384	0.023	0.044	0.51	CASP3_P420_R	CASP3
25	0.0067145	1.69	3.8	0.44	CEACAM1_P44_R	CEACAM1
26	0.0084435	1.11	4.92	0.23	SLC22A18_P216_R	SLC22A18
27	0.0087821	11.71	5.03	2.33	IL1RN_P93_R	IL1RN
28	0.0097452	0.27	0.54	0.49	FANCE_P356_R	FANCE
Ulceration						
No.	**Parametric p-value**	**Geom mean of ratios in ulcerated melanomas**	**Geom mean of ratios in non-ulcerated**	**Relative difference**	**UniqueID**	**Symbol**
1	9.90E-06	0.67	6.8	0.098	SLC22A18_P216_R	SLC22A18
2	4.62E-05	0.19	1.37	0.14	SEPT9_P374_F	SEPT9
3	5.19E-05	0.72	3.68	0.2	MMP14_P13_F	MMP14
4	0.0002047	5.18	12.31	0.42	CSF3R_P472_F	CSF3R
5	0.0002503	32.84	7.26	4.52	LTA_E28_R	LTA
6	0.0002507	16.43	59.6	0.28	SLC22A18_P472_R	SLC22A18
7	0.0002598	2.66	5.57	0.48	SPI1_E205_F	SPI1
8	0.0003156	0.12	0.26	0.44	ERBB3_P870_R	ERBB3
9	0.0004063	0.063	0.089	0.71	EPHA5_E158_R	EPHA5
10	0.0004115	11.83	3.29	3.6	RAN_P581_R	RAN
11	0.0004456	0.19	0.65	0.29	IL8_E118_R	IL8
12	0.0005009	10.45	26.64	0.39	PECAM1_E32_R	PECAM1
13	0.0005072	0.09	0.14	0.66	E2F3_P840_R	E2F3
14	0.0005219	12.51	36.42	0.34	MPO_E302_R	MPO
15	0.0005343	0.13	0.35	0.38	TNK1_P41_R	TNK1
16	0.0006093	0.016	0.044	0.36	TP73_E155_F	TP73
17	0.0006262	24.53	84.65	0.29	PI3_P274_R	PI3
18	0.0010723	0.043	0.057	0.75	EPHB2_E297_F	EPHB2
19	0.0011891	0.94	6.74	0.14	EVI2A_P94_R	EVI2A
20	0.0015447	3.41	7.97	0.43	MMP9_P189_F	MMP9
21	0.0016651	0.21	0.57	0.38	MMP14_P208_R	MMP14
22	0.0018694	70.49	32.89	2.14	LCK_E28_F	LCK
23	0.0022024	0.083	0.15	0.55	MATK_P64_F	MATK
24	0.0022253	1.99	7.14	0.28	EMR3_E61_F	EMR3

25	0.0033658	4.63	15.27	0.3	HOXA5_P1324_F	HOXA5
26	0.0034126	4.89	14.02	0.35	SYK_P584_F	SYK
27	0.0035637	3.72	7.39	0.5	SLC5A5_E60_F	SLC5A5
28	0.0038353	20.99	72.8	0.29	LCN2_P141_R	LCN2
29	0.0038367	0.057	0.13	0.44	PDGFRA_P1429_F	PDGFRA
30	0.0040761	0.85	1.6	0.53	TNK1_P221_F	TNK1
31	0.0042385	0.074	0.14	0.52	ABL1_P53_F	ABL1
32	0.0044323	7.99	23.75	0.34	LCN2_P86_R	LCN2
33	0.0050332	7	16.72	0.42	TIE1_E66_R	TIE1
34	0.0051026	0.15	0.23	0.68	PKD2_P336_R	PKD2
35	0.005227	25.81	13.86	1.86	MMP19_P306_F	MMP19
36	0.0052399	0.13	0.28	0.45	DCC_P471_R	DCC
37	0.0052404	3.01	7.8	0.39	SEPT9_P58_R	SEPT9
38	0.0054813	0.2	0.3	0.65	PALM2-AKAP2_P183_R	PALM2-AKAP2
39	0.0056944	0.09	0.19	0.49	ERCC1_P440_R	ERCC1
40	0.0057924	14.72	21.97	0.67	EGF_P242_R	EGF
41	0.0059886	1.82	4.08	0.44	HBII-52_E142_F	SNORD115-1
42	0.0060112	0.32	0.62	0.52	SPARC_P195_F	SPARC
43	0.006511	0.12	0.14	0.85	CTNNA1_P382_R	CTNNA1
44	0.0069379	7	16.05	0.44	TMPRSS4_P552_F	TMPRSS4
45	0.0069745	7.21	23.49	0.31	PGR_E183_R	PGR
46	0.007184	0.044	0.061	0.71	CDKN1A_E101_F	CDKN1A
47	0.0077282	0.31	0.84	0.37	HTR1B_E232_R	HTR1B
48	0.0077897	0.19	0.33	0.59	TYRO3_P366_F	TYRO3
49	0.0078122	0.22	0.36	0.62	P2RX7_P119_R	P2RX7
50	0.0079161	0.12	0.21	0.58	MLF1_E243_F	MLF1
51	0.0081179	1.91	0.82	2.34	E2F5_P516_R	E2F5
52	0.0093064	0.049	0.067	0.73	CDK10_E74_F	CDK10
53	0.0094069	76.11	103.24	0.74	HLA-DOB_P1114_R	HLA-DOB
54	0.0094608	44.38	21.19	2.09	WEE1_P924_R	WEE1
55	0.0097514	7.72	4.87	1.59	C4B_E171_F	C4B
56	0.0099344	0.28	0.11	2.65	CEBPA_P1163_R	CEBPA

Histologic subtype						
No.	**Parametric p-value**	**Geom mean of ratios in nodular melanomas**	**Geom mean of ratios in superficial spreading melanomas**	**Relative difference**	**UniqueID**	**Symbol**
1	0.0002157	3.28	5.12	0.64	LMTK2_P1034_F	LMTK2
2	0.0004854	30.07	7.04	4.27	AATK_P709_R	AATK
3	0.0006996	29.82	13.96	2.14	MMP19_P306_F	MMP19
4	0.0007049	18.72	51.69	0.36	GABRG3_E123_R	GABRG3
5	0.0009665	2.03	6.17	0.33	PGR_P790_F	PGR
6	0.0010637	0.1	0.075	1.39	POMC_P53_F	POMC

7	0.0013798	15.55	50.59	0.31	SLC22A18_P472_R	SLC22A18
8	0.0017386	69	27.44	2.51	AATK_E63_R	AATK
9	0.0021607	2.93	6.59	0.44	NOS3_P38_F	NOS3
10	0.0021634	0.56	1.37	0.41	ELL_P693_F	ELL
11	0.0022497	0.18	0.57	0.32	IL8_E118_R	IL8
12	0.0022853	0.078	0.14	0.54	MATK_P64_F	MATK
13	0.002342	4.68	1.06	4.43	HOXA11_E35_F	HOXA11
14	0.002963	0.21	0.97	0.21	SEPT9_P374_F	SEPT9
15	0.0031124	0.26	0.12	2.25	FGF8_P473_F	FGF8
16	0.0031853	1.13	0.66	1.72	IRF5_E101_F	IRF5
17	0.0032302	15.37	2.51	6.13	HOXA9_E252_R	HOXA9
18	0.0034368	1.04	0.2	5.08	KIT_P405_F	KIT
19	0.0040743	6.04	21.84	0.28	PGR_E183_R	PGR
20	0.0043891	0.07	0.09	0.77	IRF7_P277_R	IRF7
21	0.0045714	0.82	4.21	0.19	SLC22A18_P216_R	SLC22A18
22	0.0047463	13.93	5.49	2.54	IL1RN_P93_R	IL1RN
23	0.0048047	8.29	5.57	1.49	MXI1_P1269_F	MXI1
24	0.0048393	14.59	4.84	3.02	NBL1_P24_F	NBL1
25	0.0049191	4.44	9.1	0.49	KRT1_P798_R	KRT1
26	0.0049206	5.42	0.72	7.54	MAP3K1_E81_F	MAP3K1
27	0.0050574	4.64	12.78	0.36	TFF2_P178_F	TFF2
28	0.0051178	1.83	6.17	0.3	EMR3_E61_F	EMR3
29	0.0051307	0.8	2.7	0.3	MMP14_P13_F	MMP14
30	0.0051874	0.16	0.25	0.64	DCC_P177_F	DCC
31	0.0052636	2.65	0.85	3.1	FZD9_E458_F	FZD9
32	0.0055036	4.46	14.41	0.31	RIPK1_P744_R	RIPK1
33	0.0056252	8.97	4.85	1.85	CSF1R_P73_F	CSF1R
34	0.006112	0.28	0.13	2.1	MGMT_P281_F	MGMT
35	0.0062975	0.23	0.4	0.58	RUNX1T1_P103_F	RUNX1T1
36	0.006408	6.23	1.24	5.02	TNFRSF10A_P171_F	TNFRSF10A
37	0.0066185	0.39	0.12	3.12	TJP1_P390_F	TJP1
38	0.0066264	16.28	7.39	2.2	FGFR3_P1152_R	FGFR3
39	0.0066347	0.27	0.14	1.92	TJP1_P326_R	TJP1
40	0.0070373	1.13	0.33	3.4	CD81_P211_F	CD81
41	0.0075823	18.66	6.25	2.99	MST1R_E42_R	MST1R
42	0.0077807	3.87	2.3	1.68	LEFTY2_P561_F	LEFTY2
43	0.0079985	0.34	0.16	2.07	EPHB6_E342_F	EPHB6
44	0.0085793	11.49	33.31	0.34	S100A12_P1221_R	S100A12
45	0.0087402	23.82	12.73	1.87	SLC22A3_P634_F	SLC22A3
46	0.0089654	1.28	0.28	4.53	DIO3_P674_F	DIO3
47	0.0089993	0.043	0.055	0.79	EPHB2_E297_F	EPHB2
48	0.0091353	9.31	39.36	0.24	PGR_P456_R	PGR
49	0.0093387	0.34	0.45	0.76	FGF9_P1404_F	FGF9
50	0.0096424	0.16	0.058	2.73	TIMP3_seq_7_S38_F	TIMP3
51	0.0099707	6.43	2.54	2.53	CRIP1_P274_F	CRIP1

Appendix 2

Differentially methylated gene sets associated with *BRAF*^{V600E} mutation

No.	KEGG Pathway description	Symbol	EntrezID	Part of CpG Island
1	Cell Communication	GJB2	2706	YES
2	Cell Communication	COL1A2	1278	NO
3	Cell Communication	THBS1	7057	YES
4	Cell Communication	COL1A2	1278	YES
5	Cell Communication	COL1A2	1278	YES
6	Cell Communication	ITGB4	3691	YES
7	Cell Communication	LAMC1	3915	YES
8	Cell Communication	GJB2	2706	YES
9	Cell Communication	LAMC1	3915	YES
10	Cell Communication	KRT13	3860	NO
11	Cell Communication	GJB2	2706	YES
12	Cell Communication	COL1A1	1277	YES
13	Cell Communication	KRT1	3848	NO
14	Cell Communication	DSG1	1828	NO
15	Cell Communication	TNC	3371	YES
16	Cell Communication	THBS1	7057	YES
17	Cell Communication	DSG1	1828	NO
18	Cell Communication	THBS2	7058	NO
19	Cell Communication	VIM	7431	YES
20	Cell Communication	COL1A1	1277	YES
21	Cell Communication	KRT5	3852	NO
22	Cell Communication	DES	1674	YES
23	Cell Communication	LAMB1	3912	YES
24	Cell Communication	ITGA6	3655	YES
25	Cell Communication	COL6A1	1291	YES
26	Cell Communication	SPP1	6696	NO

27	Cell Communication	DSC2	1824	NO
28	Cell Communication	DSC2	1824	YES
1	ECM-receptor interaction	COL1A2	1278	NO
2	ECM-receptor interaction	THBS1	7057	YES
3	ECM-receptor interaction	COL1A2	1278	YES
4	ECM-receptor interaction	COL1A2	1278	YES
5	ECM-receptor interaction	ITGB4	3691	YES
6	ECM-receptor interaction	LAMC1	3915	YES
7	ECM-receptor interaction	LAMC1	3915	YES
8	ECM-receptor interaction	ITGB1	3688	YES
9	ECM-receptor interaction	COL1A1	1277	YES
10	ECM-receptor interaction	TNC	3371	YES
11	ECM-receptor interaction	THBS1	7057	YES
12	ECM-receptor interaction	GP1BB	2812	YES
13	ECM-receptor interaction	THBS2	7058	NO
14	ECM-receptor interaction	CD44	960	YES
15	ECM-receptor interaction	COL1A1	1277	YES
16	ECM-receptor interaction	LAMB1	3912	YES
17	ECM-receptor interaction	ITGA6	3655	YES
18	ECM-receptor interaction	COL6A1	1291	YES
19	ECM-receptor interaction	SPP1	6696	NO
20	ECM-receptor interaction	ITGA2	3673	YES

Appendix 3

Significant copy number (CN) alterationsof primary melanomas associated with Breslow thickness

Region	Type of CN alteration	Q-Bound	G-Score
chr1:103,945,640-104,115,640	Loss	0.016	2.941
chr4:132,814,794-133,128,048	Loss	0.002	3.823
chr7:61,060,787-61,528,861	Loss	0.027	2.793
chr9:45,309,492-46,508,968	Loss	0.013	3.192
chr9:67,589,512-68,129,501	Loss	0.013	3.073
chr14:18,138,113-18,227,290	Loss	0.027	2.823
chr21:9,882,805-10,202,296	Loss	0.001	4.112
chr11:68,712,379-69,473,364	Gain	0.022	4.010

Appendix 4

ORIGINAL PUBLICATIONS